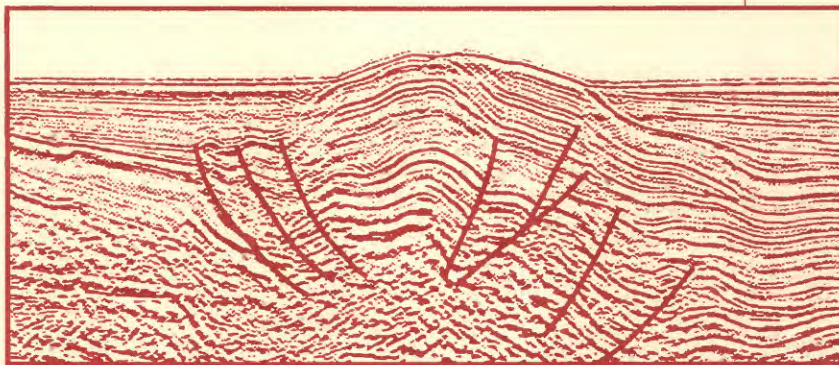


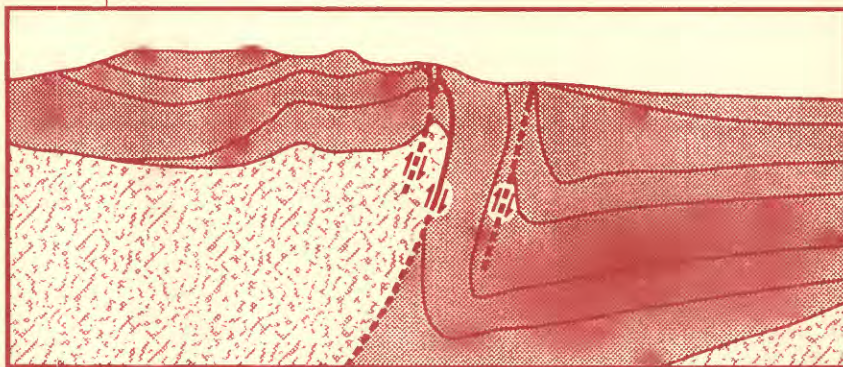
Cenozoic Deformation of the Franciscan Complex, Eastern Santa Maria Basin, California

Regional Thermal Maturity of Surface Rocks, Onshore Santa Maria Basin and Santa Barbara–Ventura Basin Area, California

Bulletin 1995–W, X



Geophysical section offshore Santa Maria basin



Geologic section onshore Santa Maria basin

Availability of Publications of the U.S. Geological Survey

Order U.S. Geological Survey (USGS) publications from the offices listed below. Detailed ordering instructions, along with prices of the last offerings, are given in the current-year issues of the catalog "New Publications of the U.S. Geological Survey."

Books, Maps, and Other Publications

By Mail

Books, maps, and other publications are available by mail from—

USGS Information Services
Box 25286, Federal Center
Denver, CO 80225

Publications include Professional Papers, Bulletins, Water-Supply Papers, Techniques of Water-Resources Investigations, Circulars, Fact Sheets, publications of general interest, single copies of permanent USGS catalogs, and topographic and thematic maps.

Over the Counter

Books, maps, and other publications of the U.S. Geological Survey are available over the counter at the following USGS Earth Science Information Centers (ESIC's), all of which are authorized agents of the Superintendent of Documents:

- Anchorage, Alaska—Rm. 101, 4230 University Dr.
- Denver, Colorado—Bldg. 810, Federal Center
- Menlo Park, California—Rm. 3128, Bldg. 3, 345 Middlefield Rd.
- Reston, Virginia—Rm. 1C402, USGS National Center, 12201 Sunrise Valley Dr.
- Salt Lake City, Utah—2222 West, 2300 South (books and maps available for inspection only)
- Spokane, Washington—Rm. 135, U.S. Post Office Building, 904 West Riverside Ave.
- Washington, D.C.—Rm. 2650, Main Interior Bldg., 18th and C Sts., NW.

Maps only may be purchased over the counter at the following USGS office:

- Rolla, Missouri—1400 Independence Rd.

Electronically

Some USGS publications, including the catalog "New Publications of the U.S. Geological Survey" are also available electronically on the USGS's World Wide Web home page at <http://www.usgs.gov>

Preliminary Determination of Epicenters

Subscriptions to the periodical "Preliminary Determination of Epicenters" can be obtained only from the Superintendent of

Documents. Check or money order must be payable to the Superintendent of Documents. Order by mail from—

Superintendent of Documents
Government Printing Office
Washington, DC 20402

Information Periodicals

Many Information Periodicals products are available through the systems or formats listed below:

Printed Products

Printed copies of the Minerals Yearbook and the Mineral Commodity Summaries can be ordered from the Superintendent of Documents, Government Printing Office (address above). Printed copies of Metal Industry Indicators and Mineral Industry Surveys can be ordered from the Center for Disease Control and Prevention, National Institute for Occupational Safety and Health, Pittsburgh Research Center, P.O. Box 18070, Pittsburgh, PA 15236-0070.

Mines FaxBack: Return fax service

1. Use the touch-tone handset attached to your fax machine's telephone jack. (ISDN [digital] telephones cannot be used with fax machines.)
2. Dial (703) 648-4999.
3. Listen to the menu options and punch in the number of your selection, using the touch-tone telephone.
4. After completing your selection, press the start button on your fax machine.

CD-ROM

A disc containing chapters of the Minerals Yearbook (1993-95), the Mineral Commodity Summaries (1995-97), a statistical compendium (1970-90), and other publications is updated three times a year and sold by the Superintendent of Documents, Government Printing Office (address above).

World Wide Web

Minerals information is available electronically at <http://minerals.er.usgs.gov/minerals/>

Subscription to the catalog "New Publications of the U.S. Geological Survey"

Those wishing to be placed on a free subscription list for the catalog "New Publications of the U.S. Geological Survey" should write to—

U.S. Geological Survey
903 National Center
Reston, VA 20192

Cenozoic Deformation of the Franciscan Complex, Eastern Santa Maria Basin, California

By ARTHUR D. WAHL

Regional Thermal Maturity of Surface Rocks, Onshore Santa Maria Basin and Santa Barbara– Ventura Basin Area, California

By NANCY D. NAESER, CAROLINE M. ISAACS, and
MARGARET A. KELLER

Chapters W and X are issued as a single volume
and are not available separately

U.S. GEOLOGICAL SURVEY BULLETIN 1995

EVOLUTION OF SEDIMENTARY BASINS/ONSHORE OIL AND GAS INVESTIGATIONS—
SANTA MARIA PROVINCE

Edited by Margaret A. Keller

U.S. DEPARTMENT OF THE INTERIOR
BRUCE BABBITT, Secretary



U.S. GEOLOGICAL SURVEY
Charles G. Groat, Director

Any use of trade, product, or firm names
in this publication is for descriptive purposes only
and does not imply endorsement by the U.S. Government

UNITED STATES GOVERNMENT PRINTING OFFICE, WASHINGTON: 1998

For sale by
U.S. Geological Survey
Information Services
Box 25286
Denver Federal Center
Denver, CO 80225

Library of Congress Cataloging-in-Publication Data

Wahl, Arthur D.

Cenozoic deformation of the Franciscan Complex, eastern Santa Maria Basin, California / by Arthur D. Wahl. Regional thermal maturity of surface rocks, onshore Santa Maria basin and Santa Barbara-Ventura basin area, California / by Nancy D. Naeser, Caroline M. Isaacs, and Margaret A. Keller. p. cm. — (U.S. Geological Survey bulletin ; 1995)

(Evolution of sedimentary basins/onshore oil and gas investigations—Santa Maria Province ; ch. W, X)

“Chapters W and X are issued as a single volume and are not available separately.”

Includes bibliographical references.

Supt. of Docs. no.: I 19.3:1995-W, X

1. Geology, Stratigraphic—Cenozoic. 2. Geology—California—Santa Maria Basin. 3. Petroleum—Geology—California—Santa Maria Basin. 4. Petrology—California—Santa Maria Basin. I. Isaacs, Caroline M. II. Keller, Margaret A. III. Naeser, Nancy D. Regional thermal maturity of surface rocks, onshore Santa Maria basin and Santa Barbara-Ventura basin area, California. IV. Title. V. Title: Regional thermal maturity of surface rocks, onshore Santa Maria basin and Santa Barbara-Ventura basin area, California. VI. Series. VII. Series: Evolution of sedimentary basins/onshore oil and gas investigations—Santa Maria Province ; ch. W, X.

QE75.B9 no. 1995-W, X
[QE690]

557.3s—dc21
[551.7'.8'09794]

98-11348
CIP

Chapter W

Cenozoic Deformation of the Franciscan Complex, Eastern Santa Maria Basin, California

By ARTHUR D. WAHL

U.S. GEOLOGICAL SURVEY BULLETIN 1995-W

EVOLUTION OF SEDIMENTARY BASINS/ONSHORE OIL AND GAS INVESTIGATIONS—
SANTA MARIA PROVINCE

Edited by Margaret A. Keller

CONTENTS

Abstract	W1
Introduction	W1
Acknowledgments	W3
Purpose and scope	W3
Geologic setting	W4
Mélange structure	W7
Hidden Potrero Fault	W8
Coast Range Fault	W9
Coherent rocks belt	W11
Oso syncline	W12
Late Cenozoic history	W15
Summary and discussion	W17
Conclusions	W18
References cited	W19

PLATE

[Plate is in pocket]

1. Map and cross sections showing geology of San Rafael Mountains mélange, Santa Cruz Creek, California

FIGURES

- 1–3. Maps showing:
 1. Regional geology of Franciscan Complex, Sur-Obispo terrane, Salinian terrane, and major faults **W2**
 2. General geology of onshore Santa Maria basin, San Rafael Mountains, Santa Ynez-Topa Topa Mountains, including Franciscan rocks, local crustal blocks, and major faults **W4**
 3. General geology of study area including folds and faults and exposed Franciscan rocks and Espada Formation **W6**
- 4–5. Schematic cross sections showing mélange structure:
 4. During early phase (Late Cretaceous) deformation **W9**
 5. At present **W10**
6. General tectonic cross section of Oso study-area region during Paleocene time after thrusting of mélange **W13**
7. Schematic cross section of Oso syncline showing pre- and post-Sespe Formation unconformities and basal thrust faults **W14**

TABLES

1. Local and regional crustal blocks, terranes, and tectonic provinces in study area **W5**
2. Correlation of rock units and events in Santa Maria basin study area **W12**

Cenozoic Deformation of the Franciscan Complex, Eastern Santa Maria Basin, California

By Arthur D. Wahl¹

Abstract

Mesozoic Franciscan basement rocks consisting of *mélange* and minor, coherent thrust sheets are exposed in the San Rafael Mountains of the southernmost Coast Ranges in California. *Mélange* is located on the Little Pine Mountain block that lies at the south edge of the regionally extensive crustal blocks of the Sur-Obispo and Salinian terranes. South of the Little Pine Mountain block lie the San Marcos block of the Santa Maria basin, which includes a coherent rocks belt of the Franciscan Complex near Lake Cachuma, and the Santa Ynez block of the western Transverse Ranges.

The origin and evolution of Franciscan *mélanges* are commonly associated with Farallon-North American Plate interaction. Detailed mapping, combined with general lithologic and structural observations, reveals that the *mélange* of this study formed during Late Cretaceous time as a contractional, vertical, brittle-ductile shear zone. This information is combined with investigation of the nearby Hidden Potrero Fault (a part of the Coast Range Fault System), the coherent rocks belt of the Franciscan Complex, and the Oso syncline to reveal Cenozoic deformation of this *mélange*. The results of this study indicate that this *mélange* was thrust beneath the Great Valley sequence during Paleocene time and reformed by late Eocene or early Oligocene to Quaternary tectonism that reflects transpression.

The transpressional structures found in this *mélange* and in the adjacent rocks are associated with the Little Pine Fault, which steepens with depth, faults the *mélange*, and separates the Little Pine Mountain block from the San Marcos block. This fault initially formed during late Eocene or early Oligocene time when anastomosing, steeply dipping reverse or reverse-oblique-slip faults and shear fractures in the *mélange* were reactivated and injected with much serpentinite. The reactivation of these structures clearly postdates regional Paleocene thrusting.

The Little Pine Fault Zone originated in *mélange* below a set of right-stepping anticlines. These anticlines were faulted to form southwest-directed flower structures. These flower structures are indicative of a lateral component of displacement along the Little Pine Fault. The orientation

of the right-stepping anticlines relative to the strike of the Little Pine Fault indicates dextral transpression; however, the Little Pine Fault probably has post-Miocene, reverse-oblique slip. The pre-Miocene slip on the Little Pine Fault is unknown, as is the slip on this fault beyond where it disappears southeastward beneath the Santa Ynez block.

The post-Paleocene transpressional structures of this *mélange* are related to the movement of local crustal blocks. These structures resulted, in part, from the oblique convergence of the San Marcos block beneath Little Pine Mountain block. The asymmetry of the Little Pine Fault, as depicted in cross section, is also a result of sinistral shear on the Big Pine and Santa Ynez Faults. The *mélange* of the Little Pine Mountain block, with its thick serpentinite basement, was transpressionally reformed and uplifted as a result of the northward convergence of the San Marcos block combined with westward movement of the blocks of the Sur-Obispo and Salinian terranes. This convergence formed local uplifts and contractional basins where *mélange* is exposed along the Little Pine Fault and caused differences in sedimentation along this fault.

In summary, the timing and tectonic style of the Late Eocene or early Oligocene diastrophism indicate that the Little Pine Mountain block formed a buttress against the northward translation of the San Marcos block by about 35 Ma. This diastrophism is related to the establishment of the known transform boundary that formed later, during Miocene time, and the local, oblique-convergent geometry this plate boundary must have had as the western Transverse Ranges subsequently rotated around this buttress.

INTRODUCTION

The Franciscan Complex forms much of the basement rock in the Coast Ranges of western California, which lie between the Great Valley and the Pacific Ocean (Bailey and others, 1964; fig. 1). The complex is a stratigraphically, structurally, and tectonically mixed composite terrane that generally consists of oceanic crust and terrigenous rocks with domains of diverse age, paleogeography, and degree of metamorphism (Blake and others, 1984). In northern California, the domains have been grouped by similar lithology and tectonic style into three northwest-trending

¹Geologist, 516 Pearson Road, Port Hueneme, CA 93041.

Manuscript approved for publication August 22, 1997.

Edited by Sean M. Stone

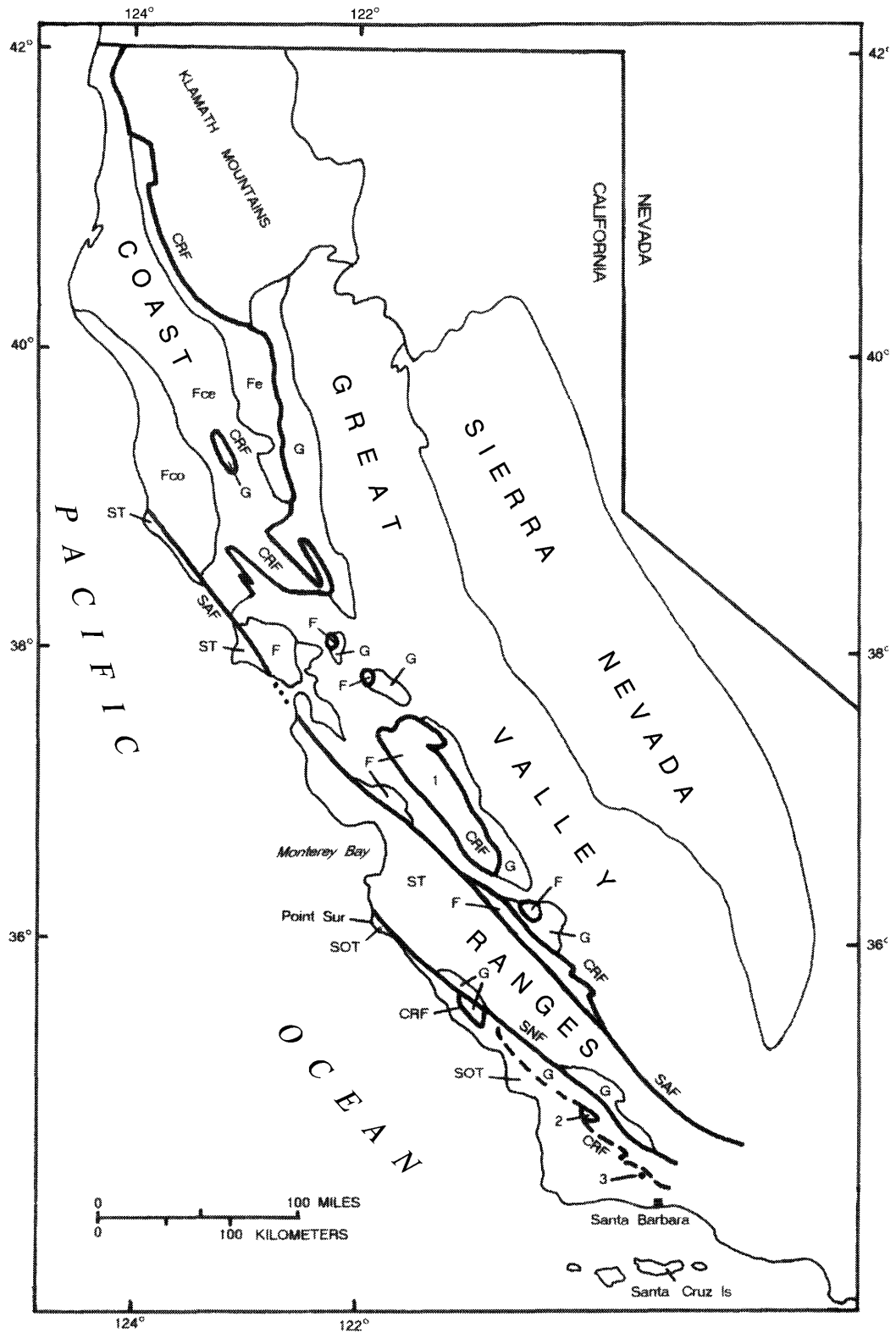


Figure 1. Regional geologic map of the Franciscan Complex, Sur-Obispo terrane, Salinian terrane, and major faults (modified from Bailey and others, 1970).

EXPLANATION

Map unit	
F	Franciscan Complex, undivided—Locally divided into:
Fco	Coastal belt
Fce	Central belt
Fe	Eastern Franciscan belt
G	Great Valley sequence and (or) Coast Range ophiolite
SOT	Sur-Obispo terrane—Basement consists of Franciscan Complex and Coast Range ophiolite
ST	Salinian terrane—Basement consists of continental margin, high-temperature metamorphic and batholithic rocks
<u>SAF</u>	Fault—Dashed where discontinuous segments are locally exposed; dotted where concealed
CRF	Coast Range Fault System
SAF	San Andreas Fault
SNF	Sur-Nacimiento Fault Zone of Page (1981)
	Features discussed in text
1	Diablo Range
2	Stanley Mountain
3	Mapped area—See plate 1

belts (Blake and Jones, 1981). These belts are related by an overall increase in age and degree of high-pressure, low-temperature metamorphism from west to east (Ernst, 1970). The Coastal belt primarily consists of low-grade lower Tertiary sedimentary rocks that are structurally coherent. The Central belt is a regional-scale mélangé (Blake and Jones, 1974). Mélangé, in general, is a chaotic zone of dismembered and mixed blocks that are commonly separated by a ductile matrix of pervasively fractured and faulted mudstone and (or) serpentinite. The Eastern Franciscan belt consists of coherent blueschist-facies terranes (Jayko and Blake, 1989; fig. 1).

In central California, Franciscan rocks form a belt of coherent thrust sheets and mélanges (Hsü, 1968) that structurally and lithologically resemble the Central belt observed farther north, although Coastal belt and Eastern Franciscan belt counterparts are not found onshore (Page, 1981). The Franciscan belts lie structurally beneath the forearc basin Great Valley sequence that conformably overlies the Upper Jurassic Coast Range ophiolite (Bailey and others, 1970; Hopson and others, 1981). Many Franciscan rocks may represent the accretionary wedge complex of a western North American subduction zone that developed initially during Late Jurassic time (Hamilton, 1969; Dickinson, 1970).

The Franciscan Complex formed as a result of Farallon-North American Plate convergence (Page, 1972); however, several questions about the origin and evolution of the mélanges still remain. Franciscan mélanges are com-

monly problematic because of their chaotic nature and their complex structure. This has led to wide differences of opinion in the interpretation of a mélangé and contrasting conclusions regarding the Mesozoic paleogeography of western California. For example, in central California, blocks of blueschist are present in a mudstone-matrix tectonic (and minor sedimentary) mélangé that formed as a result of regional crustal shortening (Warner, 1992; Wahl, 1995), which suggests, in part, that not all Franciscan oceanic crust is far-traveled (Blake and Jones, 1978; Page, 1981; Wahl, 1995).

ACKNOWLEDGMENTS

The author gratefully acknowledges permission granted to access the study area by Mr. Mike Galvin of Rancho San Fernando Rey and thanks Mr. Jim McKibbin, ranch manager, for his considerate involvement in this project. The author greatly appreciates the reviews of this manuscript by Margaret Keller, Craig Nicholson, Ed Keller, Lynn Tennyson, Sean Murphy Stone, and Art Sylvester.

PURPOSE AND SCOPE

The purpose of this report is to present the Cenozoic deformational history of a mélangé that is located in central California (fig. 1). This mélangé is exposed in the southwestern foothills of the San Rafael Mountains of the southernmost Coast Ranges (fig. 2). These foothills are bordered by the Santa Maria basin to the west and the Santa Ynez Mountains of the western Transverse Ranges to the south. The study of Mesozoic Franciscan mélanges involves the recognition and removal of the Cenozoic structures. This report is based in part on this analysis of the younger deformation identified in these older Mesozoic rocks. Results from this study are then applied to local Pacific-North American Plate interactions.

This mélangé is complexly deformed, but some details of its history may become clearer when other structures in the area are used for comparison. For this reason, analysis of the Coast Range Fault, the Hidden Potrero Fault (part of the Coast Range Fault System), the Oso syncline, and the local, Franciscan coherent rocks belt is included. This analysis is combined with some discussion of the depositional history and paleogeography of the local cover rocks. As background, this report summarizes several previously expressed conclusions regarding the Late Cretaceous and Paleocene history of this mélangé (Wahl, 1995). With this additional information, the middle and late Cenozoic structure of this mélangé is related to the movement of local crustal blocks, and microplate interactions that reflect transpression.

Table 1. Local and regional crustal blocks, terranes, and tectonic provinces in study area

LOCAL CRUSTAL BLOCK	REGIONAL CRUSTAL BLOCK	TERRANE	TECTONIC PROVINCE
Little Pine Mountain	Sur-Obispo	Sur-Obispo	
Santa Ynez		?	Western Transverse Ranges
San Marcos	Sur-Obispo	Sur-Obispo	Santa Maria
	Salinian	Salinian	

EXPLANATION

Map unit	SCF	San Cayetano Fault
F Franciscan Complex (of Sur-Obispo terrane)	SGF	San Gabriel Fault
CB Coherent rocks belt (of Franciscan Complex)	SJF	San Jose-Mesa Faults
LPM Little Pine Mountain block	SYF	Santa Ynez Fault
SMB San Marcos block	WHF	West Huasna Fault
SOT Sur-Obispo terrane (includes Great Valley sequence and Coast Range ophiolite)		Syncline—Showing trace of axial plane; arrow shows direction of plunge; queried where inferred. Major synclines labeled:
ST Salinian terrane (continental magmatic arc)	HDS	Hurricane Deck syncline
SYB Santa Ynez block	LPS	Loma Prieta syncline
<u>SAF</u> Fault—Dotted where concealed. Major faults labeled:		Anticline—Showing trace of axial plane
BPF Big Pine Fault		Santa Maria River
CRF Coast Range Fault		Geologic features discussed in text
CHF Cachuma Fault	A	Ynezan orogeny of Dibble (1991) unconformity—Two locations
CUF Camuesa Fault	B	Espada Formation of Dibble (1966)—Two locations
EHF East Huasna Fault		Features discussed in text
FCF Foxen Canyon Fault	1	Blue Canyon
GF Garlock Fault	2	Foxen Canyon
HF Hildreth Fault	3	Cañada Honda Creek
HPF Hidden Potrero Fault (local part of Coast Range Fault System)	4	San Rafael Mountains
LPF Little Pine Fault	5	Santa Maria basin
OMF Old Man Fault	6	Sisquoc Canyon
PMF Pine Mountain Fault	7	Stanley Mountain
RF Rinconada Fault (Nacimiento segment) of Dibblee (1991)	8	Santa Ynez-Topa Topa Mountains
RMF Red Mountain Fault		
SAF San Andreas Fault		

ture, in Blue Canyon, lies a semi-coherent Franciscan exposure that is presumably part of the Santa Ynez block, being bounded by the Santa Ynez Fault Zone (Dibblee, 1986a). The mélangé is separated from rocks to the northeast by the nearly vertical, northwest-striking Camuesa Fault. Northeast of the Camuesa Fault lies a closely folded, thick section of the Upper Jurassic and Lower Cretaceous Espada Formation (Dibblee, 1966) and the Upper Cretaceous Cachuma Formation (Dibblee, 1991; Atascadero Formation, J.G. Vedder, oral commun., 1993). These formations have been assigned to the Great Valley sequence because they conformably overlie the Coast Range ophiolite at Stanley Mountain (Hopson and others, 1981; Vedder and others, 1989). In Cachuma Canyon (fig. 3), the Little Pine Fault branches and cuts Pleistocene rocks (Dibblee, 1993). Also in Cachuma Canyon, the Camuesa Fault deflects the east-west-striking Big Pine Fault that apparently joins the high-angle, northwest-striking Cachuma Fault here (Dibblee, 1991). The Big Pine Fault cuts the Rinconada Fault, and is itself cut by the San Andreas Fault to the east (fig. 2).

The San Rafael Mountains mélangé consists primarily of a chaotic assemblage of dismembered and mixed blocks of terrigenous rock, upper-level oceanic crust, and serpentinized mantle peridotite that are, at various scales, separated or enveloped by matrix. Matrix is commonly mudstone and (or) fine-grained serpentinite. A minor(?)

amount of matrix consists of greenstone and chert. All matrix is pervasively fractured and faulted, and all contacts between blocks and matrix are presently structural. Sparse, isolated blocks of metagraywacke, glaucophane schist, greenschist, and amphibolite are also found in the mélangé. The sandstone (graywacke) has been subjected to diagenetic alteration (Warner, 1992). Basal chert overlying greenstone (altered basalt) is Kimmeridgian and Pliensbachian in age, but the chert is as young as early Tithonian (Pessagno, 1977; Hopson and others, 1981). One late Tithonian *Buchia* (mollusk; W.P. Elder, written commun., 1992) was found in a sandstone block during mapping (pl. 1). The only known age of mudstone in the mélangé is Late Cretaceous (based on microfossils identified by J.S. Clark, in Dibblee, 1991).

In Horse Canyon near Santa Cruz Creek, the Little Pine Fault intersects the gently north-dipping Loma Alta Fault (pl. 1; fig. 3). The Loma Alta Fault bends southeastward around Loma Alta peak, where it separates thrust Miocene rocks from underlying Pleistocene rocks (Dibblee, 1987a). A probable eastern extension of the Loma Alta Fault (Schussler, 1981) locally faults a 10-km-long Franciscan coherent rocks belt located in Aliso, lower Oso, and lower Red Rock Canyons. The coherent rocks belt consists of Upper Jurassic, upper-level oceanic crust, sandstone, and shale that dips moderately northeast (Schussler, 1981) and forms a series of thin thrust sheets. A blueschist

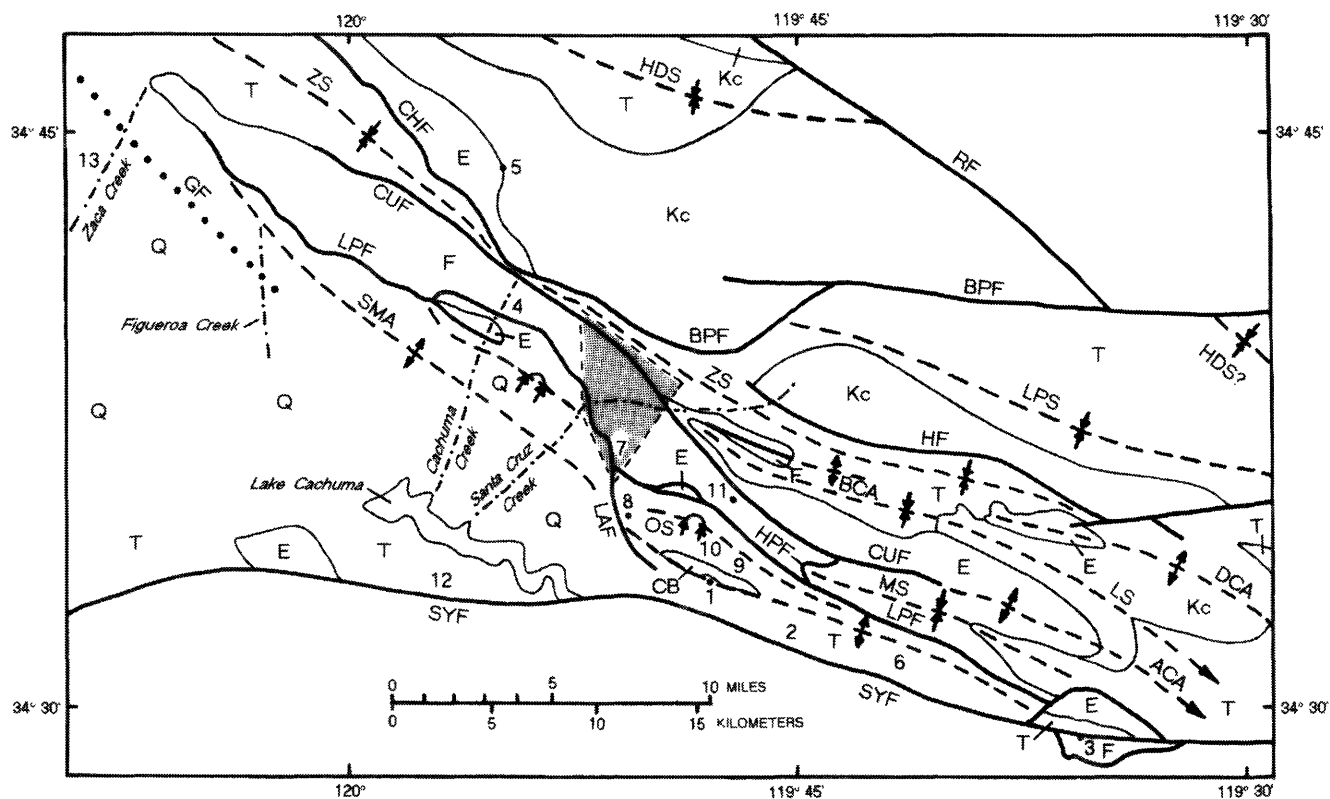


Figure 3. General geologic map of study area including folds and faults and exposed Franciscan rocks and Espada Formation (modified from Dibblee, 1991). Area of plate 1 shaded.

block is also present (A.G. Sylvester, oral commun., 1993), but serpentinite is absent. The Eocene Sierra Blanca Limestone depositionally overlies this belt and the contact is well exposed in Aliso Canyon (Dibblee, 1950).

A small exposure of Franciscan mélangé is located in the far western part of the Santa Ynez Mountains near Cañada Honda Creek where shale of the Upper Jurassic(?) or Cretaceous Honda Formation and Espada Formation crops out (Dibblee, 1950, 1982; fig. 2, loc. B). At Point Sal, 35 km north of Cañada Honda Creek, there is an excellent exposure of Coast Range ophiolite (Hopson and others, 1981), although Franciscan rocks are not exposed there.

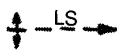
The landforms of the San Rafael Mountains mélangé generally consist of rolling hills and low mountains that are covered by tall grass and lesser amounts of chaparral and oak trees. Rounded to sharply angular mélangé blocks form outcrops of high relief, and the deflection of several creeks by erosionally resistant blocks has caused complex drainage patterns. Several large landslides are clearly present in the study area, but locally it is difficult to distinguish in-place mélangé from landslide debris.

MÉLANGE STRUCTURE

Although many of the mélangé blocks are separated by matrix, detailed mapping of the mélangé exposed along Santa Cruz Creek (fig. 3) reveals that several types of rocks form at least locally continuous, map-scale, lithologic bands (pl. 1). These bands consist of contiguous monolithic and polygenetic blocks that are separated by minor faults. The trends of these bands are roughly parallel to the strike of the matrix foliation (closely spaced cleavage consisting of anastomosing ductile shear fractures); to the strike of the high-angle, reverse and oblique-slip faults that bound the contiguous blocks; and to the strike of the bedding in the blocks. The structure of the blocks and matrix is concordant with the trends of lithologic bands, and the lithologic bands reflect the structural order present in the mélangé.

Much of the structure of the mélangé is nearly vertical. Faults, foliation, axial surfaces of folds, and bedding commonly dip steeply. Fold axes locally plunge steeply. The mélangé is a complex of tectonically arranged lithologic bands, which together with the concordant matrix

EXPLANATION

	Map unit		LS	Syncline—Arrow shows direction of plunge. Queried where inferred. Major synclines labeled:
CB	Coherent rocks belt (of Franciscan Complex)		HDS	Hurricane Deck syncline
E	Espada Formation of Dibblee (1966)		LS	Little Pine syncline
F	Franciscan Complex		LPS	Loma Prieta syncline
Kc	Cachuma Formation of Dibblee (1991)		MS	Mono syncline
Q	Quaternary rocks (general distribution)		ZS	Zaca syncline
T	Tertiary rocks			OS
<u>RF</u>	Fault—Dotted where concealed. Major faults labeled:		OS	Oso syncline
BPF	Big Pine Fault			Features discussed in text
CHF	Cachuma Fault		1	Aliso Canyon
CUF	Camuesa Fault		2	Arroyo Burro
GF	Garey Fault		3	Blue Canyon
HF	Hildreth Fault		4	Cachuma Canyon
HPF	Hidden Potrero Fault (local part of Coast Range Fault System)		5	Cachuma Peak
LAF	Loma Alta Fault		6	Devils Canyon
LPF	Little Pine Fault		7	Horse Canyon
RF	Rinconada Fault (Nacimiento segment) of Dibblee (1991)		8	Loma Alta
SYF	Santa Ynez Fault		9	Lower Oso Canyon
	Fold—Showing trace of axial plane		10	Lower Red Rock Canyon
	SMA	Anticline—Arrow shows direction of plunge. Major anticlines labeled:	11	Red Rock
ACA	Auga Caliente anticline		12	Tequepis Canyon
BCA	Buckhorn Creek anticline		13	Zaca Canyon
DCA	Diablo Canyon anticline			
SMA	San Marcos anticline			

foliation and a block-shape foliation, form a map-scale "shear foliation" that has the appearance of a crude flow structure. The abundance and near-vertical structure of serpentinite, combined with its tectonic envelopment of overlying blocks that include blueschist, indicate that a thick, regionally extensive body of serpentinite lies at the structural base of the *mélange*. The presence of upright and steeply inclined, tightly folded chert and greenstone beds, combined with the presence of opposite-facing chert that lies along the margins of several greenstone blocks, indicate that map-scale folding, rather than mere thrusting alone, caused the repetition of chert and greenstone across the *mélange* belt.

Serpentinite forms the most extensive bands in the *mélange*. These tectonic bands of serpentinite cut those of chert and greenstone, and presumably cut the foliation of the Upper Cretaceous(?) mudstone matrix. Considering the relict igneous texture, the abundance, and the upward mobility of serpentinite, the trace amount of sedimentary serpentinite found in sandstone was most likely derived from a minor (Jurassic?, Cretaceous?) source, and the abundant serpentinite in the *mélange* was emplaced by (Cenozoic) tectonism. The structure of the serpentinite clearly indicates that it was squeezed-up and injected along high-angle shear fractures and reverse faults in the *mélange*, at least during Quaternary time. The serpentinite bands, in contrast to the chert and greenstone bands, are not truncated by the Little Pine and Camuesa Faults (pl. 1). The serpentinite bands within the *mélange* become the serpentinite bands that follow the traces of these two faults. This serpentinite tectonism occurred during or after initial displacement on the Little Pine and Camuesa Faults. The local Quaternary reverse slip on the Little Pine Fault conclusively indicates that the tectonic emplacement of the major serpentinite bands within the *mélange* is related to crustal shortening during Quaternary (Pleistocene) time (Warner, 1992, pl. 1; pl. 1).

Lithologic study, detailed mapping, and structural observations reveal a stratigraphic and structural order in the *mélange* (Wahl, 1995). The *mélange* apparently developed in place, when coherent, undeformed greenstone, chert, and terrigenous rocks were being deformed into map-scale, upright folds (fig. 4). Continued horizontal shortening vertically extruded all of these rocks on conjugate and anastomosing, high-angle reverse faults that cut the folds. The principal direction of horizontal shortening roughly bisects the obtuse angle between the conjugate faults in greenstone blocks, which is opposite to that seen in brittle faulting. These structures have geometric and kinematic properties that are found in known contractional, vertical, brittle-ductile shear zones (Ramsay and Huber, 1987). The shortened serpentinite basement was ductily deformed and squeezed-up into the overlying rocks along high-angle shear fractures and faults in the *mélange* (figs. 4, 5).

The initial folding and faulting to form the *mélange* occurred during Late Cretaceous time (see below, Hidden Potrero Fault). Plate convergence may have been directed slightly(?) oblique to the strike of the structure at this time to form doubly plunging folds and anastomosing, high-angle reverse faults. Before or during this tectonism, however, regional thrusting is inferred to have juxtaposed the coherent upper crust with contractionally uplifted metamorphic rocks (for example, Wahl, 1995, pls. 3a–5; also see below, Coherent Rocks Belt), which suggests high-angle convergence. The *mélange* itself has not been subjected to large-scale, strike-slip faulting on the basis of sedimentary and other rock-type distributions (Warner, 1992). Later regional thrusting during latest Cretaceous and Paleocene time (see below) further suggests that convergence was directed approximately perpendicular to the strike of the structure during all of Late Cretaceous time. Middle to late Cenozoic deformation includes high-angle, reverse and oblique-slip faulting, and the injection of much serpentinite, which complicated the polyphase structure of the *mélange*. Considering the apparent distension of the structure along strike (pl. 1), the direction of convergence was probably oblique during this time.

HIDDEN POTRERO FAULT

The Hidden Potrero Fault is a low-angle fault that is exposed between the Camuesa and Little Pine Faults along the Camuesa Ridge fire road, 0.5 km west of Hidden Potrero (Dibblee, 1986b, mapped as depositional contact; fig. 3). This fault separates the *mélange* from the overlying Espada Formation. Displacement on the Hidden Potrero Fault postdates most of the tectonism that formed the *mélange*, because most of the steeply dipping structures of the *mélange* are truncated by this low-angle fault; however, the bands of serpentinite are a major exception.

The age of the Hidden Potrero Fault is presumably Paleocene. Its maximum age is inferred to be Paleocene, because the Cachuma Formation (Upper Cretaceous) unconformably overlies the Espada Formation without angular discordance (J.G. Vedder, oral commun., 1993; T.W. Dibblee, Jr., oral commun., 1994). It is clear that the faulting took place before Eocene time because the Eocene Sierra Blanca Limestone that is located on the southeast side of Cachuma Canyon and surrounded by a splay of the Little Pine Fault (Dibblee, 1993) depositionally overlies both the *mélange* and a small exposure of moderately dipping, well-bedded Espada Shale (Dibblee, 1993, mapped as Franciscan Shale). Furthermore, in Cachuma Canyon, the adjacent, large block composed of the Espada Formation overlies this *mélange* of undoubted Franciscan rocks along a low-angle fault (Dibblee, 1993, mapped as depositional contact), without any intervening Eocene strata. The

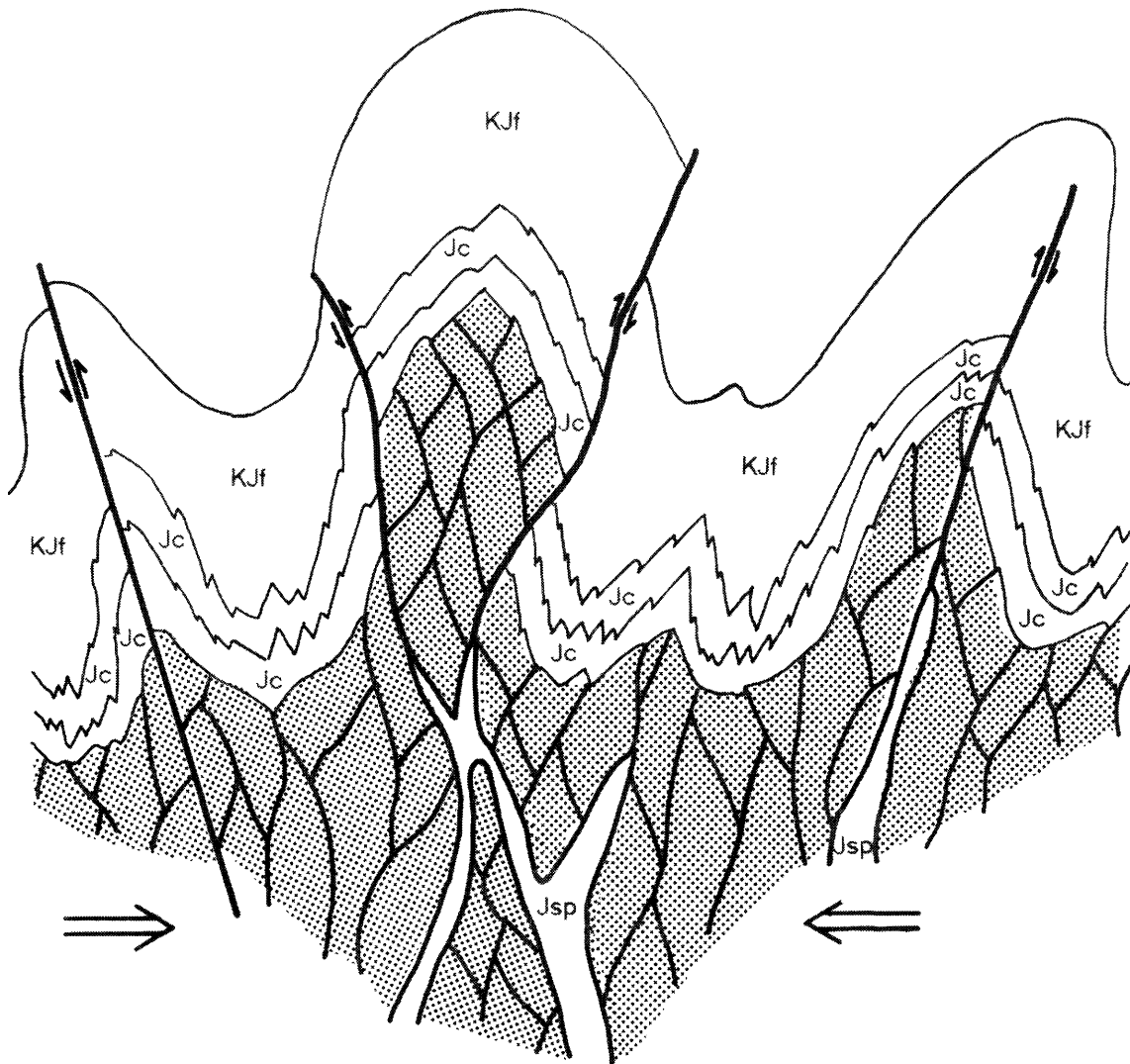
Sierra Blanca Limestone commonly contains Franciscan-derived detritus.

The Hidden Potrero Fault presently is a northeast-dipping thrust fault. Displacement on the Hidden Potrero Fault resulted in the removal of the basal (Jurassic) Espada Formation and its underlying Coast Range ophiolite stratigraphic basement, and accounts for the presence of unshered blocks composed of the Cretaceous section of the Espada Formation and mélangé in the Little Pine Fault Zone. The unshered blocks are klippen that have since been folded, faulted, and eroded; they thus reflect the later

Tertiary deformational history of the mélangé. Judging from its trace, the Hidden Potrero Fault has been slightly folded by vertical displacements associated with the mélangé and the Little Pine and Camuesa Faults.

COAST RANGE FAULT

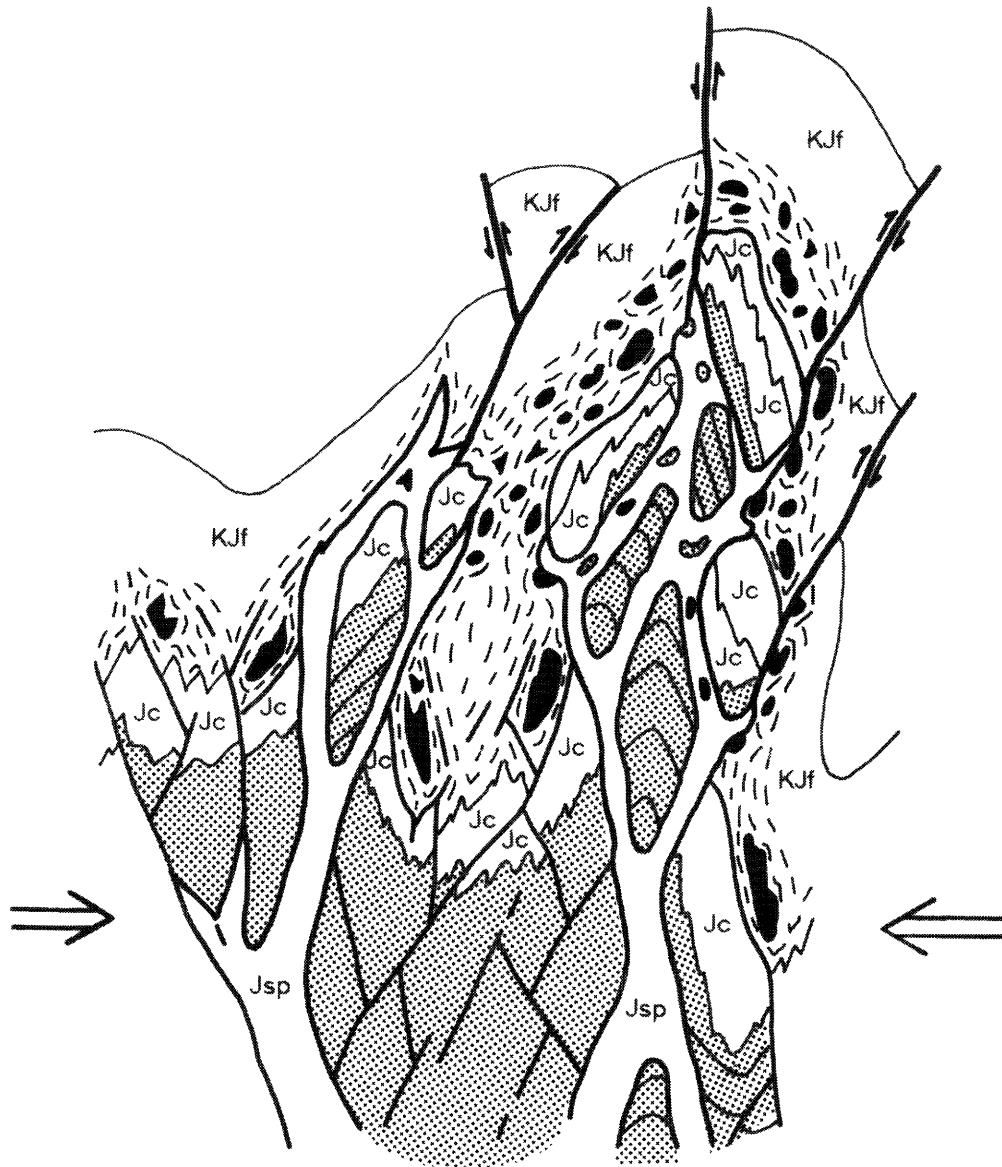
The mélangé was thrust beneath the Espada Formation along the Hidden Potrero Fault during Paleocene time. This fault is part of the Coast Range Fault System, on the



EXPLANATION

- KJf Terrigenous rocks (Early Cretaceous and Late Jurassic)
- Jc Chert (Late to Early Jurassic)
-  Greenstone (Early Jurassic)
- Jsp Serpentinite (Jurassic)
-  Fault—Arrows indicate direction of relative movement
-  Direction of compressional force

Figure 4. Schematic cross section of mélangé structure during early phase (Late Cretaceous) deformation. Coherent oceanic crust and overlying terrigenous rocks are deformed into map-scale, upright folds. Minor injection of serpentinite is shown along conjugate and anastomosing, high-angle reverse faults and ductile shear fractures in greenstone. Section is simplified by omission of possible low-angle faulting and interbedded chert and greenstone.



EXPLANATION

- | | |
|---|---|
| KJf | Terrigenous rocks (Early Cretaceous and Late Jurassic)—Includes matrix, shown with foliation (short dashes) and chert fragments (black) |
| Jc | Chert (Late to Early Jurassic) |
|  | Greenstone (Early Jurassic)—Some blocks show layering (parallel-line pattern) |
| Jsp | Serpentinite (Jurassic)—Includes matrix (Cretaceous?) (foliation not shown) |
|  | Fault—Arrows indicate direction of relative movement |
|  | Direction of compressional force |

Figure 5. Schematic cross section of mélangé structure at present. Section includes chert fragments, anastomosing and conjugate faults, and the injection of serpentinite along high-angle, ductile shear fractures and reverse faults. Section is simplified by omission of possible Campanian(?) sedimentary mélangé and low-angle Paleocene(?) faulting.

basis of the ages and types of rocks it displaces and on its shallow dip, age, and location (Bailey and others, 1970; Page, 1981; figs. 1–3), although the Coast Range ophiolite is absent along its trace. Farther north, the Sur-Nacimiento Fault Zone separates the Franciscan basement of the Sur-Obispo terrane from the continental margin-magmatic arc basement of the Salinian terrane. Parts of the Salinian terrane are surrounded by *mélange* near Point Sur, as are parts of the Coast Range ophiolite and the Great Valley sequence (Hall, 1991). In contrast, the trace of the Rinconada Fault is roughly linear (Dibblee, 1976, 1991), which suggests that the Sur-Obispo and Salinian terranes were juxtaposed, at least in part, by strike-slip faulting (fig. 1).

Considering the contractional nature of the Sur-Nacimiento Fault Zone during Paleocene time, as proposed by Page (1970, 1972, 1981) and Hall (1991), the joining of the Sur-Obispo and Salinian terranes is primarily related to the development of the Coast Range Fault. The Coast Range Fault is located east of the Salinian terrane in the Diablo Range where the Great Valley sequence structurally overlies the Franciscan Complex (Bailey and others, 1970; fig. 1). This fault is truncated by the San Andreas Fault to the south, which strongly suggests that this part of the Coast Range Fault was joined along strike to the Sur-Nacimiento Fault Zone. Apparently, most of the Sur-Obispo terrane was west of the Salinian terrane during Late Cretaceous time. The two terranes were then juxtaposed by thrusting along the Coast Range Fault during Paleocene time (or possibly earlier, by transform faulting during Late Cretaceous time, Vedder and others, 1983). Lateral and vertical displacement along the Sur-Nacimiento Fault Zone (and the Rinconada Fault) may have cut the thrust structure and, therefore, that displacement is younger than middle Eocene and unrelated to the Coast Range Fault. The Coast Range ophiolite and Great Valley sequence evidently were being thrust beneath the Salinian terrane while Franciscan *mélange* was being thrust beneath both the forearc and the continental margin-arc terrane.

COHERENT ROCKS BELT

The coherent rocks belt of the Franciscan Complex is exposed in lower Oso, lower Red Rock, and Aliso Canyons (fig. 3). The geologic history of this orderly belt may indirectly reveal more about the Mesozoic history of the *mélange*. The coherent rocks belt is also noteworthy because of its late Eocene or early Oligocene to Quaternary structure (see below, Oso Syncline).

During Late Cretaceous time, prior to the structural imbrication of the coherent rocks belt, the terrigenous section was thinned, presumably by erosion. Additionally, serpentinite and crustal ultramafic rocks are absent from this belt, as are plutonic and intrusive rocks that are comagmatic with its greenstone. The abyssal rocks that

were originally present in this belt were structurally removed by subduction before(?) imbrication.

The thrust sheets of the coherent rocks belt dip moderately, in contrast to the near-vertical structures of the *mélange*, although *mélange* bearing blueschist is believed to partially underlie and envelope this belt. After its thinning and imbrication, the coherent rocks belt was thrust southwestward, with respect to its present orientation, over blueschist-bearing *mélange* that did not contain serpentinite. In this account, post-imbricational thrusting took place during Paleocene time when the presently exposed *mélange* was thrust beneath the Espada Formation along the Hidden Potrero Fault (Alisan orogeny of Dibblee, 1991; table 2). During Late Cretaceous and Paleocene time, the *mélange* and the coherent rocks belt were apparently evolving together as a fold and thrust belt. The folds were faulted to form tectonic *mélange* that was then thrust beneath the coherent rocks (thrust) belt and the Espada Formation.

The specific fault that juxtaposed the coherent rocks belt with the Espada Formation before and (or) during the Paleocene regional thrusting is not precisely known, but it is thought to be related to the contractional detachment faults that separated these terranes from their respective basements during Late Cretaceous time (fig. 6; assuming the paleogeography presented above). Thrusting on a Coast Range Fault, however, cannot easily explain the presence of the Espada Formation along the north side of the Santa Ynez Fault near Lake Cachuma (Dibblee, 1987b; loc. B in fig. 2, fig. 3), because the Espada Formation may not have been thrust over the coherent rocks belt south of the Oso syncline (fig. 3). A similar condition exists between the Franciscan *mélange*, the overlying Coast Range ophiolite, and the Espada Formation at Stanley Mountain (Brown, 1968; Vedder and others, 1989), and the Coast Range ophiolite at Point Sal (fig. 2). At Stanley Mountain, the Coast Range ophiolite only overlies the *mélange* on its northeast side, whereas Cretaceous strata of the Espada Formation overlie the *mélange* on its southwest side. Southwest displacement by thrusting, therefore, does not easily account for the presence of the Coast Range ophiolite at Point Sal. Alternatively, it may be that strike-slip faulting of the San Marcos block displaced the fragments of the Coast Range ophiolite and Espada Formation into their outboard position. Near Cañada Honda Creek, pervasively fractured and faulted Honda shale and unshaped Espada shale overlie Franciscan *mélange* (Dibblee, 1950; 1982; fig. 2, loc. B); presumably, these rocks were originally juxtaposed along a Coast Range Fault as well. Paleocene(?) strike-slip faulting may have occurred after thrusting, and, in this case, plate convergence apparently was oblique.

An exposure of semi-coherent Franciscan rocks is located at Blue Canyon (fig. 3). These Franciscan rocks may have been rotated with the other rocks of the Santa Ynez block (for example, Luyendyk and others, 1985), includ-

ing the batholithic(?) rocks exposed on Santa Cruz Island (Gordon and Weigand, 1994; fig. 1). The contact between these Franciscan rocks and the overlying, uppermost Cretaceous strata to the south may be an unconformity in the subsurface. If so, then the Espada Formation is not present on the Santa Ynez block, at least locally. Furthermore, these uppermost Cretaceous strata overlying Franciscan rocks may correlate with the uppermost Cretaceous strata that overlie Salinian crystalline basement (Vedder and others, 1983). Alternatively, the subsurface contact may be a Coast Range Fault. In either case, a major fault (Paleocene and (or) Late Cretaceous faulting) apparently separates these undoubted Franciscan rocks from the nearby batholithic rocks on Santa Cruz Island. Considering these uncertainties, the specific paleogeography of the basement rocks of the Little Pine Mountain block relative to the San Marcos block and the Santa Ynez block during Paleocene time is not well known.

OSO SYNCLINE

After Paleocene tectonism, a thick sequence of lower and middle Eocene strata was deposited on the mélange and on an erosionally and tectonically thinned klippe of the Espada Formation and the coherent rocks belt. Before the deposition of the coarse sediments of the upper middle Eocene to lower Miocene Sespe Formation (Vedder, 1972; Howard, 1987, 1995, locally upper Oligocene, possibly lower Miocene at Loma Alta), the mélange was uplifted and most of the overlying Eocene sequence was eroded. Only a small part of this sequence is preserved in Cachuma Canyon (Dibblee, 1993; fig. 3). Fortunately, a nearly complete section of pre-late Eocene rocks is found in the Oso syncline where it depositionally overlies the coherent rocks belt with an angular unconformity of about 25° (Schussler, 1981; figs. 3, 7).

Table 2. Correlation of rock units and events. All rock units and structural and orogenic events described by Dibblee (1991) except where otherwise noted. References: 1, Ages in parentheses are uncertain; 2, Thomas and others (1988); 3, Howard (1995); 4, Hopson and others (1981); 5, Bailey and others (1964); 6, Hall (1981); 7, Atwater (1989); 8, Luyendyk and others (1985)

Age			Unit	Structure	Orogeny	Plate boundary type		Comments
Ma ¹	Period	Epoch				Transform ⁷	Transpression	
0.01	Quaternary	Holocene	Alluvium	Loma Alta fault	Late Coast Range	Transform ⁷	Transpression	Major serpentinite
1.65		Pleistocene	Paso Robles Fm					
	Tertiary	Pliocene	Careaga Ss	Garey fault ⁶ ; San Marcos anticline	Early Coast Range	Transform ⁷	Transpression	San Rafael Mts uplifted
5			Tequepis Fm					
(11)		Miocene	Monterey Fm	Volcanism Reactivated Oso syncline	Rafaelian	Transform ⁷	Transpression	Local deformation involving mélange
		Hurricane Deck Fm ²						
(20)		Early	Rincon Fm	Oso syncline: Hurricane Deck syncline; Little Pine fault	Lompocan (ended)	Oblique	Transpression	Begin rotation of Transverse Ranges ⁸
24		Vaqueros Fm						
(30)		Oligocene	Sespe Fm ³	Oso syncline: Hurricane Deck syncline; Little Pine fault	Ynezan (ended)	Oblique	Transpression	Regional angular unconformity
38		Eocene	Coldwater Ss, Cozy Del Sh, Matilija Ss, Juncal Fm.					
(50)		Paleocene	Sierra Blanca Ls	Hidden Potrero fault (Coast Range fault)	Alisan	Convergent (high angle?)	Transpression	Reactivation of mélange structures; serpentinite(?); regional angular unconformity
55			undivided					
66	Cretaceous	Late	Cachuma Fm	Folding, high-angle faulting Low-angle faulting	Larimide ⁷	Convergent (high angle?)	Transpression	Truncation of mélange structure
96		Early	Espada Fm					
138	Jurassic		Coast Range Ophiolite ⁴					Mélangé formation Separation from abyssal crust; blueschist uplift; lessening of subduction zone dip ⁷

The axis of the locally recumbent, southwest-verging Oso syncline lies between, and parallel to, the Little Pine Fault Zone and the presently exposed coherent rocks belt in lower Red Rock Canyon. On the north limb of the syncline, steeply dipping Eocene beds lie beneath the unconformable, gently folded Sespe Formation and younger strata. The south limb of the syncline dips moderately northeast, with one exception near Loma Alta where the Eocene Sierra Blanca Limestone is vertically dipping beneath unconformable, gently dipping Sespe Formation (Schussler, 1981, pl. 1). On the overturned north limb, pieces of Franciscan float rest on gently dipping, overturned Sierra Blanca Limestone. This float was presumably derived from overturned beds of the coherent rocks belt.

A block composed of Lower Cretaceous strata (Schussler, 1981) of the Espada Formation lies in the Little Pine Fault Zone and structurally overlies the overturned limb

of the Oso syncline. This isolated block composed of the Espada Formation is enveloped by Franciscan mélangé containing blueschist and serpentinite. The Paleocene Hidden Potrero Fault evidently separates this block in the subsurface from the underlying mélangé. A Paleocene basal thrust fault is inferred to underlie the coherent rocks belt in the subsurface as well, separating it from locally underlying mélangé that does not contain serpentinite (fig. 7).

In summary, both the coherent rocks belt and the Espada Formation were contractionally detached from their respective basements during Late Cretaceous time, thrust over tectonic mélangé as a result of Paleocene diastrophism, and then covered by the Sierra Blanca Limestone during Eocene time. The coherent rocks belt and the Espada Formation were, in this case, roughly adjacent and at approximately the same structural level before the develop-

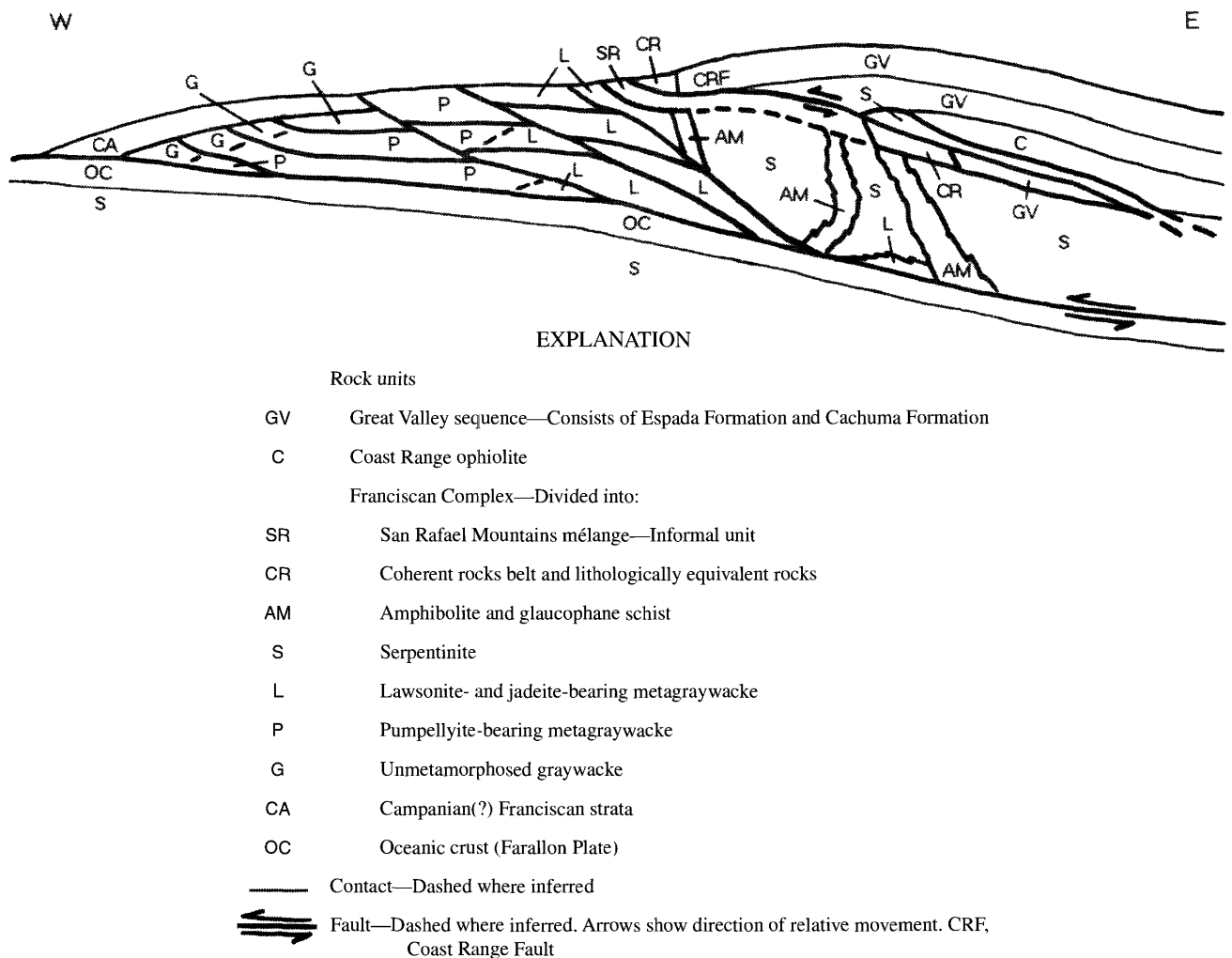


Figure 6. General tectonic cross section of study-area region during Paleocene time after thrusting of mélangé beneath coherent rocks belt and Espada Formation along the Coast Range Fault. Serpentinite including minor metamorphic rock generally underlies mélangé.

ment of the Oso syncline and the Little Pine Fault. During late Eocene or early Oligocene time, the Oso syncline formed as the pre-late Eocene sequence and the underlying coherent rocks belt were folded almost to their present structure (Ynezan orogeny of Dibblee, 1991; table 2). The syncline formed as a result of crustal shortening that is related to the folding of the coherent rocks belt beneath the Espada Formation. This origin is indicated because this locally recumbent, southwest-verging fold lies structurally beneath the southwest-thrusted block composed of the Espada Formation.

The geometry and kinematics of the Oso syncline suggest a change in tectonic style from Late Cretaceous and Paleocene thrusting to late Eocene or early Oligocene folding and high-angle, reverse faulting. The presence of the structurally overlying Espada Formation above the overturned limb of this fold suggests that the Little Pine Fault originated as a result of Ynezan tectonism. Ynezan tectonism apparently must have reformed the mélangé, considering the amount of shortening indicated by the Oso syncline, combined with the propensity of the mélangé,

with its weak serpentinite basement and inherited Cretaceous structure, to be squeezed upward. As a result, the pre-late Eocene rocks overlying the mélangé were uplifted and mostly eroded, whereas the pre-late Eocene rocks in the Oso syncline were preserved.

Angular unconformities that may reflect Ynezan tectonism are found at two other locations in the region. Along the northeast side of the Rinconada Fault, near Stanley Mountain (fig. 2, loc. A), redbeds of Oligocene(?) strata overlie strata of Paleocene(?) to Eocene age with an angular unconformity of 70° (Vedder and Brown, 1968). Farther southeast, the Rinconada Fault is offset by the Big Pine Fault, and continues southeast as the Pine Mountain Fault (Vedder and Brown, 1968). Near the junction of the Big Pine and Pine Mountain Faults (fig. 2, loc. A), Oligocene rocks overlie synclinally folded Eocene rocks with an angular unconformity of about 25° (estimated from Dibblee, 1991, fig. 9, section J-K). On the basis of its age, asymmetry, and proximity to the Pine Mountain Fault, the tectonic history of this syncline may be broadly analogous to that of the Oso syncline, although this syncline appears

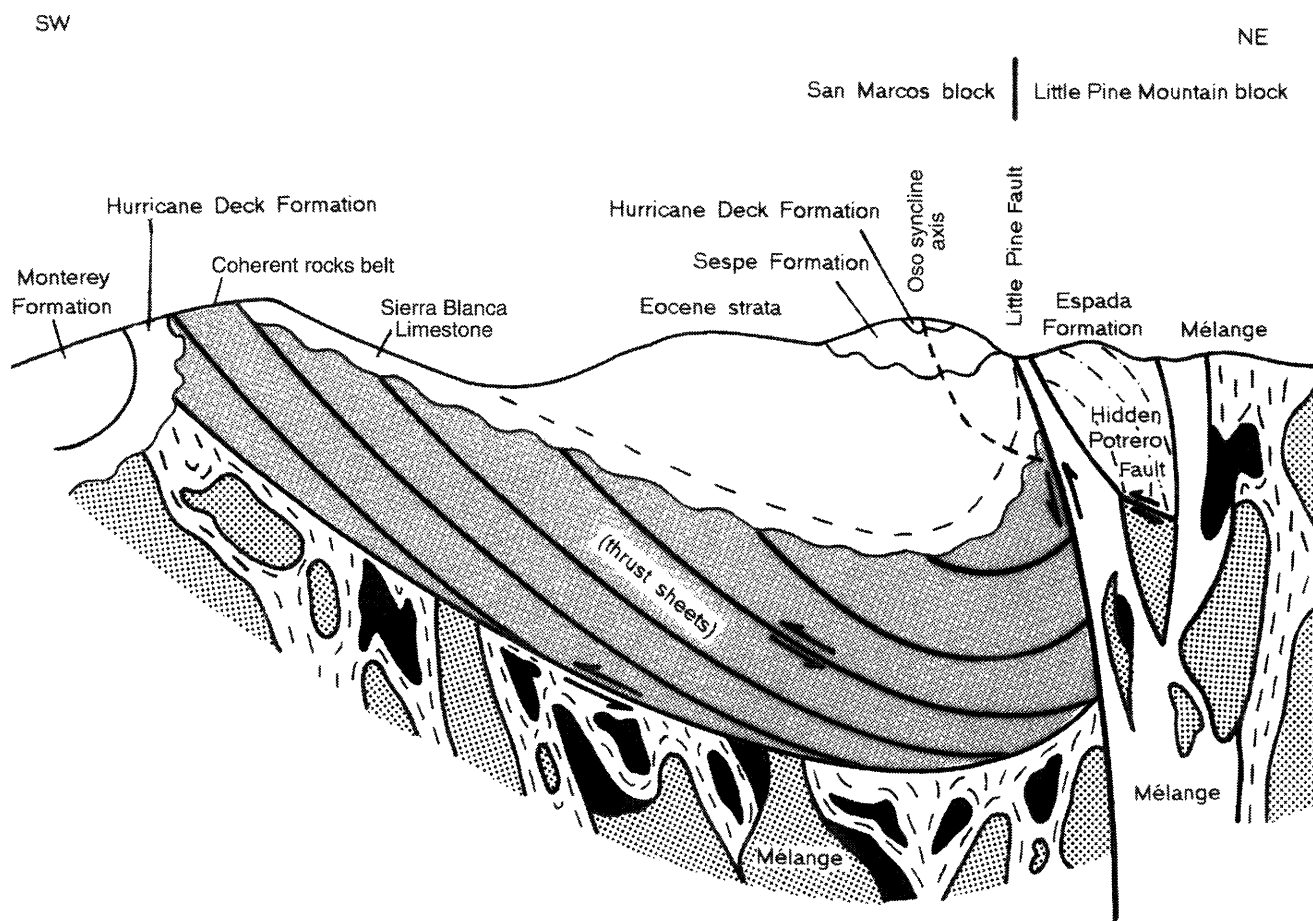


Figure 7. Schematic cross section of Oso syncline showing pre- and post-Sespe Formation unconformities and basal thrust faults that lie beneath coherent rocks belt of the Franciscan Complex and Espada Formation (modified from Schussler, 1981).

likely be a right-step of the Hurricane Deck syncline (see below, Late Cenozoic History).

During late Oligocene time, coarse sediments of the Sespe Formation that included much Franciscan-derived detritus were deposited on the deformed, pre-late Eocene rocks that overlie the coherent rocks belt in the Oso syncline. These sediments were deposited directly on the coherent rocks belt where the pre-late Eocene rocks were completely eroded (Dibblee, 1987a), and probably on mélangé as well. During early Miocene time, the coherent rocks belt and the mélangé were uplifted (see below, Late Cenozoic History). The Sespe Formation was then eroded off most of the presently exposed coherent rocks belt, but it is found along the axis of the Oso syncline overlying the pre-late Eocene rocks. This distribution of the Sespe Formation suggests renewed folding of the Oso syncline and further contractional deformation and uplift of the coherent rocks belt and the mélangé (Lompocan orogeny of Dibblee, 1991).

The Sespe Formation is absent on much of the San Marcos block (Hall, 1981; T.W. Dibblee, Jr., oral commun., 1993), either through erosion or nondeposition, with the Oso syncline area being one exception. The Sespe Formation is also present on the San Marcos block from Arroyo Burro to Devils Canyon, near the Oso syncline (Dibblee, 1986b, 1987a; fig. 3), and in Tequepis Canyon, near Lake Cachuma (Dibblee, 1987b; fig. 3). At these two localities, north-dipping Sespe Formation including conglomerate overlies Eocene sandstone, and underlies the upper Oligocene to lower Miocene Vaqueros Formation and the lower Miocene Rincon Formation (Dibblee, 1991) to form part of a conformable, Eocene-Oligocene-Miocene sequence (Dibblee, 1986b, 1987a, b; table 2). This sharp contrast in Oligocene stratigraphy between the Oso syncline and Devils Canyon areas indicates that the Devils Canyon area received a thick, conformable layer of Eocene to Miocene sediment both during and after the initial formation of the Oso syncline. Although this difference in stratigraphy suggests that a major fault separates the Oso syncline from the Devils Canyon area, none was found.

The Devils Canyon area evidently was synclinally down-buckled as the Oso syncline formed during Ynezian contraction. Renewed folding and faulting related to Lompocan tectonism further uplifted the coherent rocks belt and the mélangé. As a result, the Sespe Formation was eroded off most of the coherent rocks belt that is presently exposed, and off mélangé wherever it may have been present. Sand of the lower and middle Miocene Hurricane Deck Formation (Thomas and others, 1988) was then deposited unconformably (in agreement with Dibblee, 1966, cross section; Dibblee, 1987a; contrast, Dibblee, 1966, text; Schussler, 1981; Howard, 1995) on gently folded Sespe Formation in the Oso syncline area, and conformably on the Vaqueros Formation and the Rincon Formation in the Devils Canyon area.

LATE CENOZOIC HISTORY

Sand of the lower and middle Miocene Hurricane Deck Formation (Thomas and others, 1988) was deposited on the coherent rocks belt and mélangé of the Franciscan Complex. Basalt contemporaneous with vitric tuff of the Obispo Formation (Hall and others, 1979) locally overlies the Hurricane Deck Formation, prevalently along the Little Pine Fault northwest from Cachuma Canyon and along this trend to the Santa Maria River (Hall, 1981; Dibblee, 1991; fig. 2). Also, the abundance of serpentinite in the mélangé increases significantly northwest of Cachuma Canyon (Hall, 1981; Dibblee, 1993). A minor exposure of basalt lies in the upper part of Santa Cruz Creek (on the north side of the Hildreth Fault in Black Canyon, Dibblee, 1991). The Hurricane Deck Formation contains Franciscan-derived detritus (Dibblee, 1993).

The Hurricane Deck Formation is thickest (1,180 m, Dibblee, 1991) in the Hurricane Deck syncline (fig. 3), where it conformably overlies the Rincon Formation. In sharp contrast, the Hurricane Deck Formation is very thin (about 50 m, pl. 1) along the margins of the presently exposed mélangé. The Hurricane Deck Formation is locally missing in Cachuma Canyon where the Monterey Formation (Dibblee, 1989) depositionally(?) overlies the mélangé (Dibblee, 1993), and to the southeast in the Mono syncline and the Diablo Canyon anticline where the Monterey Formation overlies the Espada Formation (Dibblee, 1986b; fig. 3). Furthermore, the Hurricane Deck Formation is mostly missing on the San Marcos block (Dibblee, 1995), except for a few places near Lake Cachuma. In Devils Canyon, the Hurricane Deck Formation is about 200 m thick, and in Tequepis Canyon it is about 50 m thick (fig. 3). In both of these canyons, the Hurricane Deck Formation conformably overlies the Rincon Formation (Dibblee, 1986b, 1987a, b). The Hurricane Deck Formation is also present in the Oso syncline (about 50 m thick) and 2 km west of Blue Canyon where the Santa Ynez Fault and the Little Pine Fault merge (Dibblee, 1986a); however, in these two areas the Hurricane Deck Formation depositionally overlies the Sespe Formation without intervening Vaqueros Formation and (or) Rincon Formation.

The thinness or absence of the Hurricane Deck Formation in the southwestern foothills of the San Rafael Mountains suggests that this area was uplifted and eroded to low relief during early Miocene time. Much of the San Marcos block was evidently uplifted and eroded to expose Franciscan basement during the time that sand of the Hurricane Deck Formation was being deposited in the Devils Canyon area. Additionally, the presence of shale of the Rincon Formation in the Hurricane Deck syncline and at Hells Half Acre (2 km northeast of the mélangé belt, near Cachuma Peak, fig. 3) suggests regional submergence prior to the deposition of sand of the Hurricane Deck Formation. The Rincon Formation directly overlies the Cachuma

Formation locally at Hells Half Acre (T.W. Dibblee, Jr., unpub. map, San Rafael Mountain quadrangle). At the least, the *mélange* belt must have been covered by the Vaqueros Formation during the deposition of fine-grained sediments of the Rincon Formation because Franciscan-derived detritus reportedly has not been found in the Rincon Formation. Locally, the Sespe Formation probably covered the *mélange* as well. During early Miocene time, much of the Little Pine Mountain block and the San Marcos block apparently emerged as renewed folding of the Oso syncline occurred and the Rincon-Vaqueros-Sespe(?) sequence was eroded to expose uplifted *mélange*. Subsequently, during resubmergence, sand of the Hurricane Deck Formation unconformably covered the *mélange* belt, the coherent rocks belt, and the Sespe Formation located in the Oso syncline and near Blue Canyon; however, sand of the Hurricane Deck Formation conformably covered the Rincon sediments at Devils Canyon, Tequepis Canyon, and at Hurricane Deck. The absence of the Hurricane Deck Formation on much of the San Marcos block and, locally, in the southeastern San Rafael Mountains suggests that these areas remained elevated until middle Miocene time. The Devils Canyon area, in this case, was synclinally downbuckled as the Oso syncline reformed during Lompocan contraction.

The regionally extensive middle Miocene Monterey Formation conformably overlies the Hurricane Deck Formation in most of the San Rafael Mountains (Dibblee, 1989, 1991). Locally in the southeastern San Rafael Mountains and on much of the San Marcos block, the Monterey Formation overlies Mesozoic rocks. The Monterey Formation conformably overlies the Hurricane Deck Formation in Devils Canyon and in Tequepis Canyon (Dibblee, 1986b, 1987b). In contrast, the Monterey Formation conformably overlies the Rincon Formation in the Ventura-Santa Barbara basin (12 km south), except in the lower Piru Creek drainage, where the upper Monterey Formation abruptly onlaps deformed Rincon Formation and the plutonic basement complex (Dibblee, 1989).

The Monterey Formation is about 600 m thick in the study area (pl. 1), but more regionally its thickness significantly increases northward from the Santa Maria basin (630–1,100 m, Hall, 1978) to the San Rafael Mountains (1,500 m, Dibblee, 1991). In comparison, the Monterey Formation is about 800 m thick on most of the onshore Santa Ynez block, except where it thickens eastward near Lake Piru to 1,700 m (Dibblee, 1982; fig. 2).

The eastward thickening of the Monterey Formation reflects increasing sand content and proximity to land (L.E. Tennyson, written commun., 1996); the middle Miocene sea apparently transgressed rapidly eastward across the shelf that formed after much of the San Marcos block and the Little Pine Mountain block were uplifted and eroded to low relief during early Miocene time. Although the local absence of the Hurricane Deck Formation in the south-

eastern San Rafael Mountains suggests that this area persisted as a topographic high after Lompocan tectonism ended, it may also be possible that this area was rejuvenated during deposition of the fine-grained sediments of the lower part of the Monterey Formation. In either case, Monterey sedimentation ended when Franciscan basement that is located specifically in the area of the Little Pine Fault was uplifted during late Miocene time (Rafaelan orogeny, Dibblee, 1991; table 2).

Evidence for Rafaelan tectonism is based on the distribution of the upper Miocene and lower Pliocene Sisquoc Formation (Dibblee, 1991). Regionally, shale of the Sisquoc Formation conformably overlies the Monterey Formation. Locally, the basal Sisquoc Formation is a shallow marine sandstone that unconformably overlies exposed *mélange* near Zaca Canyon (Hall, 1981; Dibblee, 1991; fig. 3). In the subsurface, the Sisquoc Formation unconformably overlies previously folded(?) rocks of the Monterey Formation and basement rocks from the upper part of Foxen Canyon southeastward to Figueroa Creek, along the trend of the combined Little Pine-Foxen Canyon Fault Zone, the San Marcos anticline, and the Garey Fault (Hall, 1981; Dibblee, 1991; figs. 2, 3). The Sisquoc Formation contains Monterey-derived detritus (Hall, 1981), but reportedly no Franciscan-derived detritus (Dibblee, 1991). In contrast, the basal section of the upper Miocene to upper Pliocene Pismo Formation near San Luis Obispo contains Franciscan-derived detritus, including a significant amount of serpentinite (Hall and others, 1979).

As a result of Rafaelan(?) tectonism, the Monterey Formation was gently folded to initially form the San Marcos anticline and was uplifted on the Garey Fault and the Little Pine-Foxen Canyon Fault Zone. The deformed Monterey Formation was then deeply eroded near Zaca Canyon to expose the *mélange* locally before sediments of the Sisquoc Formation were deposited. In contrast, all(?) of the Monterey Formation is preserved in the lower parts of Sisquoc and Foxen canyons and near Lake Cachuma. This difference in upper Miocene to lower Pliocene stratigraphy along the combined Little Pine-Foxen Canyon Fault Zone, the San Marcos anticline, and the Garey Fault suggests that the faults were strike- or oblique-slip faults (Hall, 1981). The Garey Fault and the combined Little Pine-Foxen Canyon Fault Zone apparently formed as a set of left-stepping, oblique-slip faults under the San Marcos anticline, and other older anticlines that existed along this zone during this time. These older anticlines include the Agua Caliente and Diablo Canyon anticlines, and the breached (Ynezan) anticline that presumably existed between the Mono and Oso synclines (fig. 3). In this case, these faults and their associated folds reflect transpression that had a right-lateral component of displacement (Reading, 1980). In addition, high-angle faults in the *mélange* were reactivated at this time.

The Tequepis Formation is a nearshore, shallow-marine sandstone that is coeval with the Sisquoc Formation and lies exposed on the San Marcos block near Lake Cachuma (Dibblee, 1987a, b, 1995). In Tequepis Canyon, the Tequepis Formation is intercalated with the Sisquoc Formation and together they conformably overlie the Monterey Formation. Near the upper part of Santa Cruz Creek, the Tequepis Formation conformably overlies the Monterey Formation (pl. 1). The sandstone of the Tequepis Formation along with shale of the Sisquoc Formation indicate westward retreat of the sea.

During Pliocene time, sand of the Careaga Sandstone, which contains Franciscan-derived detritus, was deposited unconformably on the locally folded Sisquoc and Tequepis Formations and also on the Monterey Formation, the Espada Formation, and the *mélange* in the Little Pine Fault Zone (Dibblee, 1991, 1993). The primarily Pleistocene alluvial sediments of the Paso Robles Formation were then deposited mostly on Careaga Sandstone. Upsection, the Paso Robles Formation increasingly consists of Franciscan-derived detritus (Dibblee, 1991; table 2). Before the deposition of sand of the Careaga Sandstone and the alluvial sediments of the Paso Robles Formation, the *mélange* was uplifted on the Little Pine and Camuesa Faults simultaneously with renewed underfolding of the San Marcos block beneath the Little Pine Mountain block. This contractional tectonism is indicated by the presence of a strongly asymmetric and overturned, south-verging syncline of the San Marcos block that lies north of the San Marcos anticline and structurally beneath the *mélange* (fig. 3). Southwest-directed, reverse-oblique displacement of the *mélange* on the Little Pine Fault placed the San Marcos block farther beneath the Little Pine Mountain block (early Coast Range orogeny of Dibblee, 1991; table 2). The geometry and kinematics of this asymmetric syncline are analogous to those of the Oso syncline, which initially formed as the coherent rocks belt was folded beneath the Espada Formation during Ynezan tectonism. During early Coast Range tectonism, if not earlier, blocks composed of the Espada Formation lying in the Little Pine Fault Zone were enveloped significantly by squeezed-up *mélange*. The *mélange*, as well as the Espada, Monterey, Sisquoc, and Tequepis Formations, was then eroded. Sand of the Careaga Sandstone was deposited unconformably on the San Marcos block and along the southwest margin of the uplifted Little Pine Mountain block. The *mélange* continued to be contractionally deformed, uplifted, and eroded, resulting in the deposition of Monterey- and Franciscan-derived detritus along the southwest border of the *mélange* as the Paso Robles Formation.

After the deposition of sand of the Careaga Sandstone and the alluvium of the Paso Robles Formation, the *mélange* was again shortened and uplifted. As a result, the Neogene and Quaternary strata were folded back, strongly overturned, and locally thrust onto rocks of the San Marcos

block (late Coast Range orogeny of Dibblee, 1991; pl. 1; table 2). In lower Red Rock Canyon, the Tequepis Formation conformably overlies anticlinally folded Monterey Formation and Hurricane Deck Formation that are strongly overturned to the southwest and locally faulted. The north limb of this anticline becomes the south limb of the Oso syncline to the north. This anticline may have been connected to the San Marcos anticline prior to thrusting on the Loma Alta Fault during Quaternary time (fig. 3). Extensive bodies of serpentinite were injected into the high-angle faults and shear fractures in the *mélange* during this Quaternary phase, although less significant bodies may have been uplifted during any of the earlier late Eocene or early Oligocene to Pliocene deformational episodes. Serpentinite was also injected along the Little Pine and Camuesa Faults, which are steep at depth and converge with increasing depth (pl. 1). The *mélange* was subsequently eroded to form the present drainage system.

SUMMARY AND DISCUSSION

Late Eocene or early Oligocene tectonism formed major folds that include the Oso syncline and an inferred syncline in the Devils Canyon area (Ynezan orogeny). The Hurricane Deck syncline presumably began to form at this time as well, although all of its pre-late Eocene rocks were eroded. Major anticlines formed between the synclines at this time, and at least one is believed to have formed above the Little Pine Fault where the Cretaceous shear zone of Franciscan *mélange* is found. Younger tectonism reactivated all of these structures and tended to form numerous small folds and faults throughout the region. The continuity of tectonic style from the Ynezan orogeny through the late Coast Range orogeny suggests that these episodes of deformation are genetically related.

Ynezan and younger structures evidently resulted, in part, from low-angle convergence between the San Marcos block and the Little Pine Mountain block. Major folding and faulting of the San Marcos block beneath the Little Pine Mountain block occurred where *mélange* is exposed along the Little Pine Fault to form local uplifts and contractional basins. Differences in stratigraphy along the Little Pine Fault support this interpretation. The asymmetry of the combined Little Pine-Camuesa Fault Zone, as depicted in cross section (pl. 1), may also be a result of sinistral shear (Dibblee, 1982) on the Big Pine and Santa Ynez Faults. The gently dipping Loma Alta (thrust) Fault, for example, reflects the southwestward (Quaternary) displacement of the Little Pine Mountain block over the San Marcos block. The prevalence of serpentinite in the *mélange* northwest of Cachuma Canyon possibly reflects sinistral shear on the Big Pine Fault, as does the Camuesa Fault being locally overturned. The Ynezan angular unconformities that developed elsewhere in the region (fig.

2, loc. A) suggest westward movement of the Salinian terrane combined with northward movement of the Sur-Obispo terrane during late Eocene or early Oligocene time. Similarly, the *mélange* of the San Rafael Mountains was reformed and uplifted as a result of the northward convergence of the San Marcos block combined with westward movement of the Little Pine Mountain block.

The Little Pine and Camuesa Faults strike both parallel and at a low angle to Ynezan folds, such as the Oso and Hurricane Deck synclines, and to other folds, such as the San Marcos, Agua Caliente, and Buckhorn Creek anticlines (fig. 3). These two faults evolved below a zone of right-stepping anticlines that were faulted to form an asymmetric flower structure, or palm tree structure (Sylvester, 1988). The Loma Alta (thrust) Fault, the recumbently folded Oso syncline, and the large synclinally overturned, reverse-faulted block composed of the Espada Formation in Cachuma Canyon (Dibblee, 1993) are all interpreted as map-scale flower structures that formed within the combined Little Pine-Camuesa Fault System. These flower structures were produced, in part, by a lateral component of displacement on the Little Pine Fault. The orientation of the right-stepping anticlines relative to the Little Pine Fault Zone suggests dextral transpression.

The Little Pine Fault Zone and its related folds reflect the reactivation of the near-vertical, contractional structures of the *mélange*, initially during late Eocene or early Oligocene time. Reactivated, anastomosing, steeply dipping, reverse or oblique-slip faults in the *mélange* are also interpreted to be flower structures (Warner, 1992, pl. 1, Camuesa Fault Zone; pl. 1). The reactivation of these contractional structures postdates Paleocene thrusting. Major known late Cenozoic reformation of the *mélange*, as clearly reflected by the structure of serpentinite and the injection of serpentinite matrix, occurred as a result of transpression. The most extensive bands of serpentinite in the *mélange* are those that locally follow the traces of the Little Pine and Camuesa Faults. In addition, serpentinite forms the cores of several right-stepping, faulted anticlines in this area (for example, Buckhorn Creek and Agua Caliente anticlines). The Little Pine Fault has breached a serpentinite-cored anticline as well. The *mélange* has thus evolved in response to a transpressionally uplifted serpentinite basement.

The reverse component of slip on the Little Pine Fault is about 2.5 km, considering that the fault steepens with depth, that the faulted thickness of the Eocene to Quaternary strata is about 2 km and that the thickness of the coherent rocks belt is about 0.5 km. The lateral component of slip on the Little Pine Fault is uncertain, because reliable offsets were not found. The fault is buried to the northwest by upended strata of the Sisquoc Formation (Hall, 1981; Dibblee, 1991), which indicates that no significant lateral displacement on this fault has occurred after Rafealan tectonism in late Miocene time. The Little Pine

Fault Zone, including the *mélange*, probably has a maximum reverse-oblique slip of about 1.5 km during post-Miocene time (pl. 1).

At the surface, the Little Pine-Camuesa Fault Zone terminates to the southeast at the Franciscan exposure in Blue Canyon, where the greatest uplift of the Santa Ynez block has occurred (Dibblee, 1982; fig. 2). In the Blue Canyon area, the Santa Ynez Fault, which was a thrust or reverse fault during Pliocene and Pleistocene time, has been steepened and deflected southward, resulting in overturned bedding south of the fault in this area (Dibblee, 1982). East of Blue Canyon, the fold axes of the Agua Caliente and Little Pine synclines of the Little Pine Mountain block plunge beneath the Santa Ynez block, and the Santa Ynez Fault is overturned (Dibblee, 1982). The Santa Ynez block has overridden the San Marcos block and the uplifted southwest margin of the Little Pine Mountain block. Other results of this overriding may include the formation of a set of faults west of Santa Barbara (for example, San Jose Fault, Mesa Fault, Dibblee, 1966; fig. 2), and the Red Mountain Fault near Ventura (Dibblee, 1982; fig. 2). The trend of the San Jose Fault leads to a set of faults west of Lake Cachuma and near a block composed of the Espada Formation (Dibblee, 1987b; loc. B in fig. 2, fig. 3); however, no major Tertiary fault younger than Paleocene(?) presumably extends farther northwest along this trend (that is, to Point Sal) because a conformable, Eocene to Miocene section is present.

The Santa Ynez Fault dies out eastward near Lake Piru into the 1,700-m-thick folded section of the Monterey Formation (Dibblee, 1982; fig. 2). The Santa Ynez block is connected to the Little Pine Mountain block at this location, where a major syncline (right step of the Hurricane Deck(?) syncline) separates the Santa Ynez Fault from the Pine Mountain Fault. The folded structure near Lake Piru may have formed, in part, as a pivot for the clockwise rotation of the Santa Ynez block; however, finding conclusive evidence to specify the faults and the slip involved in this rotation remains elusive. The Miocene (as well as Paleogene) net slip on the Little Pine Fault is unknown. Furthermore, the Little Pine Mountain block and the Little Pine Fault may extend for many kilometers southeastward in the subsurface beneath the Santa Ynez block, and the history of this region is speculative.

CONCLUSIONS

Clearly not all of the diastrophism that formed the San Rafael Mountains *mélange* occurred prior to its being thrust beneath the Espada Formation during Paleocene tectonism. The regional tectonism that followed is characterized by several, genetically related episodes of contractional folding and faulting that undoubtedly reformed the inherited Cretaceous structure of the *mélange*. The present structure of the *mélange* and overly-

ing rocks reflects the remobilization of the weak serpentinite basement during Cenozoic time.

The degree of Cenozoic dismemberment and mixing in this mélangé is believed to be related to the Little Pine Mountain block being located at the south edge of the Sur-Obispo and Salinian blocks, and north of the Santa Ynez block of the western Transverse Ranges. The timing and tectonic style of the Ynezan orogeny (late Eocene or early Oligocene) indicate that the Little Pine Mountain block formed a buttress against the northward translation of the San Marcos block by about 35 Ma. Ynezan structures, which include folds and faults in and adjacent to the mélangé, thus are related to the establishment of the known Pacific-North American-Plate transform boundary (Atwater, 1989) that formed later, during Miocene time, and the subsequent rotation of the western Transverse Ranges province (Nicholson and others, 1994) around the Little Pine Mountain block.

REFERENCES CITED

- Atwater, T.M., 1989, Plate tectonic history of the northeast Pacific and western North America, in Winterer, E.L., Hussong, D.M., and Decker, R.W., eds., *The eastern Pacific Ocean and Hawaii*: Boulder, Colo., Geological Society of America, *Geology of North America*, v. N, p. 21-71.
- Bailey, E.H., Blake, M.C., Jr., and Jones, D.L., 1970, On-land Mesozoic ocean crust in California Coast Ranges: U.S. Geological Survey Professional Paper 700-C, p. 70-81.
- Bailey, E.H., Irwin, W.P., and Jones, D.L., 1964, The Franciscan and related rocks and their significance in the geology of western California: California Division of Mines and Geology Bulletin 183, 177 p.
- Blake, M.C., Jr., Howell, D.G., and Jayko, A.S., 1984, Tectonostratigraphic terranes of the San Francisco Bay region, in Blake, M.C., Jr., ed., *Franciscan geology of northern California*: Society of Economic Paleontologists and Mineralogists, Pacific Section, v. 43, p. 5-22.
- Blake, M.C., Jr., and Jones, D.L., 1974, Origin of the Franciscan mélanges in northern California, in Dott, R.H., and Shaver, R.H., eds., *Modern and ancient geosynclinal sedimentation*: Society of Economic Paleontologists and Mineralogists Special Publication 19, p. 255-263.
- 1978, Allochthonous terranes in northern California?—A reinterpretation, in Howell, D.G., and McDougall, K.A., eds., *Mesozoic paleogeography of the western United States*: Society of Economic Paleontologists and Mineralogists, Pacific Section, Pacific Coast Paleogeographic Symposium 2, p. 397-400.
- 1981, The Franciscan assemblage and related rocks in northern California: A reinterpretation, in Ernst, W.G., ed., *The geotectonic development of California*, Rubey Volume I: Englewood Cliffs, N.J., Prentice-Hall, p. 306-328.
- Brown, J.A., Jr., 1968, Thrust contact between Franciscan Group and Great Valley sequence northeast of Santa Maria, California: Los Angeles, University of Southern California, Ph.D. dissertation, 234 p.
- Dibblee, T.W., Jr., 1950, Geology of southwestern Santa Barbara County, California: California Division of Mines and Geology Bulletin 150, 84 p., scale 1:62,500.
- 1966, Geology of the central Santa Ynez Mountains, Santa Barbara County, California: California Division of Mines and Geology Bulletin 186, 99 p., scales 1:62,500 and 1:31,680.
- 1976, The Rinconada and related faults in the southern Coast Ranges, California, and their tectonic significance: U.S. Geological Survey Professional Paper 981, 55 p.
- 1982, Geology of the Santa Ynez-Topa Topa Mountains, Southern California, in *Geology and mineral wealth of the California Transverse Ranges*: South Coast Geological Society, p. 41-56.
- 1986a, Geologic map of the Carpinteria quadrangle, Santa Barbara County, California: Santa Barbara, Calif., Thomas W. Dibblee, Jr., Geological Foundation map DF-04, scale 1:24,000.
- 1986b, Geologic map of the Little Pine Mountain quadrangle, Santa Barbara County, California: Santa Barbara, Calif., Thomas W. Dibblee, Jr., Geological Foundation map DF-05, scale 1:24,000.
- 1987a, Geologic map of the San Marcos Pass quadrangle, Santa Barbara County, California: Santa Barbara, Calif., Thomas W. Dibblee, Jr., Geological Foundation map DF-08, scale 1:24,000.
- 1987b, Geologic map of the Lake Cachuma quadrangle, Santa Barbara County, California: Santa Barbara, Calif., Thomas W. Dibblee, Jr., Geological Foundation map DF-10, scale 1:24,000.
- 1989, Mid-Tertiary conglomerates and sandstones on the margins of the Ventura and Los Angeles basins and their tectonic significance, in Colburn, I., Abbott, P., and Minch, J., eds., *Conglomerates and basin analysis*: Society of Economic Paleontologists and Mineralogists, Pacific Section, v. 62, p. 207-226.
- 1991, Geology of the San Rafael Mountains, Santa Barbara County, in Lewis, L., Hubbard, P., Heath, E., and Pace, A., eds., *Southern Coast Ranges*: South Coast Geological Society, Annual Field Trip Guide Book, no. 19, p. 3-31.
- 1993, Geologic map of the Figueroa Mountain quadrangle, Santa Barbara County, California: Santa Barbara, Calif., Thomas W. Dibblee, Jr., Geological Foundation map DF-43, scale 1:24,000.
- 1995, Tectonic and depositional environment of the middle and upper Cenozoic sequences of the coastal southern California region, in Fritsche, A.E., ed., *Cenozoic paleogeography of the western United States—II*: Society of Economic Paleontologists and Mineralogists/Society for Sedimentary Geology, Pacific Section, v. 75, p. 212-245.
- Dickinson, W.R., 1970, Interpreting detrital modes of graywacke and arkose: *Journal of Sedimentary Petrology*, v. 40, p. 695-707.
- Ernst, W.G., 1970, Tectonic contact between the Franciscan mélangé and the Great Valley Sequence, crustal expression of a Late Mesozoic Benioff zone: *Journal of Geophysical Research*, v. 75, p. 886-902.
- Gordon, J.H., and Weigand, P.W., 1994, The Willows Plutonic Complex—A slice of immature arc rocks marooned on Santa Cruz Island, California, in Weigand, P.W., Gordon, J.C., and Boles, J., eds., *Geology of Santa Cruz Island*: American Association of Petroleum Geologists/Society of Economic Paleontologists and Mineralogists, Pacific Section, Field trip to Santa Cruz Island, p. 37-52.

- Hall, C.A., Jr., 1978, Origin and development of the Lompoc-Santa Maria pull-apart basin and its relation to the San Simeon-Hosgri strike-slip fault, western California, in Silver, E.A., and Normark, W.R., San Gregorio-Hosgri Fault Zone, California: California Division of Mines and Geology Special Report, v. 137, p. 25-31.
- 1981, Geology along Little Pine Fault, California: U.S. Geological Survey Miscellaneous Field Studies Map MF-1285, scale 1:24,000.
- 1991, Geology of the Point Sur-Lopez Point region, Coast Ranges, California: A part of the southern California allochthon: Geological Society of America Special Paper 226, 40 p.
- Hall, C.A., Jr., Ernst, W.G., and Wiese, J.W., 1979, Geologic map of the San Luis Obispo-San Simeon region, California: U.S. Geological Survey Miscellaneous Investigations Series Map I-1097, scale 1:48,000.
- Hamilton, W.B., 1969, Mesozoic California and underflow of the Pacific mantle: Geological Society of America Bulletin, v. 80, p. 2409-2430.
- Hopson, C.A., Mattinson, J.M., and Pessagno, E.A., Jr., 1981, Coast Range ophiolite, western California, in Ernst, W.G., ed., The geotectonic development of California, Rubey Volume I: Englewood Cliffs, N.J., Prentice-Hall, p. 418-510.
- Howard, J.L., 1987, Paleoenvironments, provenance, and tectonic implications of the Sespe Formation, southern California: University of California Santa Barbara. Ph.D. dissertation, 306 p.
- 1995, Conglomerates of the Upper Middle Eocene to Lower Miocene Sespe Formation along the Santa Ynez fault—Implications for the geologic history of the eastern Santa Maria basin area, in Keller, M.A., ed., Evolution of sedimentary basins and onshore oil and gas investigations—Santa Maria province: U.S. Geological Survey Bulletin 1995-H, 37 p.
- Hsü, K.J., 1968, Principles of mélangé and their bearing on the Franciscan-Knoxville paradox: Geological Society of America Bulletin, v. 79, p. 1063-1074.
- Jayko, A.S., and Blake, M.C., Jr., 1989, Deformation of the eastern Franciscan belt, northern California: Journal of Structural Geology, v. 4, p. 375-390.
- Luyendyk, B.P., Kammerling, M.J., Terres, R.R., and Hornafius, J.S., 1985, Simple shear of southern California during Neogene time suggested by paleomagnetic declinations: Journal of Geophysical Research, v. 90, p. 12,454-12,466.
- Mattinson, J.M., 1988, Constraints on the timing of Franciscan metamorphism: Geochronological approaches and their limitations, in Ernst, W.G., ed., Metamorphism and crustal evolution of the western United States, Rubey Volume II: Englewood Cliffs, N.J., Prentice-Hall, p. 1036-1059.
- Nicholson, C., Sorlien, C.C., Atwater, T., Crowell, J.C., and Luyendyk, B.P., 1994, Microplate capture, rotation of the western Transverse Ranges, and the initiation of the San Andreas transform as a low-angle fault system: Geology, v. 22, p. 491-495.
- Page, B.M., 1970, Sur-Nacimiento fault-zone of California: Continental margin tectonics: Geological Society of America Bulletin, v. 81, p. 667-690.
- 1972, Oceanic crust and mantle fragment in subduction complex near San Luis Obispo, California: Geological Society of America Bulletin, v. 83, p. 957-972.
- 1981, The southern Coast Ranges, in Ernst, W.G., ed., The geotectonic development of California, Rubey Volume I: Englewood Cliffs, N.J., Prentice-Hall, p. 329-417.
- Pessagno, E.A., Jr., 1977, Upper Jurassic radiolaria and radiolarian biostratigraphy of the California Coast Ranges: Micropaleontology, v. 23, no. 1, p. 56-113.
- Ramsay, J.G., and Huber, M.I., 1987, The techniques of modern structural geology, v. 2: Folds and fractures: London, England, Academic Press, 462 p.
- Reading, H., 1980, Characteristics and recognition of strike-slip fault systems: International Association of Sedimentologists, Special Publication, v. 4, p. 7-26.
- Ross, J.A., and Sharp, W.D., 1986, $^{40}\text{Ar}/^{39}\text{Ar}$ and Sm/Nd dating of garnet amphibolite in the Coast Ranges, California: EOS, v. 67, p. 1249.
- 1988, The effects of sub-blocking temperature metamorphism on the K/Ar systematics of hornblendes: $^{40}\text{Ar}/^{39}\text{Ar}$ dating of polymetamorphic garnet amphibolite from the Franciscan Complex, California: Contributions to Mineral Petrology, v. 100, p. 213-221.
- Schusser, C., 1981, Paleogene and Franciscan Complex stratigraphy, southwestern San Rafael Mountains, Santa Barbara County, California: University of California Santa Barbara, M.A. thesis, 235 p.
- Suppe, J., and Armstrong, R.L., 1972, Potassium-argon dating of Franciscan metamorphic rocks, American Journal of Science, v. 272, p. 217-233.
- Sylvester, A.G., 1988, Strike-slip faults: Geological Society of America Bulletin, v. 100, p. 1666-1703.
- Thomas, G.D., Fritsche, A.E., and Condon, M.W., 1988, Stratigraphy and depositional environments of the Hurricane Deck Formation, a new lower and middle Miocene submarine-fan sandstone unit in the Sierra Madre and San Rafael Mountains, northeastern Santa Barbara County, California, in Bazeley W.J.M. ed., Tertiary tectonics and sedimentation in the Cuyama Basin, San Luis Obispo, Santa Barbara, and Ventura Counties, California: Society of Economic Paleontologists and Mineralogists, Pacific Section, v. 59, p. 71-86.
- Vedder, J.G., 1972, Revision of stratigraphic names for some Eocene formations in Santa Barbara and Ventura Counties, California: U.S. Geological Survey Bulletin 1354-D, 12 p.
- Vedder, J.G., and Brown, R.D., Jr., 1968, Structural and stratigraphic relations along the Nacimiento fault in the southern Santa Lucia Range and the San Rafael Mountains, California, in Dickinson, W.R., and Grantz, Arthur, eds., Geological Sciences, v. 11, p. 242-259: Stanford University Publications.
- Vedder, J.G., Howell, D.G., and McLean, Hugh, 1983, Stratigraphy, sedimentation, and tectonic accretion of exotic terranes, southern Coast Ranges, California, in Watkins, J.S., and Drake, C.L., eds., Studies in continental margin geology: American Association of Petroleum Geologists Memoir 34, p. 471-496.
- 1989, Geologic map of Chimney Peak quadrangle and part of Huasna Peak quadrangle, California: U.S. Geological Survey, Open-File Report 89-161, scale 1: 24,000.
- Wahl, A.D., 1995, The geology of the Franciscan Complex San Rafael Mountains mélangé, California: University of California Santa Barbara, M.A. thesis, 121 p.
- Warner, M.C., 1992, Geology of the Franciscan Complex in Rancho San Fernando Rey area of Santa Barbara County, California: University of California Santa Barbara, M.A. thesis, 186 p.

Chapter X

Regional Thermal Maturity of Surface Rocks, Onshore Santa Maria Basin and Santa Barbara– Ventura Basin Area, California

By NANCY D. NAESER, CAROLINE M. ISAACS, and
MARGARET A. KELLER

U.S. GEOLOGICAL SURVEY BULLETIN 1995–X

EVOLUTION OF SEDIMENTARY BASINS/ONSHORE OIL AND GAS INVESTIGATIONS—
SANTA MARIA PROVINCE

Edited by Margaret A. Keller

Regional Thermal Maturity of Surface Rocks, Onshore Santa Maria Basin and Santa Barbara-Ventura Basin Area, California

By NANCY D. NAESER, CAROLINE M. ISAACS, and MARGARET A. KELLER

Abstract

Thermal maturities of surface rocks in the onshore Santa Maria and Santa Barbara-Ventura basin region of coastal California are mapped as "vitrinite reflectance equivalent" (VRE), a numerical parameter derived from measurement of vitrinite reflectance, Thermal Alteration Index, Rock-Eval pyrolysis T_{\max} and Production Index, and hydrogen/carbon ratio. Surface-rock maturity was determined by direct measurements on outcrop samples of Late Jurassic to Miocene age in the basins and surrounding areas or, in a limited number of cases, by extrapolating data from Eocene to Pleistocene age drill-hole samples to the surface. Maturity data are reported for more than 500 samples and include data determined specifically for this study and from other published and unpublished sources.

In the onshore Santa Maria basin and southern Coast Ranges, basement rocks, including the Franciscan Complex, are assumed to be overmature with respect to oil generation (VRE>1.3 percent), although data are available from only a very few samples. Upper Jurassic and Cretaceous sedimentary rocks range between marginally mature (VRE \approx 0.6 percent) and overmature (VRE>1.3 percent) with respect to oil generation. The exposed Tertiary section, composed almost entirely of lower Miocene and younger rocks, yields VRE<0.6 percent except in limited areas where the rocks are associated with Tertiary intrusive rocks. In drill holes in the Santa Maria basin and the smaller Huasna-Pismo basin to the north, lower Miocene to lower Pliocene sediments yield VRE \leq 0.6 percent to depths at least as great as about 2,620 m (about 8,600 ft) below surface. The data thus indicate that the Neogene section is immature at the surface and to significant depths in the subsurface, but VRE values may underestimate the actual maturity of these rocks, particularly the Miocene Monterey Formation.

In the onshore Santa Barbara-Ventura basin and surrounding areas, basement and Cretaceous sedimentary rocks are generally deeply buried and therefore largely missing at the surface except for limited areas south of the Santa Ynez fault and in the Simi Hills and Santa Monica

Mountains. The main source of maturity information is the Tertiary section, which, in contrast to the Santa Maria basin, includes an extensive, thick Paleogene section. South of the Santa Ynez fault, maturity decreases from VRE>1.3 percent in Cretaceous and Eocene rocks near the fault to VRE<0.6 percent in younger strata to the south. Within the Eocene section maturity also decreases from east to west, from the California State Highway 33 (Wheeler Gorge) area north of Ventura toward Point Conception, probably reflecting at least in part a westward decrease in the estimated maximum burial depth of Eocene rocks. The Neogene section along the Santa Barbara coast and in the Ventura area generally yields VRE<0.6 percent at the surface and to depths of greater than 5,700 m (18,700 ft) in the subsurface. The only Neogene surface rocks known to have VRE>0.6 percent are in the Santa Monica Mountains.

INTRODUCTION

The study area encompasses the onshore California coastal area west and south of the Nacimiento and Big Pine faults and north of the Santa Monica fault, extending from about 36° N. to 34° N. and covering parts of the Monterey, San Luis Obispo, Santa Maria, and Los Angeles 1:250,000 quadrangles. It lies in the Santa Maria basin and Ventura basin assessment provinces of Gautier and others (1995) and includes as the main areas of interest the onshore Santa Maria and Santa Barbara-Ventura basins and surrounding southern Coast Ranges and western Transverse Ranges (figs. 1, 2). The Coast Ranges-western Transverse Ranges junction and surrounding region are geologically, structurally, and tectonically complex, as exemplified by the contrasting structural grain of the west-trending Transverse Ranges and the northwest-trending Coast Ranges (Bailey and Jahns, 1954; Vedder and others, 1969). The Santa Maria and Santa Barbara-Ventura basins are rich in oil and gas resources, particularly in the Neogene section, stimulating much interest and research since the first oil field was discovered almost 130 years ago (Crawford, 1971; Curran and others, 1971; Nagle and Parker, 1971; Curran, 1982; references *in* Tomson, 1988). Many recently discovered aspects of the regional geologic evolution are elu-

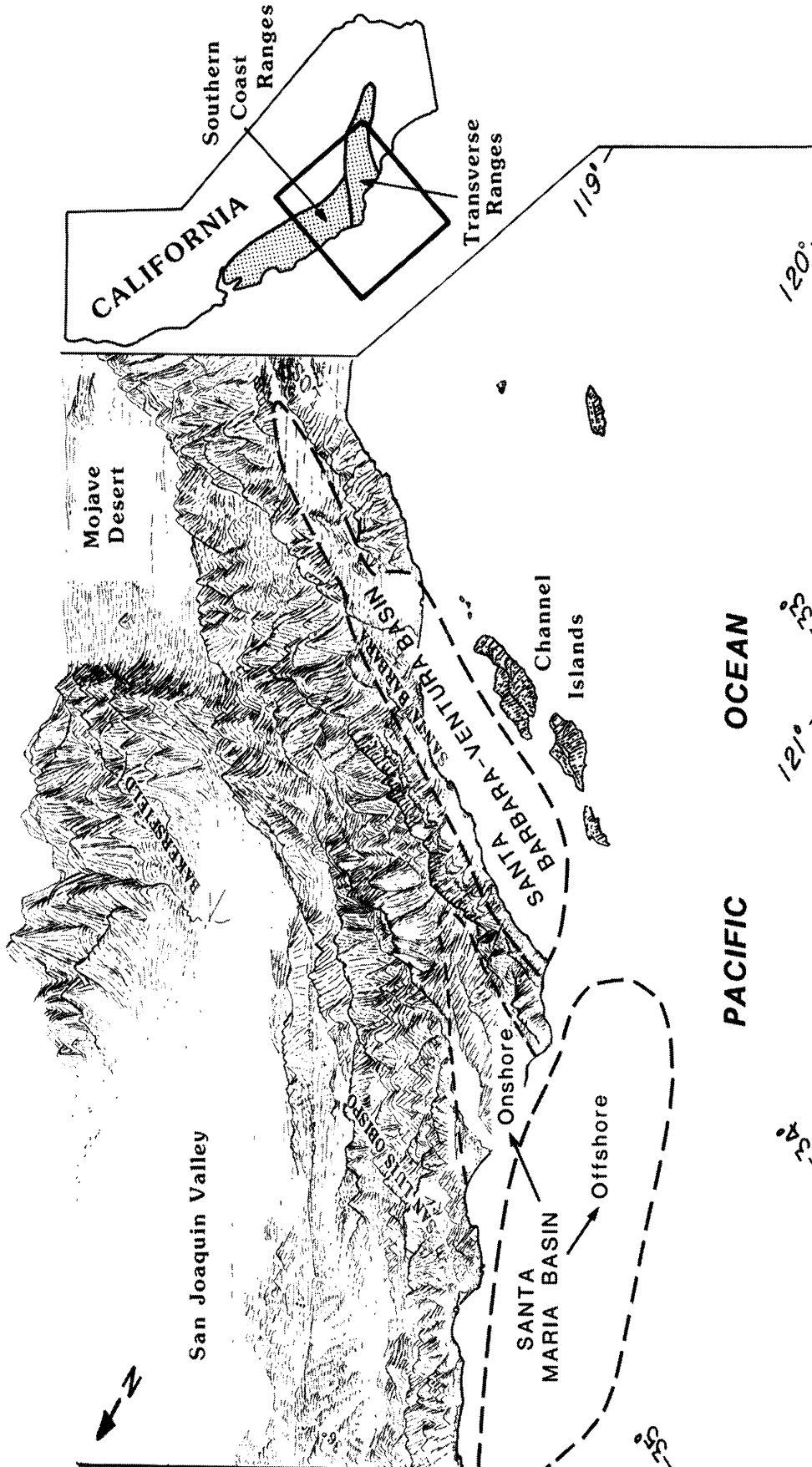


Figure 1. Oblique map of southern California, showing location of Santa Maria and Santa Barbara-Ventura basins. From Keller (1990); base from Alpha and others (1988).

culated in other chapters of U.S. Geological Survey Bulletin 1995.

The Santa Barbara-Ventura basin sedimentary sequence is dominated by marine beds of Cretaceous to Pleistocene age, with two intercalated nonmarine sequences of Eocene to Oligocene and Pleistocene age (fig. 3); the compiled sedimentary section has an estimated maximum thickness of approximately 15,240 m (50,000 ft), including at least 6 km (about 19,500 ft) of Pliocene and Pleistocene marine clastic strata (Bailey and Jahns, 1954; Vedder and others, 1969; Bostick and others, 1978; Ingle, 1981; Howard, 1995). No one stratigraphic column is representative of the entire basin because strata vary laterally in thickness and lithology and many of the formation boundaries are time transgressive (for example, Howard, 1995, fig. 11).

Stratigraphy of the adjacent onshore Santa Maria basin (fig. 4) is similar except that most of the pre-Miocene part of the sedimentary section is not present or, where

present along the basin margins, is much thinner than in the Santa Barbara-Ventura area (Dibblee, 1950; Woodring and Bramlette, 1950; Stanley and others, 1991). A tectonically emplaced assemblage of Mesozoic rocks, including the Upper Jurassic and Cretaceous Franciscan Complex, forms the basement in the region (Vedder and others, 1983; Howell and others, 1987; McLean, 1991).

Several important periods of tectonism initiated or punctuated basin formation and deformed the sedimentary section (Nagle and Parker, 1971; Crowell, 1976; Yeats, 1983; Hornafius and others, 1986; Luyendyk and Hornafius, 1987; Namson, 1987). Formation of both the Santa Maria and the Neogene Santa Barbara-Ventura basins began with Miocene subsidence (Vedder and others, 1969; Crowell, 1987; Johnson and Stanley, 1994). Miocene and older tectonic episodes are not as well understood as the younger period of compression that has overprinted most earlier deformation, forming a major fold and thrust belt in the Santa Barbara-Ventura basin during

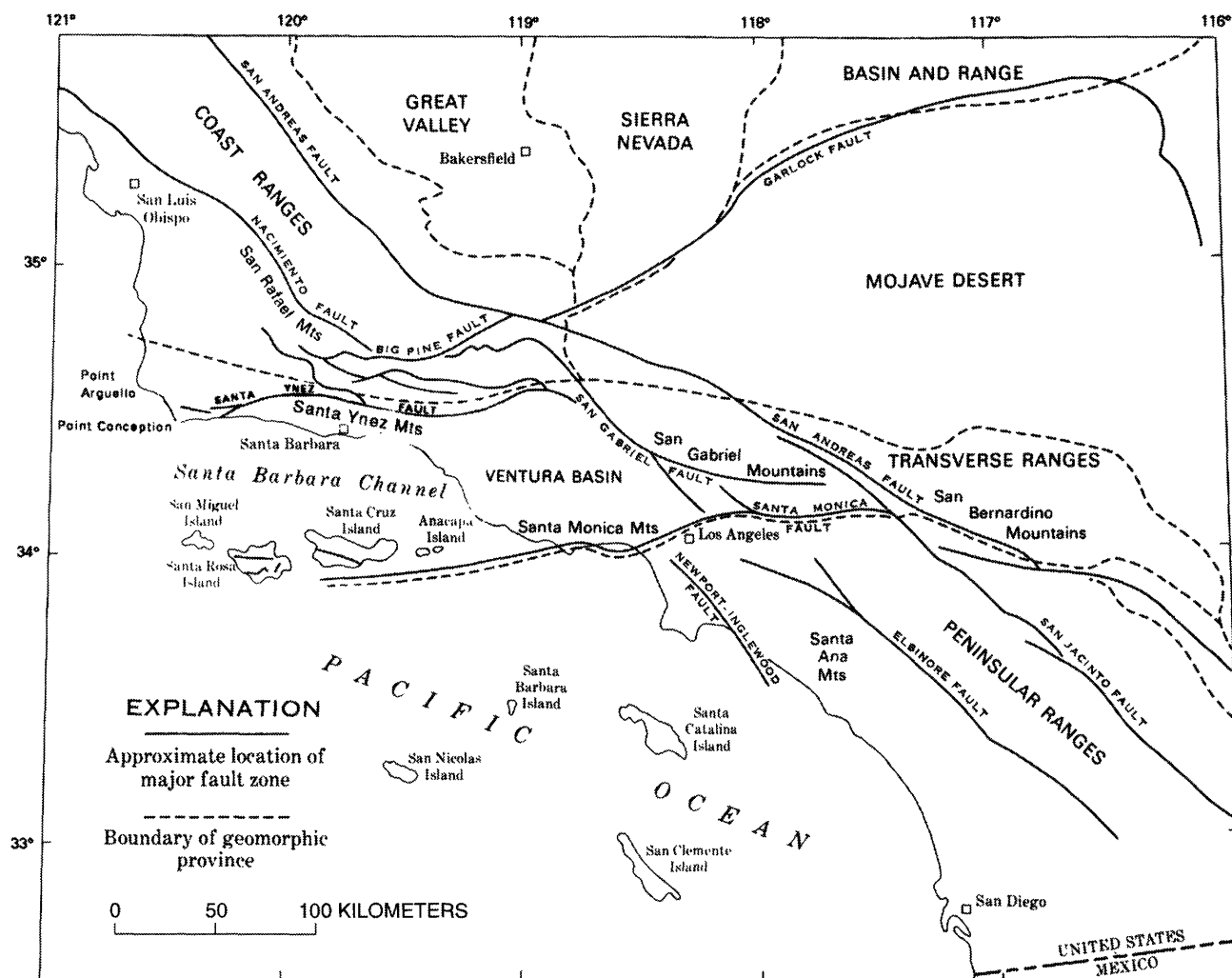


Figure 2. Index map showing major faults and geomorphic provinces of southern California. From Vedder and others (1969), as modified from Yerkes and others (1965).

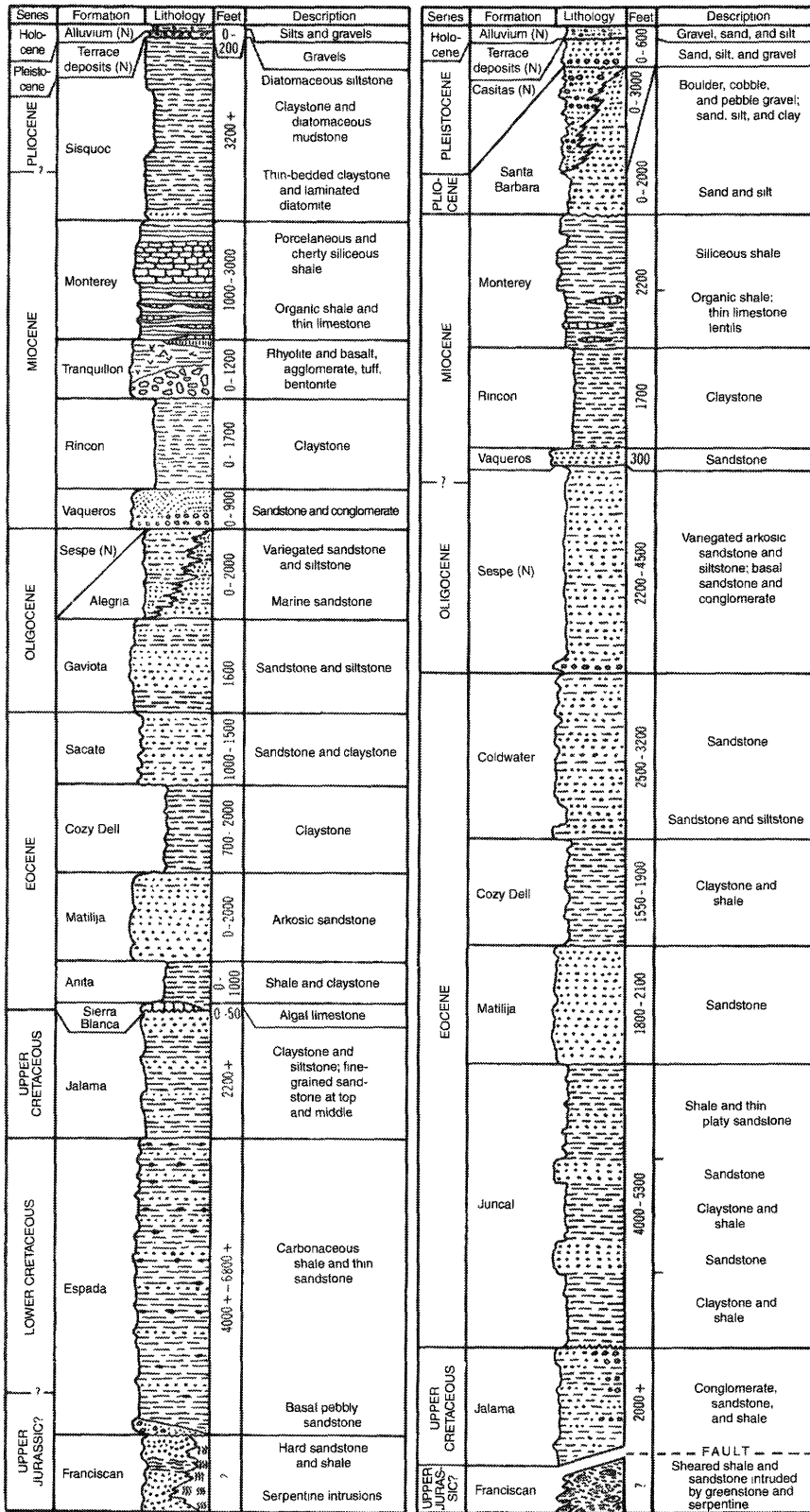


Figure 3. Representative stratigraphic columns from the onshore Santa Barbara-Ventura basin. *A*, western Santa Ynez Mountains. *B*, central Santa Ynez Mountains. (N), nonmarine unit. Note that because of the variable stratigraphy in different parts of the basin, some of the sampled formations (table 4) do not appear in these stratigraphic columns, and the age range of some formations is greater than shown (for example, Howard, 1995, fig. 11). The depth of burial of rocks suggested by thicknesses shown here is influenced by the extreme rates of deposition since about 3.5 Ma and so is somewhat misleading in terms of the thermal exposure and potential maturity of the rocks. From Vedder and others (1969), as modified from Dibblee (1950, 1966).

A

B

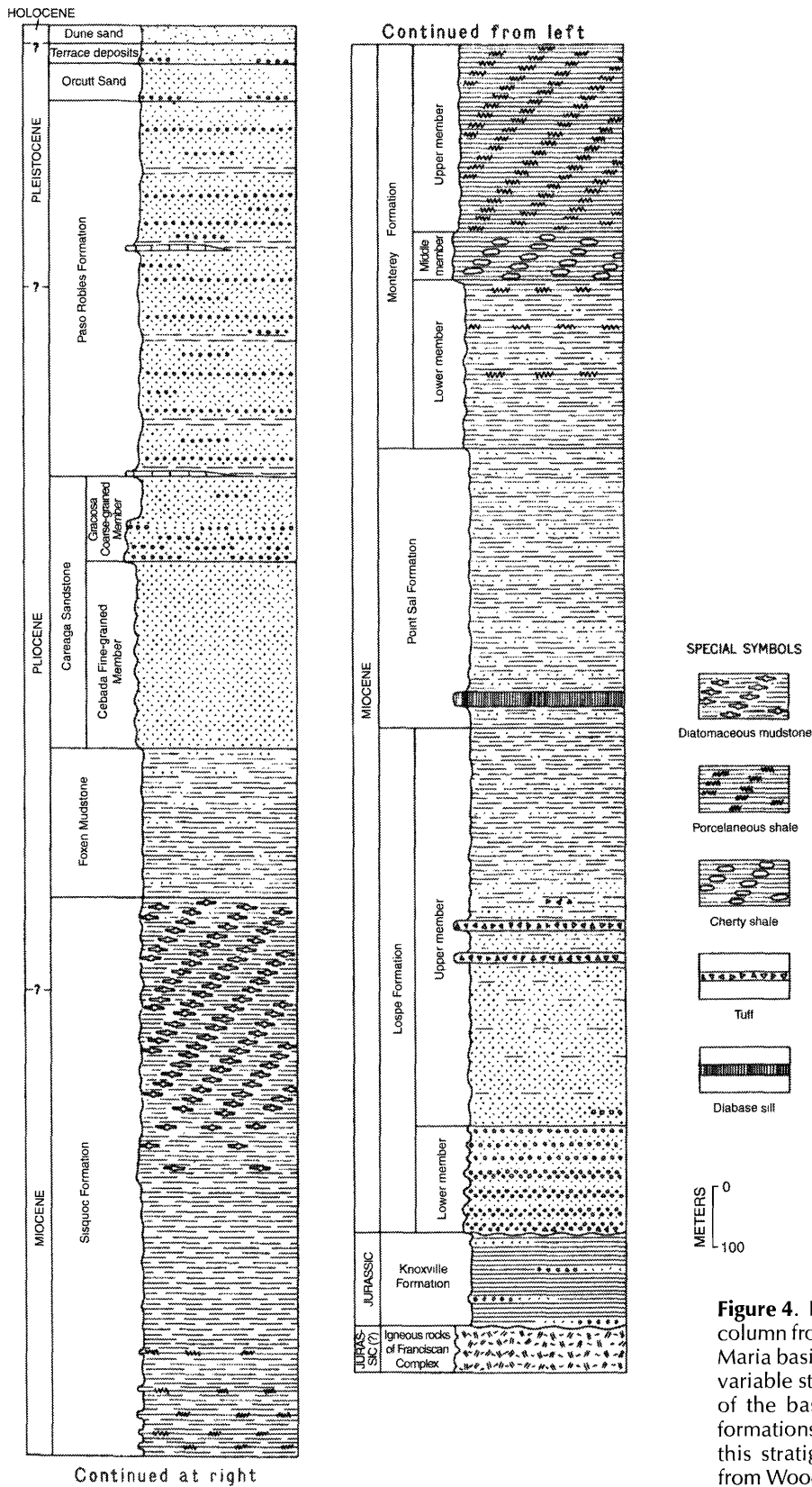


Figure 4. Representative stratigraphic column from the central onshore Santa Maria basin. Note that because of the variable stratigraphy in different parts of the basin, some of the sampled formations (table 4) do not appear in this stratigraphic column. Modified from Woodring and Bramlette (1950).

the Pliocene and Pleistocene (Yeats, 1983; Crowell, 1987; Namson, 1987). The main structural downwarp that is a conspicuous product of this deformation is the onshore Ventura basin and its founded offshore extension, the modern Santa Barbara basin.

Nearly all of the sedimentary units in these basins have produced oil and gas somewhere in the region; however, the most important production is from rocks in the Miocene to Pleistocene section in the Santa Barbara-Ventura basin and the Miocene section in the Santa Maria basin. The deep-marine Miocene deposits of these basins are the source of an important volume of oil as well as the host of important oil reservoirs. The pre-Miocene section is largely missing in the Santa Maria basin, and in the onshore Santa Barbara-Ventura basin it accounts for only about 15 percent of total basin production (Nagle and Parker, 1971). The oil-rich Santa Barbara-Ventura and Santa Maria basins are among the largest hydrocarbon-producing areas in California, with eight giant oil fields (>100 million barrels) in the onshore and at least five in the offshore, and they contain some of the oldest and youngest areas with respect to exploration and development (California Division of Oil and Gas, 1991). These basins also include important areas on land and in the adjacent offshore that have been explored only minimally (Crawford, 1971; Nagle and Parker, 1971; Curran, 1982; Keller, 1993, 1995; Tennyson, 1995). Therefore, significant undiscovered oil and gas resources undoubtedly remain. One key to finding undiscovered resources, in unexplored areas as well as in existing fields, might be a better understanding of the thermal history of this complex region (for example, Williams and others, 1994). Determining thermal maturity of organic matter in rocks provides a basis for assessing maximum temperatures to which rocks were exposed, one component in reconstructing regional thermal history and assessing petroleum resources. In the present paper, regional thermal maturity of surface rocks in the onshore Santa Maria and Santa Barbara-Ventura basin area is mapped on the basis of maturity data compiled from samples analyzed specifically for this study and from other published and unpublished sources.

ACKNOWLEDGMENTS

This paper includes one of several regional maps developed as an outgrowth of a project begun by USGS in the 1980's to produce 1:2,500,000 maps of the thermal maturity of surface and subsurface rocks of the United States. We would like to thank Norman Frederiksen, Peter van de Kamp, Leslie Magoon, Thane McCulloh, and Michael Underwood for supplying unpublished data that have been incorporated into the map and text. Mark Pawlewicz (U.S. Geological Survey, Denver) determined vitrinite reflectance of samples analyzed for the present

study, and Ted Daws (U.S. Geological Survey, Denver) performed the Rock-Eval analyses. We would like to thank Neely Bostick, Ted Daws, Thane McCulloh, and Vito Nuccio for discussion and comments that greatly improved the paper. Work was funded by USGS National Cooperative Geologic Mapping, Evolution of Sedimentary Basins, and Onshore Oil and Gas Investigations Programs.

THERMAL MATURITY INDICATORS

Many techniques have been proposed for assessing thermal maturity of organic matter, based on various modelling procedures and on direct measurements on organic and inorganic components in the rocks (for example, Tissot and Welte, 1978; Poole and Claypool, 1984; Bustin and others, 1985; Waples, 1985; Claypool and Magoon, 1988; Naeser and McCulloh, 1989). Vitrinite reflectance of dispersed kerogen in sedimentary rocks is currently one of the most widely used and widely accepted indicators of thermal maturity (for example, Bustin and others, 1985; Waples, 1985), and accordingly it is the parameter that we have chosen to express the thermal maturity of surface rocks in the Santa Maria basin-Santa Barbara-Ventura basin region.

Although relatively few actual vitrinite reflectance measurements have been reported for the Santa Maria and Santa Barbara-Ventura basins, maturity data are available in the form of Thermal Alteration Index (TAI), Rock-Eval pyrolysis temperature of maximum rate of pyrolytic yield (T_{max}) and Production Index (PI), and hydrogen/carbon ratio (H/C) data. Consequently, we have expressed surface-rock thermal maturity in terms of "vitrinite reflectance equivalent" (VRE), a value derived from correlating the available maturity data to vitrinite reflectance (tables 1, 2).

Correlating various indicators of thermal maturity is a complex problem, complicated by the inherent imprecision of each of the methods and, more importantly, by the wide range of factors that can influence results in the various techniques. The correlation of vitrinite reflectance, T_{max} , PI, and H/C adopted herein (table 1) is derived from correlation schemes proposed by Poole and Claypool (1984), Waples (1985), Peters (1986), and Claypool and Magoon (1988). Correlation of TAI and vitrinite reflectance presents special problems because numerical values of colors on the TAI scale (see below) have not been standardized among laboratories; to interpret TAI in terms of vitrinite reflectance it is necessary to know the TAI-vitrinite reflectance correlation used in the particular laboratory that determined a specific TAI value (Waples, 1985). The equivalency charts reported by the laboratories that measured the TAI data listed in table 5 are given in table 2. The uses, advantages, and disadvantages of the various indicators of thermal maturity are discussed more fully below.

Vitrinite Reflectance

Vitrinite reflectance is the measure of reflectance of incident light by polished vitrinite particles in coal or in kerogen in sedimentary rocks, measured using a specialized microscope. The use of vitrinite reflectance to determine maturity is based on the observation that reflectance increases with increasing thermal exposure (table 1). Ideally 50 to 100 vitrinite particles are measured per sample, although in many samples fewer particles are measured because of the scarcity of suitable material. The individual measurements are plotted as a histogram and usually reported as either mean or median R_o (vitrinite reflectance measured in immersion oil). Success in measuring and interpreting results depends on the ability of the analyst to distinguish primary from reworked

vitrinite particles and vitrinite from other kerogen macerals and solidified bitumen in the sample. Other problems in vitrinite reflectance analysis may include the following: lack of sufficient material in some samples; presence of different types of vitrinite that mature at different rates; contamination of drill-hole samples by organic matter from cavings or from drilling mud; uncertainty in the time-temperature (kinetics) of vitrinite maturation; the question of how closely the change in reflectance of vitrinite parallels kerogen maturation in general and specifically oil generation from kerogen; and, finally, possible suppression of R_o , probably related to the presence of significant Type I or Type II kerogen macerals in intimate and abundant association with the vitrinite, high concentrations of hydrogen in the vitrinite macerals, and (or) oil staining (Walker and others, 1983; Price, 1984; Price and Barker,

Table 1. Correlation among indicators of thermal maturity of organic matter and stages of hydrocarbon generation and preservation adopted herein, modified from Poole and Claypool (1984), Waples (1985), Peters (1986), Claypool and Magoon (1988), and Johnsson and others (1993)

[The zone between 0.6 and 1.3 percent R_o corresponds to the conventional oil window (see text discussion); rocks with R_o greater than 1.3 percent are considered overmature with respect to oil generation. R_o , mean random vitrinite reflectance, measured in oil; TAI, Thermal Alteration Index; T_{max} , temperature of maximum rate of pyrolytic yield of S₂, determined by Rock-Eval pyrolysis; PI, Production Index, S₁/(S₁ + S₂), derived from Rock-Eval pyrolysis; H/C, atomic ratio of hydrogen to carbon in sapropelic (S) and humic (H) kerogen]

Stages of organic matter transformation	Qualitative interpretation of organic matter thermal history with respect to oil generation	Stages of oil generation and preservation	Vitrinite reflectance (percent R_o)	TAI	Rock-Eval pyrolysis		H/C	
					T_{max} (°C)	PI	S	H
DIAGENESIS	IMMATURE	ONSET OF OIL GENERATION	0.6	See table 2	≈435-445	≈0.1	1.1	0.8
		LIMIT OF OIL GENERATION	1.3		≈470	≈0.4	0.8	0.6
CATAGENESIS	OVERMATURE	LIMIT OF OIL PRESERVATION	1.75		≈490	≈0.5	0.65	0.55
		LIMIT OF CONDENSATE/WET GAS PRESERVATION	2.0				0.6	0.5
		METAGENESIS						

measurement requires knowing the TAI-vitrinite reflectance correlation that characterizes data from the measuring laboratory (Bustin and others, 1985; Waples, 1985). The relatively large range of R_o values covered by some TAI numbers (table 2) also affects the accuracy of the TAI- R_o correlation.

More than half of the available TAI data in the study area (see table 5) are from Frederiksen (1985; written commun., 1986). When Frederiksen's TAI values are interpreted using his TAI- R_o correlation (table 2), they yield anomalously low maturities compared with most other maturity data available for these rocks (for example, table 3). The reason for this discrepancy is not established, but part of the explanation may be that Frederiksen calibrated his TAI data against vitrinite reflectance values (from Helmold, 1980) that appear to be anomalously low, particularly in the range from about 0.6 to 1.3 percent R_o . Frederiksen's TAI calibration in this range (table 2) is based on vitrinite reflectance data from Eocene rocks in the California State Highway 33 (Wheeler Gorge) [map numbers (map no.) 61-63 on map A, pl. 1] and Gibraltar Road (map no. 66-68) sections. Several other laboratories have reported maturity data for the State Highway 33 section (see table 5). Direct comparison of Helmold's (1980) vitrinite reflectance data to other maturity data is complicated by uncertainty about the stratigraphic relationship of samples analyzed by the various laboratories, but in general Helmold's (1980) R_o values appear to be low in comparison both to R_o values determined by P.C. van de Kamp (written

commun., 1987) and to VRE interpreted from Rock-Eval pyrolysis data (Frizzell and Claypool, 1983), particularly in the range from about 0.6 to 1.3 percent R_o . If Helmold's (1980) measurements are anomalously low, it would explain in part why Frederiksen's (1985) TAI values appear to predict anomalously low maturity in some samples. Further work would be required to thoroughly clarify both the suggested interdependency and the resulting effect on the values reported by Frederiksen (1985).

Rock-Eval Pyrolysis Temperature of Maximum Rate of Pyrolytic Yield (T_{max}) and Production Index (PI)

Pyrolysis is in effect a laboratory attempt to simulate the effects of slow natural thermal maturation of organic matter by briefly heating a sample in the absence of oxygen to bring about thermal decomposition reactions. Several pyrolysis instruments are available; Rock-Eval is one of the most widely used. Rock-Eval pyrolysis data are used for assessing both the type and the thermal maturity of organic matter in a rock. The analysis yields two values used to assess maturity: (1) maximum temperature of pyrolytic yield (T_{max}), that is, the temperature (in degrees Celsius) at which the maximum rate of pyrolysis occurs (the temperature at the top of the S2 peak); and (2) the Production Index (PI) (or Transformation Ratio), $S1/S1+S2$, where S1 is a measure of hydrocarbons present in the rock since deposition plus those already

Table 3. Comparison of TAI and other thermal maturity indicators for selected samples, onshore Santa Maria and Santa Barbara-Ventura basin area, California

[Locality data and lithology are given in table 5. Sample locations are plotted (by map numbers) in map A (pl. 1). R_o , mean random vitrinite reflectance, measured in oil; TAI, Thermal Alteration Index; T_{max} , temperature of maximum rate of pyrolytic yield of S2, determined by Rock-Eval pyrolysis; PI, Production Index (Transformation Ratio) $S1/(S1 + S2)$, derived from Rock-Eval pyrolysis; H/C, atomic ratio of hydrogen to carbon; VRE, vitrinite reflectance equivalent, interpreted from listed R_o , TAI, T_{max} , and (or) PI values, based on correlation given in tables 1 and 2 (see text)]

Map No.	Sample No.	Stratigraphic age ¹ (Formation)	R_o ² (percent)	TAI	T_{max} (°C)	PI	Approximate VRE (percent)	Reference ³
52	BUC-2	Late Jurassic-Early Cretaceous (KJe)	0.95±0.11 --	3.0 1+/2-	-- --	-- --	1.0 <0.2	1 2
	BUC-3-2	-----do-----	0.75±0.08 --	2.5-2.7 1+	447 --	0.0 --	0.7 <0.2	1 2
89	SIM-3	Late Cretaceous (Kc)	0.53±0.03 --	2.5 1+	426 --	0.0 --	0.5 <0.2	1 2
	SIM-4	-----do-----	0.55±0.03 --	-- 1+/2-	-- --	-- --	0.6 <0.2	1 2
	SUS-1B	-----?do-----	0.50±0.03 --	-- 1+/2-	-- --	-- --	0.5 <0.2	1 2

¹Kc, Chatsworth Formation (Colburn and others, 1981); KJe, Espada Formation (Dibblee, 1950).

²Uncertainty calculated as 95 percent confidence limits.

³References:

1 = present study

2 = N.O. Frederiksen (written commun., 1986)

naturally generated in subsurface, and S2 represents the remaining hydrocarbon generative capacity.

In theory, both T_{\max} and PI should increase with increasing thermal maturity (table 1). However, considerable care must be used in interpreting maturity from pyrolysis data because of the number of factors that can influence T_{\max} and PI. The basic assumption in pyrolysis analysis is that the analyzed rock behaved as a closed system in which (1) the only petroleum products in the sample are indigenous, that is, those that were originally deposited in the sediment or were generated after deposition from organic matter present only in that rock; and (2) any petroleum generated in the rock has not migrated away but is still present in the sample. Migration of hydrocarbons into or out of the rock, combined with a number of other complicating factors, including effects of weathering, kerogen type, and low total organic carbon (TOC), can affect T_{\max} and PI values to the extent that Waples (1985) suggests that isolated T_{\max} values are not trustworthy indicators of thermal maturity and PI values in general are not a reliable maturity indicator. Ideally, interpretations should always be supported by other maturity data (Peters, 1986).

Because of the potential problems associated with pyrolysis data, more weight has been given to direct vitrinite reflectance measurements for interpreting thermal maturity than to pyrolysis data, and in turn more weight has been placed on T_{\max} than on PI values.

Hydrogen/Carbon Ratio (H/C)

The hydrogen/carbon atomic ratio of kerogen varies with organic type and maturity, in general decreasing with increasing maturity. Maturity-related H/C values for sapropelic (Type II) and humic (Type III) kerogen (Poole and Claypool, 1984; Claypool and Magoon, 1988) are listed in table 1. Some problems associated with such measurements devolve from adverse influences of weathering, even in fresh-appearing rocks, and from the decreased precision of measurements in low-TOC rocks (T.H. McCulloh, written commun., 1995).

THERMAL MATURITY—ONSHORE SANTA MARIA AND SANTA BARBARA-VENTURA BASIN AREA

The stratigraphic column in the Santa Maria and Santa Barbara-Ventura basins and surrounding areas can be divided into three packages—basement rocks, including the Franciscan Complex (lower package); Upper Jurassic and Cretaceous sedimentary rocks (middle package); and Tertiary and Quaternary sedimentary rocks (upper package). Tectonically emplaced basement and structurally overlying Upper Jurassic and Cretaceous rocks, along with Tertiary and Quaternary rocks, were deformed, displaced, and overprinted during complex Paleogene and Neogene tectonic episodes and basin-forming events. This complex history has brought rocks

with different thermal histories, and hence different thermal maturity, into contact along fault, erosional, or major tectonic discontinuities (for example, Vedder and others, 1983; Crowell, 1987; Howell and others, 1987; Luyendyk and Hornafius, 1987; De Rito and others, 1989; Tennyson, 1989; McLean, 1991; Crouch and Suppe, 1993; Williams and others, 1994). Hence, in many areas the *total* thermal exposure of rocks in different blocks must be viewed more or less independently. The thermal exposure of older rocks is probably in general as great as or greater than that of younger rocks, but immature and overmature rocks can be in contact with no intervening mature rock.

In the onshore Santa Maria basin and smaller Huasna-Pismo basins to the north, the oldest widespread strata in the Tertiary section are middle Miocene in age, and these strata everywhere yield vitrinite reflectance equivalent less than 0.6 percent at the surface. Basement rocks are everywhere assumed to be overmature with respect to oil generation (VRE greater than 1.3 percent); this assumption may not be strictly true, but, because this package largely consists of Franciscan Complex *mélange*, the effort to determine details of the thermal maturity would be excessive and probably of little value. This essentially leaves the Upper Jurassic and Cretaceous package, which crops out mainly in the southern Coast Ranges to the north and east of the basins, as the main source of complexity in mapping VRE of surface rocks in the Santa Maria area.

In the onshore Santa Barbara-Ventura basin, on the other hand, the major source of complexity in mapping surface-rock thermal maturity is the Tertiary and Quaternary section, which, in contrast to the Santa Maria basin, includes extensive outcrops of Paleogene strata. Pre-Tertiary rocks are only locally exposed, and their extent is generally too small to show on maps A and B (pl. 1).

In the present study, thermal maturity of surface rocks in the onshore Santa Maria and Santa Barbara-Ventura basins and surrounding area was determined by direct measurements on outcrop samples or, in a limited number of cases, by extrapolation of drill-hole data to the surface. Maturity data are reported from more than 500 samples collected from Upper Jurassic to Miocene surface rocks and Eocene to Pleistocene drill-hole samples (map A, pl. 1; tables 4-5).

For purpose of discussion, the study area has been divided into 16 regions (map B, pl. 1), each dominated by one of three packages of rock—basement (predominantly Franciscan Complex), Jurassic and Cretaceous sedimentary rocks, or Tertiary and Quaternary upper sedimentary rocks. Surface-rock thermal maturity of each region is discussed below. Thermal maturity is classified (table 5; map A, pl. 1) as VRE < 0.6 percent, 0.6-1.3 percent, or > 1.3 percent, based on the maturity data in table 5 and correlations given in tables 1 and 2. R_o values of 0.6 and 1.3 percent are typically related to the lower and upper limits of the main oil-generation window (for example, Claypool and Magoon, 1988; Johnsson

and others, 1993) (table 1). In any given area, however, the actual R_o values at the boundaries of the oil window and the ability of rocks within this zone to generate petroleum will depend not only on thermal maturity, but also on the type and

quantity of organic matter present in the rock (for example, Waples (1985) and discussion under "Region 7").

Data listed in table 5 include R_o , TAI, T_{max} , and PI measurements from samples analyzed specifically for this study

Table 4. Sampled formations, onshore Santa Maria and Santa Barbara-Ventura basin region, California

Stratigraphic age	Formation	Sample location		Symbol	
		Santa Maria basin area	Santa Barbara-Ventura basin area		
Pliocene and Pleistocene	Santa Barbara Formation	—	x	QTsb	
	Pico Formation	—	x	QTp	
Late Miocene and early Pliocene	Sisquoc Formation	x	—	Ts	
Miocene	Monterey Formation	x	x	Tm	
	Rincon Shale	—	x	Tr	
	Topanga Formation	—	x	Tt	
	Point Sal Formation	x	—	Tps	
	Lospe Formation	x	—	Tl	
Oligocene and early Miocene	Simmler Formation	x	—	Tsi	
Eocene and Oligocene	Gaviota Formation	—	x	Tg	
Eocene	Sacate Formation ¹	—	x	Tsa	
	Coldwater Sandstone	—	x	Tcw	
	Cozy Dell Shale	x	x	Tcd	
	Matilija Sandstone	—	x	Tma	
	Juncal Formation	x	x	Tj	
Paleocene and Eocene	Anita Formation	—	x	Ta	
Cretaceous	Late Cretaceous	Jalama Formation	—	x	Kj
		Chatsworth Formation ²	—	x	Kc
	Early Cretaceous	Jollo Formation	x	—	Kjo
Late Jurassic and Early Cretaceous	Toro Formation	x	—	KJt	
	Espada Formation ³	x	—	KJe	
Late Jurassic and Cretaceous	Franciscan Complex	x	—	KJf	
Late Jurassic	Santa Monica Slate	—	x	Jsm	

¹Of Kelley (1943)

²Of Colburn and others (1981)

³Of Dibblee (1950)

Table 5. Locality, stratigraphic age, lithology, and thermal maturity data for surface and drill-hole samples, onshore Santa Maria and Santa Barbara-Ventura basin area, California

[Sample locations are plotted (by map numbers) in map A (pl. 1). R_o , mean random vitrinite reflectance measured in oil; TAI, Thermal Alteration Index; T_{max} , temperature of maximum rate of pyrolytic yield of S2, determined by Rock-Eval pyrolysis; PI, Production Index (Transformation Ratio) S1/(S1 + S2), derived from Rock-Eval pyrolysis; H/C, atomic ratio of hydrogen to carbon; VRE, vitrinite reflectance equivalent, interpreted from listed R_o , TAI, T_{max} , PI, and (or) H/C values, based on correlations given in tables 1 and 2 (see text). VRE is queried where maturity parameters for a given sample give conflicting results; the listed VRE is based on the maturity parameter judged most reliable (see text)]

Map No.	Sample No. ¹	Location	Depth below surface (ft)	Stratigraphic age ² (Formation)	Lithology ³	R_o ⁴ (%)	TAI	T_{max} (°C)	PI	H/C	VRE (%)	Reference ⁵
1	BM 840A	sec. 25, T. 24 S., R. 6 E. 35°49'12" N., 121°16'26" W.	--	Late Jr-Early K (KJt)	slts.-sh.	3.07±0.14	4.0	--	--	--	>1.3	A
	BM845A	sec. 25, T. 24 S., R. 6 E. 35°49'05" N., 121°16'26" W.	--	-----do-----	---do---	3.22±0.10	--	--	--	--	>1.3	A
2	-- ⁶	T. 27 S., R. 8 E.; T. 28 S., R. 8 E.; and T. 28 S., R. 9 E.	--	K	?	-- ⁶	--	--	--	--	0.6-1.3	B
3	Toro-1	T. 29 S., R. 11 E. 35°25'40" N., 120°44'55" W.	--	?	slts.-sh.	1.73±0.10	4.0	--	--	--	>1.3	A
	Toro-2	-----do-----	--	?	---do---	1.99±0.07	3.5-3.7	--	--	--	>1.3	A
	Toro-3	-----do-----	--	?	---do---	1.81±0.09	3.5	--	--	--	>1.3	A
4	VF-81C-1048 (152)	T. 30 S., R. 14 E.	--	Miocene (Tm)	---do---	--	--	429	0.05	--	<0.6	C
	VF-81C-1043 (151)	T. 31 S., R. 14 E.	--	-----do-----	---do---	--	--	411	0.02	--	<0.6	C
5	VF-81C-1052 (160)	T. 30 S., R. 14 E.	--	K	---do---	--	--	442	0.11	--	0.6-1.3 (=0.6)	C
6	VF-81C-1060 (153)	T. 30 S., R. 14 E.	--	Miocene (Tm)	---do---	--	--	421	0.05	--	<0.6	C
	FM-81C-237 (159)	-----do-----	--	-----do-----	---do---	--	--	413	0.06	--	<0.6	C
	FM-81C-235 (158)	T. 30 S., R. 13 E.	--	-----do-----	---do---	--	--	415	0.04	--	<0.6	C
7	FM-81C-260 (161)	T. 30 S., R. 13 E.	--	K	---do---	--	--	505	0.50	--	>1.3	C
8	VF-81C-1021 (150)	-----do-----	--	Miocene (Tm)	---do---	--	--	420	0.04	--	<0.6	C
	FM-81C-221 (154)	-----do-----	--	-----do-----	---do---	--	--	414	0.04	--	<0.6	C
	FM-81C-222 (155)	-----do-----	--	-----do-----	---do---	--	--	417	0.05	--	<0.6	C
	FM-81C-224 (156)	-----do-----	--	-----do-----	---do---	--	--	410	0.04	--	<0.6	C
	FM-81C-225 (157)	-----do-----	--	-----do-----	---do---	--	--	414	0.07	--	<0.6	C
9	R2770	sec. 6, T. 31 S., R. 15 E.	--	?Oligocene-early Miocene (?Tsi)	?	--	2	--	--	--	<0.6	D
10	Well a:	sec. 35, T. 31 S., R. 14 E.										
	--	--	surface	--	--	--	--	--	--	--	?<0.6 ⁷	--
	--	--	200	Miocene (Tm)	?	--	--	--	0.15	--	--	E
11	VF-81C-353 (140)	T. 32 S., R. 17 E.	--	K	slst.-sh.	--	--	450	0.06	--	?0.6-1.3	C
12	VF-81C-378 (147)	T. 32 S., R. 16 E.	--	K	---do---	--	--	447	0.85	--	?0.6-1.3	C
13	VF-81C-372 (146)	-----do-----	--	K	---do---	--	--	455	0.15	--	0.6-1.3	C

Table 5. Locality, stratigraphic age, lithology, and thermal maturity data for surface and drill-hole samples, onshore Santa Maria and Santa Barbara-Ventura basin area, California—Continued

Map No.	Sample No. ¹	Location	Depth below surface (ft)	Stratigraphic age ² (Formation)	Lithology ³	R _o ⁴ (%)	TAI	T _{max} (°C)	PI	H/C	VRE (%)	Reference ⁵
14	Well b:	sec. 24, T. 32 S., R. 14 E.										
	--	--	surface	--	--	--	--	--	--	--	<0.6 ⁷	--
	--	--	1,600 to 2,500	Miocene (Tm)	?	--	--	--	0.06	--		E
	Well c:	?sec. 25, T. 32 S., R. 14 E.										
	--	--	surface	--	--	--	--	--	--	--	<0.6 ⁷	--
	--	--	1,200 to 4,000	Miocene (Tm)	?	--	--	--	<0.06	--		E
15	Well d:	sec. 5, T. 32 S., R. 13 E.										
	--	--	surface	--	--	--	--	--	--	--	<0.6 ⁷	--
	E-4510	--	4,510	Miocene (Tm)	?	--	2-	--	--	1.20		F
	E-4754	--	4,754	-----do-----	?	--	2-	--	--	0.83		F
	E-4985	--	4,985	-----do-----	?	--	2-	--	--	1.11		F
	E-5172	--	5,172	-----do-----	?	--	2-	--	--	0.94		F
	E-5572	--	5,572	-----do-----	?	--	2- to 2	--	--	--		F
	E-5807	--	5,807	-----do-----	?	--	2- to 2	--	--	--		F
	E-5809	--	5,809	-----do-----	?	--	--	--	--	1.17		F
	E-6137	--	6,137	-----do-----	?	--	2	--	--	0.95		F
	E-6398	--	6,398	-----do-----	?	--	2	--	--	1.12		F
	E-6926	--	6,926	-----do-----	?	--	2	--	--	1.13		F
	E-6934	--	6,934	-----do-----	?	--	2	--	--	--		F
	Well e:	sec. 6, T. 32 S., R. 13 E.										
	--	--	surface	--	--	--	--	--	--	--	<0.6 ⁷	--
	N-2013	--	2,013	Miocene (Tm)	?	--	1+	--	--	1.19		F
	N-2530	--	2,530	-----do-----	?	--	2-	--	--	1.22		F
	N-2620	--	2,620	-----do-----	?	--	2-	--	--	1.18		F
	N-2841	--	2,841	-----do-----	?	--	2-	--	--	1.22		F
	N-3062	--	3,062	-----do-----	?	--	2-	--	--	1.29		F
	N-3762	--	3,762	-----do-----	?	--	2-	--	--	1.26		F
	N-3935	--	3,935	-----do-----	?	--	2-	--	--	0.95		F
16	NSB-5	sec. 10, T. 32 S., R. 12 E.	--	-----do-----	?	--	2-	--	--	1.31	<0.6	F
	NSB-7	-----do-----	--	-----do-----	?	--	2-	--	--	1.29	<0.6	F
	PO-24	-----do-----	--	-----do-----	?	--	2-	--	--	1.29	<0.6	F
17	ALC-1	T. 12 N., R. 32 W.	--	Early K (Kjo)	concretion	1.13 ⁸	--	465	0.29	--	0.6-1.3	A
	ALC-2	35°05'16" N., 120°15'07" W.	--	-----do-----	-----do-----	1.26±0.37	--	467	0.21	--	0.6-1.3	A
	ALC-4	-----do-----	--	-----do-----	-----do-----	--	--	471	0.30	--	0.6-1.3	A
	ALC-5	-----do-----	--	-----do-----	mdst.	1.27±0.02	3.2	471	0.19	--	0.6-1.3	A
18	ALC-3	-----do-----	--	-----do-----	concretion	--	--	477	0.50	--	>1.3	A
19	VF-81C-359 (141)	T. 11 N., R. 30 W.	--	K	sist.-sh.	--	--	519	0.45	--	>1.3	C
20	VF-81C-361 (142)	T. 11 N., R. 31 W.	--	K	---do---	--	--	499	0.12	--	?>1.3	C
21	VF-81C-351 (148)	-----do-----	--	KJf	---do---	--	--	490	0.08	--	?>1.3	C
22	NF-81C-57 (149)	T. 11 N., R. 32 W.	--	KJf	---do---	--	--	482	0.05	--	?>1.3	C
23	VF-81C-349 (139)	-----do-----	--	K	---do---	--	--	468	0.09	--	?0.6-1.3	C
24	Well f:	sec. 11, T. 11 N., R. 33 W.										
	--	--	surface	--	--	--	--	--	--	--	<0.6 ⁷	--
	--	--	750	Miocene (Tm)	?	--	--	--	<0.05	--		E

Table 5. Locality, stratigraphic age, lithology, and thermal maturity data for surface and drill-hole samples, onshore Santa Maria and Santa Barbara-Ventura basin area, California—Continued

Map No.	Sample No. ¹	Location	Depth below surface (ft)	Stratigraphic age ² (Formation)	Lithology ³	R _o ⁴ (%)	TAI	T _{max} (°C)	PI	H/C	VRE (%)	Reference ⁵
25	477-27-5	T. 10 N., R. 30 W. (SE.) 34°55'00" N., 120°01'14" W.	--	Late K	?	0.81±0.07	--	435	0.04	--	?0.6-1.3	A
26	VF-81C-362 (143)	T. 10 N., R. 31 W.	--	K	slst.-sh.	--	--	430	0.02	--	<0.6	C
	VF-81C-364 (144)	-----do-----	--	K	---do---	--	--	444	0.03	--	?0.6-1.3 (=0.6)	C
	--	-----do-----	--	K-early T	?	--	2-/2	--	--	--	<0.6	D
27	Well g:	sec. 25, T. 10 N., R. 34 W.										
	--	--	surface	--	--	--	--	--	--	--	<0.6 ⁷	--
	6	--	3.165	late Miocene-early Pliocene (Ts)	siliceous sh.	--	1.1	--	--	1.12	--	G, H
	7	--	3.734	Miocene (Tm)	-----do-----	--	1.3	--	--	1.29	--	G, H
	8	--	3.765	-----do-----	-----do-----	--	1.3	--	--	1.28	--	G, H
	9	--	3.922	-----do-----	-----do-----	--	1.5	--	--	1.30	--	G, H
28	Well h:	sec. 11, T. 9 N., R. 34 W.										
	--	--	surface	--	--	--	--	--	--	--	<0.6 ⁷	--
	30	--	8,075-8,088	Miocene (Tm)	calcareous siliceous sh.	--	2.0	--	--	1.30	--	G, H
	31	--	8,075-8,088	-----do-----	-----do-----	--	2.0	--	--	1.29	--	G, H
	32	--	8,581-8,593	-----do-----	-----do-----	0.30±0.08	2.1	--	--	1.28	--	G, H
	33	--	8,692-8,704	-----do-----	-----do-----	0.30±0.02	2.3	--	--	1.14	--	G, H
	34	--	8,757-8,767	-----do-----	-----do-----	0.33±0.12	2.3	--	--	1.25	--	G, H
	35	--	8,791-8,799	-----do-----	-----do-----	0.33±0.01	2.3	--	--	1.26	--	G, H
	36	--	9,106-9,124	-----do-----	-----do-----	0.36±0.01	2.3	--	--	1.09	--	G, H
	37	--	9,155	-----do-----	-----do-----	0.38 ⁸	2.3	--	--	1.15	--	G, H
29	Well i:	sec. 25, T. 9 N., R. 34 W.										
	--	--	surface	--	--	--	--	--	--	--	<0.6 ⁷	--
	22	--	520-540	late Miocene-early Pliocene (Ts)	clayey siliceous sh.	0.21 ⁸	2.3	--	--	1.43	--	G, H
	23	--	1,191-1,216	-----do-----	-----do-----	0.35±0.07	2.3	--	--	1.14	--	G, H
	24	--	2,033-2,041	Miocene (Tm)	-----do-----	--	1.1	--	--	1.36	--	G, H
	25	--	2,435-2,447	-----do-----	-----do-----	--	1.1	--	--	1.32	--	G, H
	26	--	2,447-2,463	-----do-----	-----do-----	--	1.1	--	--	1.34	--	G, H
	27	--	2,785-2,790	-----do-----	-----do-----	0.31 ⁸	1.1	--	--	1.27	--	G, H
	28	--	3,247-3,265	Miocene (Tps)	-----do-----	--	1.3	--	--	1.30	--	G, H
	29	--	3,491-3,509	-----do-----	-----do-----	0.41±0.17	1.3	--	--	1.21	--	G, H
30	-- ⁹	T. 9 N., R. 36 W.		early Miocene (Tl and Tps)	sh., mdst., and ss.	-- ⁹	--	--	--	--	ranges from 0.6-1.3 to >1.3	I
31	FIG-2	T. 8 N., R. 29 W. 34°44'18" N., 119°55'23" W.	--	Late Jr-Early K (KJe)	concretion	1.00±0.05	3.0	454	0.03	--	0.6-1.3	A
	FIG-3	T. 8 N., R. 29 W. 34°44'22" N., 119°55'31" W.	--	-----do-----	-----do-----	1.06±0.11	--	467	0.05	--	0.6-1.3	A
	R2440A	sec. 16, T. 8 N., R. 29 W.	--	-----do-----	?	--	3-	--	--	--	0.6-1.3	D
	R2440B	-----do-----	--	-----do-----	?	--	3-/3	--	--	--	0.6-1.3	D
	2439A	-----do-----	--	-----do-----	?	--	3-	--	--	--	0.6-1.3	D
	2438A	-----do-----	--	-----do-----	?	--	3-	--	--	--	0.6-1.3	D
	2438B	sec. 21, T. 8 N., R. 29 W.	--	-----do-----	?	--	3	--	--	--	0.6-1.3	D
	2438C	-----do-----	--	-----do-----	?	--	3-	--	--	--	0.6-1.3	D
	2438D	-----do-----	--	-----do-----	?	--	3-/3	--	--	--	0.6-1.3	D
	2438E	-----do-----	--	-----do-----	?	--	3-/3	--	--	--	0.6-1.3	D
	R2437B	-----do-----	--	-----do-----	?	--	2+/3-	--	--	--	0.6-1.3 (0.6)	D
	R2437A	sec. 27, T. 8 N., R. 29 W.	--	-----do-----	?	--	2+/3-	--	--	--	0.6-1.3 (0.6)	D

Table 5. Locality, stratigraphic age, lithology, and thermal maturity data for surface and drill-hole samples, onshore Santa Maria and Santa Barbara-Ventura basin area, California—Continued

Map No.	Sample No. ¹	Location	Depth below surface (ft)	Stratigraphic age ² (Formation)	Lithology ³	R _o ⁴ (%)	TAI	T _{max} (°C)	PI	H/C	VRE (%)	Reference ⁵
32	Well j:	sec. 12, T. 8 N., R. 34 W.	surface	--	--	--	--	--	--	--	<0.67	--
	10	--	6,112-6,122	late Miocene-early Pliocene (Ts)	clayey siliceous sh.	0.32±0.05	1.8	--	--	1.22	--	G, H
	11	--	8,006-8,021	Miocene (Tm)	-----do-----	--	2.1	--	--	1.30	--	G, H
	12	--	8,006-8,021	-----do-----	-----do-----	--	2.1	--	--	1.23	--	G, H
	13	--	8,794-8,812	-----do-----	-----do-----	0.33±0.05	2.3	--	--	1.30	--	G, H
	14	--	9,509-9,515	-----do-----	-----do-----	--	2.5	--	--	1.03	--	G, H
	15	--	9,509-9,515	-----do-----	-----do-----	0.35±0.03	2.5	--	--	1.04	--	G, H
33	VF-80C-544 (87)	T. 7 N., R. 21 W.	--	Eocene (Tj)	slst.-sh.	--	--	446	0.09	--	0.6-1.3 (=0.6)	C
34	VF-80C-566 (101)	-----do-----	--	-----do-----	-----do-----	--	--	432	0.04	--	<0.6	C
35	VF-80C-569 (102)	T. 7 N., R. 22 W.	--	-----do-----	-----do-----	--	--	472	0.37	--	0.6-1.3 (=1.3)	C
	VF-80C-574 (105)	-----do-----	--	-----do-----	-----do-----	--	--	437	0.25	--	?0.6-1.3 (?=0.6)	C
36	VF-80C-570 (103)	-----do-----	--	-----do-----	-----do-----	--	--	436	0.06	--	<0.6	C
	VF-80C-573 (104)	-----do-----	--	-----do-----	-----do-----	--	--	421	0.17	--	?<0.6	C
	VF-80C-575 (106)	-----do-----	--	-----do-----	-----do-----	--	--	424	0.04	--	<0.6	C
	VF-80C-577 (107)	-----do-----	--	-----do-----	-----do-----	--	--	434	0.64	--	?<0.6	C
	R2735A	sec. 10, T. 7 N., R. 22 W.	--	?	?	--	2/2+	--	--	--	<0.6	D
	R2735B	-----do-----	--	?	?	--	2	--	--	--	<0.6	D
37	VF-80C-586 (108)	T. 7 N., R. 22 W.	--	Eocene (Tj)	slst.-sh.	--	--	455	0.20	--	0.6-1.3	C
	VF-80C-587 (109)	-----do-----	--	-----do-----	-----do-----	--	--	445	0.71	--	?0.6-1.3	C
	VF-80C-588 (110)	-----do-----	--	-----do-----	-----do-----	--	--	441	0.15	--	0.6-1.3	C
	R2535	sec. 16, T. 7 N., R. 22 W.	--	?	?	--	2+/3-	--	--	--	0.6-1.3 (0.6)	D
38	R2731G	sec. 30, T. 7 N., R. 23 W.	--	Eocene (Tcd)	?	--	2	--	--	--	<0.6	D
	R2731H	-----do-----	--	-----do-----	?	--	2/2+	--	--	--	<0.6	D
	R2731F	sec. 25, T. 7 N., R. 24 W.	--	-----do-----	?	--	2+	--	--	--	<0.6	D
	R2731D	sec. 36, T. 7 N., R. 24 W.	--	Eocene (Tma)	?	--	2+	--	--	--	<0.6	D
	R2731A	-----do-----	--	-----do-----	?	--	2+	--	--	--	<0.6	D
	R2741C	-----do-----	--	-----do-----	?	--	2+	--	--	--	<0.6	D
	R2730L	-----do-----	--	-----do-----	?	--	2+	--	--	--	<0.6	D
	R2730J	-----do-----	--	-----do-----	?	--	2/2+	--	--	--	<0.6	D
	R2730G	-----do-----	--	-----do-----	?	--	2	--	--	--	<0.6	D
39	R2730C	-----do-----	--	Eocene (Tcd)	?	--	2+/3-	--	--	--	0.6-1.3 (0.6)	D
	R2730D	-----do-----	--	-----do-----	?	--	2/2+	--	--	--	<0.6	D
	R2730E	-----do-----	--	-----do-----	?	--	2+	--	--	--	<0.6	D
	R2730F	-----do-----	--	-----do-----	?	--	2+/3-	--	--	--	0.6-1.3 (0.6)	D
40	Well k:	sec. 6, T. 7 N., R. 33 W.	surface	--	--	--	--	--	--	--	<0.67	--
	1	--	1,390-1,415	late Miocene-early Pliocene (Ts)	clayey siliceous sh.	0.34±0.30	1.1	--	--	1.27	--	G, H
	2	--	1,815-1,828	-----do-----	-----do-----	0.33±0.09	1.1	--	--	1.21	--	G, H
	3	--	2,600-2,618	Miocene (Tm)	-----do-----	0.37 ⁸	1.1	--	--	1.28	--	G, H
	4	--	2,751-2,755	-----do-----	-----do-----	--	1.1	--	--	1.30	--	G, H
	5	--	2,911-2,945	-----do-----	-----do-----	0.32±0.10	1.1	--	--	1.22	--	G, H
41	VF-81C-278 (22)	T. 6 N., R. 18 W.	--	Eocene (Tj)	slst.-sh.	--	--	493	0.16	--	?>1.3	C
42	VF-81C-966 (6)	T. 6 N., R. 19 W.	--	Miocene (Tr)	-----do-----	--	--	409	0.02	--	<0.6	C
	VF-81C-970 (7)	-----do-----	--	-----do-----	-----do-----	--	--	411	0.03	--	<0.6	C
	VF-81C-973 (8)	-----do-----	--	-----do-----	-----do-----	--	--	413	0.02	--	<0.6	C

Table 5. Locality, stratigraphic age, lithology, and thermal maturity data for surface and drill-hole samples, onshore Santa Maria and Santa Barbara-Ventura basin area, California—Continued

Map No.	Sample No. ¹	Location	Depth below surface (ft)	Stratigraphic age ² (Formation)	Lithology ³	R _o ⁴ (%)	TAI	T _{max} (°C)	PI	H/C	VRE (%)	Reference ⁵
43	VF-80C-560 (96)	T. 6 N., R. 20 W.	--	Eocene (Tj)	---do---	--	--	454	0.27	--	0.6-1.3	C
	VF-80C-561 (97)	-----do-----	--	---do---	---do---	--	--	451	0.20	--	0.6-1.3	C
	VF-80C-555 (91)	-----do-----	--	---do---	---do---	--	--	454	0.22	--	0.6-1.3	C
	VF-80C-595 (112)	-----do-----	--	---do---	---do---	--	--	2466	0.45	--	20.6-1.3	C
	VF-80C-558 (94)	-----do-----	--	---do---	---do---	--	--	438	0.14	--	0.6-1.3 (=0.6)	C
	R2740	sec. 17, T. 6 N., R. 20 W.	--	---do---	?	--	2+	--	--	--	<0.6	D
	R2445A	sec. 21, T. 6 N., R. 20 W.	--	---do---	?	--	3-	--	--	--	0.6-1.3	D
	R2445B	-----do-----	--	---do---	?	--	3-	--	--	--	0.6-1.3	D
	R2445C	-----do-----	--	---do---	?	--	3-	--	--	--	0.6-1.3	D
VF-80C-554 (90)	T. 6 N., R. 21 W.	--	---do---	slst.-sh.	--	--	450	0.16	--	0.6-1.3	C	
44	VF-80C-543 (86)	T. 6 N., R. 21 W.	--	---do---	---do---	--	--	437	0.05	--	<0.6	C
	VF-80C-542 (85)	-----do-----	--	---do---	---do---	--	--	410	0.03	--	<0.6	C
	VF-80C-540 (83)	-----do-----	--	---do---	---do---	--	--	428	0.19	--	?<0.6	C
	VF-80C-541 (84)	-----do-----	--	---do---	---do---	--	--	419	0.09	--	<0.6	C
	R2738B	sec. 3, T. 6 N., R. 21 W.	--	---do---	?	--	2-/2	--	--	--	<0.6	D
	R2738A	sec. 4, T. 6 N., R. 21 W.	--	---do---	?	--	2	--	--	--	<0.6	D
45	VF-80C-579 (80)	T. 6 N., R. 21 W.	--	Eocene (Tcd)	slst.-sh.	--	--	449	0.59	--	20.6-1.3	C
46	VF-80C-581 (78)	T. 6 N., R. 22 W.	--	---do---	---do---	--	--	452	0.36	--	0.6-1.3	C
47	VF-80C-592 (77)	-----do-----	--	Eocene (Tcw)	---do---	--	--	469	0.64	--	20.6-1.3 (?=1.3)	C
48	VF-80C-475 (55)	T. 6 N., R. 22 W.	--	Eocene (Tj)	---do---	--	--	450	0.15	--	0.6-1.3	C
	R2647L	sec. 30, T. 6 N., R. 22 W.	--	---do---	?	--	2/2+	--	--	--	<0.6	D
	R2647J	-----do-----	--	Eocene (Tma)	?	--	2/2+	--	--	--	<0.6	D
	R2647F	sec. 36, T. 6 N., R. 23 W.	--	Eocene (Tcd)	?	--	2/2+	--	--	--	<0.6	D
	R2647E	sec. 31, T. 6 N., R. 22 W.	--	---do---	?	--	2	--	--	--	<0.6	D
	TS-80C-206 (44)	T. 6 N., R. 23 W.	--	---do---	slst.-sh.	--	--	454	0.37	--	0.6-1.3	C
	TS-80C-204 (43)	-----do-----	--	---do---	---do---	--	--	443	0.16	--	0.6-1.3	C
	TS-80C-203 (42)	-----do-----	--	---do---	---do---	--	--	447	0.13	--	0.6-1.3	C
	VF-80C-474 (36)	T. 6 N., R. 22 W.	--	Eocene (Tcw)	---do---	--	--	452	0.11	--	0.6-1.3	C
R2647D	sec. 36, T. 6 N., R. 23 W.	--	---do---	?	--	2	--	--	--	<0.6	D	
49	Well I:	sec. 11, T. 6 N., R. 23 W.										
	--	--	surface	--	--	--	--	--	--	--	<0.6 ⁷	
	.. ¹⁰	--	771	Eocene	?	0.48 ¹⁰	--	--	--	--	--	J
50	R2650E	sec. 21, T. 6 N., R. 23 W.	--	Eocene (Tcd)	?	--	2/2+	--	--	--	<0.6	D
	R2650D	sec. 22, T. 6 N., R. 23 W.	--	---do---	?	--	2/2+	--	--	--	<0.6	D
	R2650C	-----do-----	--	---do---	?	--	2/2+	--	--	--	<0.6	D
	R2650B	-----do-----	--	---do---	?	--	2+	--	--	--	<0.6	D
	R2650A	-----do-----	--	---do---	?	--	2+	--	--	--	<0.6	D
	VF-80C-483 (56)	T. 6 N., R. 23 W.	--	Eocene (Tj)	slst.-sh.	--	--	446	0.07	--	20.6-1.3 (?=0.6)	C
	VF-80C-484 (57)	-----do-----	--	---do---	---do---	--	--	448	0.38	--	0.6-1.3	C
	R2648D	sec. 23, T. 6 N., R. 23 W.	--	---do---	?	--	2+	--	--	--	<0.6	D
	R2648E	-----do-----	--	---do---	?	--	2+	--	--	--	<0.6	D
R2648H	-----do-----	--	---do---	?	--	2+	--	--	--	<0.6	D	

Table 5. Locality, stratigraphic age, lithology, and thermal maturity data for surface and drill-hole samples, onshore Santa Maria and Santa Barbara-Ventura basin area, California—Continued

Map No.	Sample No. ¹	Location	Depth below surface (ft)	Stratigraphic age ² (Formation)	Lithology ³	R _o ⁴ (%)	TAI	T _{max} (°C)	PI	H/C	VRE (%)	Reference ⁵
51	R2650H	sec. 18, T. 6 N., R. 23 W.	--	Eocene (Tcw)	?	--	2	--	--	--	<0.6	D
	R2650G	-----do-----	--	Eocene (Tcd)	?	--	2/2+	--	--	--	<0.6	D
	R2650F	-----do-----	--	-----do-----	?	--	2/2+	--	--	--	<0.6	D
	TS-80C-250 (50)	T. 6 N., R. 23 W.	--	-----do-----	slst.-sh.	--	--	446	0.61	--	?0.6-1.3	C
	TS-80C-207 (45)	-----do-----	--	-----do-----	-----do-----	--	--	446	0.60	--	?0.6-1.3	C
	TS-80C-209 (46)	-----do-----	--	-----do-----	-----do-----	--	--	446	0.21	--	0.6-1.3	C
	TS-80C-211 (58)	-----do-----	--	Eocene (Tj)	-----do-----	--	--	451	0.24	--	0.6-1.3	C
	TS-80C-212 (59)	-----do-----	--	-----do-----	-----do-----	--	--	452	0.24	--	0.6-1.3	C
	TS-80C-215 (60)	-----do-----	--	-----do-----	-----do-----	--	--	445	0.10	--	0.6-1.3(=0.6)	C
	TS-80C-217 (61)	-----do-----	--	-----do-----	-----do-----	--	--	450	0.09	--	?0.6-1.3	C
	TS-80C-218 (62)	-----do-----	--	-----do-----	-----do-----	--	--	452	0.05	--	?0.6-1.3	C
	TS-80C-221 (63)	-----do-----	--	-----do-----	-----do-----	--	--	454	0.15	--	0.6-1.3	C
	TS-80C-222 (64)	-----do-----	--	-----do-----	-----do-----	--	--	459	0.11	--	0.6-1.3	C
	TS-80C-223 (65)	-----do-----	--	-----do-----	-----do-----	--	--	451	0.18	--	0.6-1.3	C
	TS-80C-225 (51)	-----do-----	--	Eocene (Tma)	-----do-----	--	--	461	0.14	--	0.6-1.3	C
	TS-80C-226 (52)	-----do-----	--	-----do-----	-----do-----	--	--	453	0.61	--	?0.6-1.3	C
	TS-80C-228 (53)	-----do-----	--	-----do-----	-----do-----	--	--	457	0.58	--	?0.6-1.3	C
	TS-80C-229 (47)	T. 6 N., R. 24 W.	--	Eocene (Tcd)	-----do-----	--	--	451	0.28	--	0.6-1.3	C
	TS-80C-230 (48)	T. 5 N., R. 24 W.	--	-----do-----	-----do-----	--	--	460	0.16	--	0.6-1.3	C
	TS-80C-231 (49)	-----do-----	--	-----do-----	-----do-----	--	--	449	0.04	--	?0.6-1.3	C
	TS-80C-234 (66)	-----do-----	--	Eocene (Tj)	-----do-----	--	--	450	0.16	--	0.6-1.3	C
	TS-80C-237 (67)	-----do-----	--	-----do-----	-----do-----	--	--	453	0.51	--	?0.6-1.3	C
	TS-80C-238 (68)	-----do-----	--	-----do-----	-----do-----	--	--	459	0.16	--	0.6-1.3	C
	TS-80C-239 (54)	-----do-----	--	Eocene (Tma)	-----do-----	--	--	464	0.21	--	0.6-1.3	C
52	BUC-1B	T. 6 N., R. 27 W.	--	Late Jr-Early K (KJe)	concretion	1.05±0.09	--	454	0.0	--	0.6-1.3	A
	BUC-2	34°35'07" N., 119°43'12" W.	--	-----do-----	-----do-----	0.95±0.11	3.0	--	--	--	0.6-1.3	A
		34°34'57" N., 119°43'21" W.	--			--	1+/-	--	--	--	<0.6	K
	BUC-3-2	T. 6 N., R. 27 W.	--	-----do-----	-----do-----	0.75±0.08	2.5-2.7	447	0.0	--	0.6-1.3	A
		34°34'51" N., 119°43'29" W.	--			--	1+	--	--	--	<0.6	K
	CAM-1-2	T. 6 N., R. 27 W.	--	-----do-----	slst.-sh.	0.74±0.05	--	454	0.08	--	0.6-1.3	A
		34°33'47" N., 119°42'20" W.	--			--	--	--	--	--	--	--
53	R2659C	T. 6 N., R. 31 W.	--	Eocene (Tcd)	?	--	1+/-	--	--	--	<0.6	D
54	R2658A	sec. ?13, T. 6 N., R. 32 W.	--	Late Jr-Early K (KJe)	?	--	2	--	--	--	<0.6	D
	R2658B	sec. ?24, T. 6 N., R. 32 W.	--	-----do-----	?	--	2	--	--	--	<0.6	D
	R2658C	-----do-----	--	-----do-----	?	--	2/2+	--	--	--	<0.6	D
	R2658E	-----do-----	--	-----do-----	?	--	2+	--	--	--	<0.6	D
55	R2657A	sec. ?25, T. 6 N., R. 34 W.	--	-----do-----	?	--	1+/-	--	--	--	<0.6	D
	R2657B	-----do-----	--	-----do-----	?	--	1+	--	--	--	<0.6	D
56	R2446	sec. ?27 (projected), T. 6 N., R. 18 W. ¹¹	--	Eocene (Tj)	?	--	2+	--	--	--	<0.6	D
	R2537	sec. 1, T. 5 N., R. 18 W.	--	?	?	--	2	--	--	--	<0.6	D
	VF-80C-598 (23)	T. 5 N., R. 18 W.	--	Eocene (Tj)	slst.-sh.	--	--	448	0.08	--	?0.6-1.3(=0.6)	C
57	--	sec. 4, T. 5 N., R. 18 W.	--	Eocene	?	0.63	--	--	--	--	0.6-1.3	L
	--	-----do-----	--	-----do-----	?	0.80	--	--	--	--	0.6-1.3	L
	--	-----do-----	--	-----do-----	?	0.67	--	--	--	--	0.6-1.3	L
	--	-----do-----	--	-----do-----	?	0.63	--	--	--	--	0.6-1.3	L
	--	-----do-----	--	-----do-----	?	0.66	--	--	--	--	0.6-1.3	L
58	VF-81C-313 (5)	T. 5 N., R. 19 W.	--	Miocene (Tr)	slst.-sh.	--	--	434	0.04	--	<0.6	C
	VF-81C-310 (4)	-----do-----	--	-----do-----	-----do-----	--	--	428	0.04	--	<0.6	C
	VF-81C-287 (2)	-----do-----	--	-----do-----	-----do-----	--	--	434	0.17	--	?<0.6	C

Table 5. Locality, stratigraphic age, lithology, and thermal maturity data for surface and drill-hole samples, onshore Santa Maria and Santa Barbara-Ventura basin area, California—Continued

Map No.	Sample No. ¹	Location	Depth below surface (ft)	Stratigraphic age ² (Formation)	Lithology ³	R _o ⁴ (%)	TAI	T _{max} (°C)	PI	H/C	VRE (%)	Reference ⁵
59	TS-80C-201 (37)	T. 5 N., R. 22 W.	--	Eocene (Tcw)	---do---	--	--	456	0.15	--	0.6-1.3	C
60	R2646J	sec. 1, T. 5 N., R. 23 W.	--	Eocene (Tcd)	?	--	2	--	--	--	<0.6	D
	VF-80C-470 (41)	T. 5 N., R. 23 W.	--	-----do-----	slst.-sh.	--	--	459	0.26	--	0.6-1.3	C
	VF-80C-468 (39)	-----do-----	--	-----do-----	---do---	--	--	456	0.15	--	0.6-1.3	C
	VF-80C-469 (40)	T. 5 N., R. 22 W.	--	-----do-----	---do---	--	--	459	0.36	--	0.6-1.3	C
	VF-80C-463 (38)	T. 5 N., R. 23 W.	--	-----do-----	---do---	--	--	459	0.45	--	0.6-1.3	C
	R2646G	sec. 1, T. 5 N., R. 23 W.	--	-----do-----	?	--	2+	--	--	--	<0.6	D
	R2646F	sec. 11, T. 5 N., R. 23 W.	--	-----do-----	?	--	2+	--	--	--	<0.6	D
	R2646E	sec. 10, T. 5 N., R. 23 W.	--	-----do-----	?	--	2+	--	--	--	<0.6	D
	R2646B	sec. 15, T. 5 N., R. 23 W.	--	-----do-----	?	--	2+	--	--	--	<0.6	D
	R2644A	sec. 14, T. 5 N., R. 23 W.	--	Eocene (Tcw)	?	--	2/2+	--	--	--	<0.6	D
	R2644C	sec. 15, T. 5 N., R. 23 W.	--	-----do-----	?	--	2+	--	--	--	<0.6	D
	R2644D	-----do-----	--	-----do-----	?	--	2+	--	--	--	<0.6	D
	R2644E	-----do-----	--	-----do-----	?	--	2+/3-	--	--	--	0.6-1.3 (0.6)	D
	R2644F	-----do-----	--	-----do-----	?	--	2+/3-	--	--	--	0.6-1.3 (0.6)	D
61	WC-15	-----do-----	--	Late K (Kj) ¹²	?	2.32±1.79	--	--	--	--	>1.3	M
	WC-1	-----do-----	--	-----do. ¹² -----	?	3.08±0.39	--	--	--	--	>1.3	M
	WC-14	-----do-----	--	-----do. ¹² -----	?	2.04±0.09	--	--	--	--	>1.3	M
	76-1-25	T. 5 N., R. 23 W.	--	K	?	2.44±0.02	--	--	--	--	>1.3	N
	WC-2	sec. 22, T. 5 N., R. 23 W.	--	Eocene (Tj) ¹²	?	1.74±0.14	--	--	--	--	>1.3	M
	WC-3	-----do-----	--	-----do. ¹² -----	?	1.94±0.04	--	--	--	--	>1.3	M
	WC-4	-----do-----	--	-----do. ¹² -----	?	1.88±0.06	--	--	--	--	>1.3	M
	WC-7	sec. 21, T. 5 N., R. 23 W.	--	-----do. ¹² -----	?	1.88±0.05	--	--	--	--	>1.3	M
	WC-8	-----do-----	--	-----do. ¹² -----	?	1.73±0.07	--	--	--	--	>1.3	M
	NF-80C-42 (27)	T. 5 N., R. 23 W.	--	-----do-----	slst.-sh.	--	--	2496	0.44	--	?>1.3	C
	NF-80C-41 (26)	-----do-----	--	-----do-----	---do---	--	--	475	0.39	--	>1.3 (=1.3)	C
	NF-80C-38 (25)	-----do-----	--	-----do-----	---do---	--	--	482	0.63	--	>1.3	C
	76-1-24	-----do-----	--	-----do-----	?	2.36±0.03	--	--	--	--	>1.3	N
	76-1-22	-----do-----	--	-----do-----	?	1.46±0.02	--	--	--	--	>1.3	N
62	WC-5	sec. 21, T. 5 N., R. 23 W.	--	-----do. ¹² -----	?	1.33±0.10	--	--	--	--	0.6-1.3 (=1.3)	M
	WC-6	-----do-----	--	-----do. ¹² -----	?	1.25±0.17	--	--	--	--	0.6-1.3 (=1.3)	M
	NF-80C-33 (24)	T. 5 N., R. 23 W.	--	-----do-----	slst.-sh.	--	--	460	0.59	--	0.6-1.3	C
	76-1-20	-----do-----	--	-----do-----	?	1.19±0.01	--	--	--	--	0.6-1.3	N
	76-1-18	-----do-----	--	Eocene (Tma)	?	1.02±0.02	--	--	--	--	0.6-1.3	N
	76-1-14	-----do-----	--	-----do-----	?	0.89±0.02	--	--	--	--	0.6-1.3	N
	WC-9	sec. 29, T. 5 N., R. 23 W.	--	-----do. ¹² -----	?	1.13±0.08	--	--	--	--	0.6-1.3	M
	WC-10	-----do-----	--	-----do. ¹² -----	?	1.33±0.06	--	--	--	--	?>1.3	M
	R2531P	-----do-----	--	-----do-----	?	--	3	--	--	--	0.6-1.3	D
	R2531K	sec. 28, T. 5 N., R. 23 W.	--	-----do-----	?	--	3	--	--	--	0.6-1.3	D
	R2531J	-----do-----	--	Eocene	?	--	3-	--	--	--	0.6-1.3	D
	NF-80C-26 (20)	T. 5 N., R. 23 W.	--	(Tma/Tcd contact) Eocene (Tcd)	slst.-sh.	--	--	468	0.39	--	0.6-1.3 (=1.3)	C
	R2645D	sec. 28, T. 5 N., R. 23 W.	--	-----do-----	?	--	2+/3-	--	--	--	0.6-1.3 (0.6)	D
	R2645G	-----do-----	--	-----do-----	?	--	2+/3-	--	--	--	0.6-1.3 (0.6)	D
	R2531I	-----do-----	--	-----do-----	?	--	3-	--	--	--	0.6-1.3	D
	R2531H	-----do-----	--	-----do-----	?	--	3-	--	--	--	0.6-1.3	D
	NF-80C-25 (19)	T. 5 N., R. 23 W.	--	-----do-----	slst.-sh.	--	--	458	0.29	--	0.6-1.3	C
	NF-80C-24 (18)	-----do-----	--	-----do-----	---do---	--	--	447	0.14	--	0.6-1.3	C
	R2531G	sec. 28, T. 5 N., R. 23 W.	--	-----do-----	?	--	3-	--	--	--	0.6-1.3	D
	R2531F	-----do-----	--	Eocene	?	--	3-	--	--	--	0.6-1.3	D
	WC-12	sec. 33, T. 5 N., R. 23 W.	--	(Tcd/Tcw contact) Eocene (Tcd) ¹²	?	0.97±0.42	--	--	--	--	0.6-1.3	M
	WC-13	-----do-----	--	-----do. ¹² -----	?	0.95±0.06	--	--	--	--	0.6-1.3	M
63	76-1-8	T. 5 N., R. 23 W.	--	-----do-----	?	0.42±0.01	--	--	--	--	<0.6	N
	76-1-7	-----do-----	--	Eocene (Tcw)	?	0.31±0.02	--	--	--	--	<0.6	N
64	MAT B2 (70)	T. 5 N., R. 24 W.	--	Eocene (Tj)	slst.-sh.	--	--	472	0.45	--	>1.3	C
	MAT B1 (69)	-----do-----	--	-----do-----	---do---	--	--	487	0.54	--	>1.3	C

Table 5. Locality, stratigraphic age, lithology, and thermal maturity data for surface and drill-hole samples, onshore Santa Maria and Santa Barbara-Ventura basin area, California—Continued

Map No.	Sample No. ¹	Location	Depth below surface (ft)	Stratigraphic age ² (Formation)	Lithology ³	R _o ⁴ (%)	TAI	T _{max} (°C)	PI	H/C	VRE (%)	Reference ⁵
65	FM-81C-141 (74)	-----do-----	--	----do----	---do---	--	--	449	0.47	--	?0.6-1.3	C
	THM M9 (73)	T. 5 N., R. 25 W.	--	----do----	---do---	--	--	438	0.07	--	?0.6-1.3 (≈0.6)	C
66	76-2-42	T. 5 N., R. 27 W.	--	Eocene (Tj) ¹³	?	2.25±0.03	--	--	--	--	>1.3	N
	76-2-46	-----do-----	--	Eocene (Tj)	?	1.52±0.04	--	--	--	--	>1.3	N
67	76-2-31	-----do-----	--	----do----	?	0.74±0.01	--	--	--	--	0.6-1.3	N
	76-2-27	-----do-----	--	----do----	?	1.20±0.02	--	--	--	--	0.6-1.3	N
	76-2-26	-----do-----	--	----do----	?	1.04±0.02	--	--	--	--	0.6-1.3	N
	76-2-25	-----do-----	--	----do----	?	1.12±0.02	--	--	--	--	0.6-1.3	N
	R2728C	sec. 27, T. 5 N., R. 27 W.	--	----do----	?	--	3-/3	--	--	--	0.6-1.3	D
	R2728B	sec. 26, T. 5 N., R. 27 W.	--	----do----	?	--	3-/3	--	--	--	0.6-1.3	D
	R2727M	-----do-----	--	----do----	?	--	3-/3	--	--	--	0.6-1.3	D
	R2727L	-----do-----	--	----do----	?	--	3	--	--	--	0.6-1.3	D
	76-2-22	T. 5 N., R. 27 W.	--	Eocene (Tma)	?	1.06±0.02	--	--	--	--	0.6-1.3	N
	76-2-14	-----do-----	--	Eocene (Ted)	?	0.61±0.01	--	--	--	--	0.6-1.3	N
	R2727K	sec. 35, T. 5 N., R. 27 W.	--	----do----	?	--	3-/3	--	--	--	0.6-1.3	D
	R2727J	-----do-----	--	----do----	?	--	3	--	--	--	0.6-1.3	D
	R2727G	-----do-----	--	----do----	?	--	3-	--	--	--	0.6-1.3	D
	R2727F	-----do-----	--	----do----	?	--	3-	--	--	--	0.6-1.3	D
	R2727E	-----do-----	--	----do----	?	--	3-	--	--	--	0.6-1.3	D
68	76-2-13	T. 5 N., R. 27 W.	--	Eocene (Tew)	?	0.56±0.01	--	--	--	--	<0.6	N
	76-2-11	-----do-----	--	----do----	?	0.61±0.02	--	--	--	--	?0.6-1.3	N
	76-2-8	-----do-----	--	----do----	?	0.50±0.01	--	--	--	--	<0.6	N
	76-2-6	-----do-----	--	----do----	?	0.31±0.02	--	--	--	--	<0.6	N
69	R2662B	sec. 17, T. 5 N., R. 28 W.	--	?	?	--	2+/3-	--	--	--	0.6-1.3 (0.6)	D
70	R2643O	sec. 6, T. 5 N., R. 30 W.	--	Paleocene-Eocene (Ta)	?	--	3-	--	--	--	0.6-1.3	D
	R2643N	-----do-----	--	-----do-----	?	--	3-	--	--	--	0.6-1.3	D
	R2643M	-----do-----	--	-----do-----	?	--	3-	--	--	--	0.6-1.3	D
71	R2643K	-----do-----	--	-----do-----	?	--	2+	--	--	--	<0.6	D
	R2441G	-----do-----	--	Eocene (Ted)	?	--	2	--	--	--	<0.6	D
	R2441E	sec. 7, T. 5 N., R. 30 W.	--	Eocene (Tsa)	?	--	2/2+	--	--	--	<0.6	D
	R2441C	-----do-----	--	-----do-----	?	--	2	--	--	--	<0.6	D
	R2441A	-----do-----	--	-----do-----	?	--	2+	--	--	--	<0.6	D
	R2643A	-----do-----	--	-----do-----	?	--	2/2+	--	--	--	<0.6	D
	R2643E	sec. 19, T. 5 N., R. 30 W.	--	Eocene-Oligocene (Tg)	?	--	2	--	--	--	<0.6	D
	R2643G	-----do-----	--	-----do-----	?	--	2	--	--	--	<0.6	D
72	DV 1	sec. 10, T. 5 N., R. 31 W.	--	Eocene (Tj) ¹⁴	?	0.63±0.02	--	--	--	--	0.6-1.3	M
	DV 2	-----do-----	--	----do. ¹⁴ ----	?	0.71±0.04	--	--	--	--	0.6-1.3	M
	DV 3	-----do-----	--	----do. ¹⁴ ----	?	0.88±0.04	--	--	--	--	0.6-1.3	M
	DV 4	-----do-----	--	----do. ¹⁴ ----	?	0.59±0.02	--	--	--	--	?0.6-1.3 (≈0.6)	M
73	--15	T. 5 N., R. 31 W.	--	Miocene (Tr)	calcareous and noncalcareous mdst., dol., sh.	--	--	--15	--	--	<0.6	O
74	R2659A	T. 5 N., R. 32 W.	--	?Eocene (?Tsa)	?	--	2/2+	--	--	--	<0.6	D

Table 5. Locality, stratigraphic age, lithology, and thermal maturity data for surface and drill-hole samples, onshore Santa Maria and Santa Barbara-Ventura basin area, California—Continued

Map No.	Sample No. ¹	Location	Depth below surface (ft)	Stratigraphic age ² (Formation)	Lithology ³	R _o ⁴ (%)	TAI	T _{max} (°C)	PI	H/C	VRE (%)	Reference ⁵
75	GAV-10-9	-----do-----	--	Miocene (Tm)	siliceous dolomitic mdst.	--	--	--	--	1.35	<0.6	G
	GAV-19-6	-----do-----	--	-----do-----	marl	--	--	--	--	1.37	<0.6	G
	GE-K-2B	-----do-----	--	-----do-----	--do--	0.33 ^{+0.45}	1.7	--	--	1.26	<0.6	H
	GE-K-3	-----do-----	--	-----do-----	--do--	-0.33	1.7	--	--	1.28	<0.6	H
76	476	sec. 22 (projected), T. 5 N., R. 33 W.	--	Late K (Kj)	?	0.82±0.10	--	--	--	--	0.6-1.3	M
	477	-----do-----	--	Paleocene-Eocene (Ta)	?	0.75±0.04	--	--	--	--	0.6-1.3	M
77	AUG-4C-11	T. 5 N., R. 33 W.	--	Miocene (Tm)	dolostone	--	--	--	--	1.38	<0.6	G
	AUG-4C-13	-----do-----	--	-----do-----	phosphatic dolostone	--	--	--	--	1.38	<0.6	G
	AUG-4C-25	-----do-----	--	-----do-----	marl	--	--	--	--	1.37	<0.6	G
	AUG-6B-14	-----do-----	--	-----do-----	--do--	--	--	--	--	1.35	<0.6	G
	AUG-6C-9	-----do-----	--	-----do-----	--do--	--	--	--	--	1.38	<0.6	G
	AUG-7B-5	-----do-----	--	-----do-----	calcareous chert	--	--	--	--	1.41	<0.6	G
	AUG-7B-15	-----do-----	--	-----do-----	calcareous siliceous sh.	--	--	--	--	1.41	<0.6	G
	AUG-6C-10B	-----do-----	--	-----do-----	dolostone	--	--	--	--	1.30	<0.6	G
78	BIX-3-3	T. 5 N., R. 34 W.	--	-----do-----	calcareous porcelanite	--	--	--	--	1.36	<0.6	G
	BIX-6B-13	-----do-----	--	-----do-----	quartz chert	--	--	--	--	1.45	<0.6	G
	BIX-7-6B	-----do-----	--	-----do-----	porcelanite	--	--	--	--	1.33	<0.6	G
	BLK-5-2	-----do-----	--	-----do-----	calcareous siliceous sh.	--	--	--	--	1.29	<0.6	G
	BLK-7A-10	-----do-----	--	-----do-----	chert	--	--	--	--	1.37	<0.6	G
	BLK-7A-13	-----do-----	--	-----do-----	porcelanite	--	--	--	--	1.36	<0.6	G
	BLK-K-1	-----do-----	--	-----do-----	calcareous siliceous sh.	--	1.5	--	--	1.37	<0.6	H
	DAM-7D-1	-----do-----	--	-----do-----	siliceous dolomitic sh.	--	--	--	--	1.38	<0.6	G
	DAM-7D-3	-----do-----	--	-----do-----	dolomitic porcelanite	--	--	--	--	1.33	<0.6	G
	DAM-8C-1	-----do-----	--	-----do-----	siliceous mdst.	--	--	--	--	1.34	<0.6	G
	DAM-8C-4	-----do-----	--	-----do-----	siliceous sh.	--	--	--	--	1.35	<0.6	G
	DAM-8C-7	-----do-----	--	-----do-----	porcelanite	--	--	--	--	1.37	<0.6	G
	WOOD-3-3	-----do-----	--	-----do-----	calcareous siliceous sh.	--	--	--	--	1.34	<0.6	G
	WOOD-4-2	-----do-----	--	-----do-----	marl	--	--	--	--	1.33	<0.6	G
	WOOD-5-1	-----do-----	--	-----do-----	quartz chert	--	--	--	--	1.41	<0.6	G
	WOOD-5-4	-----do-----	--	-----do-----	marl	--	--	--	--	1.30	<0.6	G
	WOOD-5-4dk	-----do-----	--	-----do-----	--do--	--	--	--	--	1.44	<0.6	G
	BIX-7-2	-----do-----	--	-----do-----	porcelanite	--	--	--	--	1.28	<0.6	G
	WOOD-3-1	-----do-----	--	-----do-----	marl	--	--	--	--	1.30	<0.6	G
	WOOD-9-1	-----do-----	--	-----do-----	quartz chert	--	--	--	--	1.46	<0.6	G
79	HOP-4-1E	T. 4 N., R. 19 W. 34°25'10" N., 118°49'58" W.	--	-----do-----	slst.-sh.	0.32±0.01	--	412	0.02	--	<0.6	A
80	VF-81C-288 (3)	T. 4 N., R. 19 W.	--	Miocene (Tr)	--do--	--	--	428	0.07	--	<0.6	C
	VF-81C-281 (1)	T. 4 N., R. 20 W.	--	Miocene (Tm)	--do--	--	--	416	0	--	<0.6	C

Table 5. Locality, stratigraphic age, lithology, and thermal maturity data for surface and drill-hole samples, onshore Santa Maria and Santa Barbara-Ventura basin area, California—Continued

Map No.	Sample No. ¹	Location	Depth below surface (ft)	Stratigraphic age ² (Formation)	Lithology ³	R_o^4 (%)	TAI	T_{max} (°C)	PI	H/C	VRE (%)	Reference ⁵
81	SMR-B	T. 4 N., R. 23 W. 34°24.4' N., 119°14' W.	--	-----do-----	siliceous marl	--	--	415	0.02	--	<0.6	P
	SMR-D	-----do-----	--	-----do-----	-----do-----	--	--	414	0.02	--	<0.6	P
	SMR-E	-----do-----	--	-----do-----	siliceous	--	--	423	0.0	--	<0.6	P
	SMR-G	-----do-----	--	-----do-----	calcareous sh. calcareous sh.	--	--	425	0.0	--	<0.6	P
82	RIN-K-1	T. 4 N., R.25 W. 34°22.8' N., 119°29' W.	--	-----do-----	calcareous siliceous sh.	0.24±0.05	1.5	401	0.06	1.35	<0.6	P, H
	RIN-K-3	-----do-----	--	-----do-----	-----do-----	0.24±0.06	1.7	398	0.12	1.30	<0.6	P, H
	RIN-5-1	-----do-----	--	-----do-----	calcareous	--	--	404	0.13	--	?<0.6	P
	RIN-5-10	-----do-----	--	-----do-----	porcelanite diatomaceous calcareous sh.	--	--	398	0.11	--	<0.6	P
83	UGO-2B-1B	T. 4 N., R. 28 W.	--	-----do-----	-----do-----	0.21 ^{+0.36} -0.21	1.1	408	0.07	1.47	<0.6	P, H
	UGO-2-5C	-----do-----	--	-----do-----	-----do-----	--	--	411	0.07	--	<0.6	P
	UGO-2-10	-----do-----	--	-----do-----	-----do-----	--	--	406	0.12	--	?<0.6	P
	UGO-2B-11	-----do-----	--	-----do-----	-----do-----	0.28 ⁸	1.1	408	0.10	1.37	<0.6	P, H
84	NAP-1-1	T. 4 N., R. 29 W.	--	-----do-----	siliceous sh.	--	--	--	--	1.43	<0.6	G
	NAP-11-5	-----do-----	--	-----do-----	marl	--	--	--	--	1.42	<0.6	G
	NAP-12-6	-----do-----	--	-----do-----	calcareous	--	--	--	--	1.30	<0.6	G
	NAP-13-3	-----do-----	--	-----do-----	diatomaceous sh. chert	--	--	--	--	1.34	<0.6	G
85	CAP-6R-3	T. 4 N., R. 30 W.	--	-----do-----	calcareous chert	--	--	--	--	1.40	<0.6	G
	CAP-6-4	-----do-----	--	-----do-----	marl	--	--	--	--	1.39	<0.6	G
	CAP-6-11	-----do-----	--	-----do-----	calcareous siliceous rock	--	--	--	--	1.42	<0.6	G
86	REF-6-6	T. 4 N., R. 31 W. (NE.)	--	-----do-----	calcareous siliceous mdst.	--	--	--	--	1.37	<0.6	G
87	Well m: --	T. 4 N., R. 34 W. -- --	surface to 4,606	-- Eocene (Tj) to Miocene (Tr)	-- ? ?	-- ..16 ..16	-- -- --	-- -- --	-- -- --	-- -- --	<0.6 ⁷	-- N
88	LSC-6-8	T. 3 N., R. 24 W. 34°21.8' N., 119°24.7' W.	--	Miocene (Tm)	calcareous porcelanite	--	--	403	0.07	--	<0.6	P
	LSC-6-10	-----do-----	--	-----do-----	calcareous siliceous sh.	--	--	403	0.05	--	<0.6	P
	LSC-6-11A	-----do-----	--	-----do-----	-----do-----	--	--	398	0.05	--	<0.6	P
	LSC-6-12A	-----do-----	--	-----do-----	-----do-----	--	--	397	0.07	--	<0.6	P
89	SIM-3	sec. 11, T. 2 N., R. 17 W. 34°16'29" N., 118°37'36" W.	--	Late K (Kc)	slst.-sh.	0.53±0.03	2.5	426	0.0	--	<0.6	A K
	SIM-4	sec. 11, T. 2 N., R. 17 W. 34°16'32" N., 118°37'26" W.	--	-----do-----	-----do-----	0.55±0.03	--	--	--	--	<0.6	A K
	SUS-1B	sec. 12, T. 2 N., R. 17 W. 34°16'19" N., 118°36'18" W.	--	-----do-----	-----do-----	0.50±0.03	--	--	--	--	<0.6	A K

Table 5. Locality, stratigraphic age, lithology, and thermal maturity data for surface and drill-hole samples, onshore Santa Maria and Santa Barbara-Ventura basin area, California—Continued

Map No.	Sample No. ¹	Location	Depth below surface (ft)	Stratigraphic age ² (Formation)	Lithology ³	R _o ⁴ (%)	TAI	T _{max} (°C)	PI	H/C	VRE (%)	Reference ⁵
90	Well n:	sec. 9, T. 2 N., R. 22 W. 34°16'07" N., 119°11'48" W.										
--	--	--	surface	--	--	--	--	--	--	--	<0.67	--
	272A	--	13,080-13,098	Plio-Pleistocene (QTP)	?	0.35±0.0517	--	--	--	--	--	Q
	272B	--	13,988	--do--	?	0.38±0.0617	--	--	--	--	--	Q
	272C	--	14,526-14,537	--do--	?	0.39±0.0617	--	--	--	--	--	Q
	272D	--	16,017-16,023	Pliocene ¹⁸	?	0.42±0.0617	--	--	--	--	--	Q
	272E	--	16,813-16,832	----do,18--	?	0.38±0.0517	--	--	--	--	--	Q
	272F	--	18,296-18,304	----do,18--	?	0.43±0.0717	--	--	--	--	--	Q
	272G	--	18,428-18,438	----do,18--	?	0.40±0.0617	--	--	--	--	--	Q
	272H	--	18,711-18,721	----do,18--	?	0.43±0.0717	--	--	--	--	--	Q
91	Well o:	sec. 23, T. 2 N., R. 23 W. 34°14'35" N., 119°15'06" W.										
--	--	--	surface	--	--	--	--	--	--	--	<0.67	--
	284A	--	4,343-4,352	Plio-Pleistocene (QTsb)	?	0.30±0.0517	--	--	--	--	--	Q
	284B	--	5,100-5,108	----do-----	?	0.32±0.0517	--	--	--	--	--	Q
	284C	--	6,058-6,068	Plio-Pleistocene (QTP)	?	0.29±0.0417	--	--	--	--	--	Q
	284D	--	6,746-6,756	----do-----	?	0.31±0.0517	--	--	--	--	--	Q
	284E	--	7,135-7,140	----do-----	?	(0.31) ¹⁹	--	--	--	--	--	Q
	284F	--	7,368-7,373	----do-----	?	0.34±0.0517	--	--	--	--	--	Q
	284G	--	7,925-7,935	----do-----	?	0.35±0.0417	--	--	--	--	--	Q
	284H	--	8,405-8,415	----do-----	?	0.41±0.0617	--	--	--	--	--	Q
	284I	--	8,568-8,578	----do-----	?	0.37±0.0517	--	--	--	--	--	Q
	284K	--	9,058-9,066	----do-----	?	0.37±0.0517	--	--	--	--	--	Q
	284L	--	9,422-9,442	----do-----	?	0.36±0.0517	--	--	--	--	--	Q
	284M	--	9,611-9,622	----do-----	?	0.38±0.0617	--	--	--	--	--	Q
	284N	--	9,997-10,014	----do-----	?	0.39±0.0517	--	--	--	--	--	Q
	284O	--	10,394-10,402	----do-----	?	0.30±0.0417	--	--	--	--	--	Q
	284P	--	10,763-10,779	----do-----	?	0.34±0.0517	--	--	--	--	--	Q
	284Q	--	11,168-11,185	----do-----	?	0.41±0.0617	--	--	--	--	--	Q
	284R	--	11,967-11,977	----do-----	?	0.32±0.0517	--	--	--	--	--	Q
	284S	--	12,128-12,144	----do-----	?	0.37±0.0517	--	--	--	--	--	Q
	284U	--	13,105-13,125	----do-----	?	0.34±0.0417	--	--	--	--	--	Q
	284V	--	13,473-13,477	----do-----	?	0.36±0.0517	--	--	--	--	--	Q
	284W	--	14,420-14,435	----do-----	?	0.37±0.0517	--	--	--	--	--	Q
	284X	--	15,100-15,112	----do-----	?	0.35±0.0417	--	--	--	--	--	Q
	284Y	--	16,493-16,503	Pliocene ¹⁸	?	0.40±0.0617	--	--	--	--	--	Q
	284Z	--	16,694-16,697	----do,18--	?	0.38±0.0517	--	--	--	--	--	Q
	284AA	--	16,950-16,967	----do,18--	?	0.45±0.0617	--	--	--	--	--	Q
92	MUH-2	T. 1 N., R. 16 W. 34°07'51" N., 118°32'19" W.	--	Late Jr (Jsm)	slate	2.81±0.61	--	--	--	--	>1.3	A
93	MUH-4-1	T. 1 N., R. 16 W. 34°07'35" N., 118°33'11" W.	--	Late K	sh.	0.65±0.02	--	422	0.0	--	0.6-1.3	A
94	TOP-1	T. 1 S., R. 16 W. 34°04'01" N., 118°35'08" W.	--	--do--	slst.-sh.	0.72±0.08	2.5-3.0	444	0.0	--	0.6-1.3	A
	TUN-3B	T. 1 S., R. 16 W. 34°03'18" W., 118°35'57" W.	--	?do--	---do---	0.95±0.04	3.0	--	--	--	0.6-1.3	A
95	CC-3	T. 1 S., R. 18 W. 34°04'12" N., 118°45'12" W.	--	K-early T	---do---	3.94±0.10	4.0	--	--	--	>1.3	A
	CC-2	-----do-----	--	---do---	---do---	4.16±0.77	--	--	--	--	>1.3	A
96	--	sec. 15, T. 1 S., R. 21 W.	--	Miocene (Tt)	?	0.7-1.9	--	--	--	--	0.6-1.3 to >1.3	L

Table 5. Locality, stratigraphic age, lithology, and thermal maturity data for surface and drill-hole samples, onshore Santa Maria and Santa Barbara-Ventura basin area, California—Continued

¹Wells, with operator at the time of drilling and API number (in parentheses):

- a* = Western Gulf Oil Huasna Community No. 1 (04-079-00250)
- b* = Tar Springs # 1 (probably Superior Oil Tar Springs Ranch No. 1; 04-079-00507)
- c* = Tar Springs # 2 (exact location, operator, and API number uncertain)
- d* = C.W. Colgrove Elberta No. 1-5 (04-079-00637)
- e* = Holmes No. 1 (probably Los Nietos Holmes No. 1; 04-079-00654)
- f* = Phillips Petroleum Porter D No. 2 (04-079-20517)
- g* = Union Oil of California SMVU Signal-Brown No. 1 (04-083-02834)
- h* = Los Nietos Los Nietos-Gulf S.S.T. No. 25-11 (04-083-04065)
- i* = Union Oil of California Newlove No. 51 (04-083-02306)
- j* = Union Oil of California Harris A-2 (04-083-04094)
- k* = Pinal Dome Corporation Union Annex No. 1 (04-083-01831)
- l* = Standard Oil of California Hattie Russell No. 1
- m* = Standard Oil of California Gerber No. 1
- n* = Superior Oil Limoneira No. 1
- o* = Standard Oil of California Maxwell No. 1

²Stratigraphic age based on age assignment in cited reference: Jr, Jurassic; K, Cretaceous; T, Tertiary. Formation names are abbreviated as follows: Jsm, Santa Monica Slate; Kc, Chatsworth Formation; Kj, Jalama Formation; Kjo, Jollo Formation; KJe, Espada Formation; KJf, Franciscan Complex; KJt, Toro Formation; QTsb, Santa Barbara Formation; QTp, Pico Formation; Ta, Anita Formation; Ted, Cozy Dell Shale; Tcw, Coldwater Sandstone; Tg, Gaviota Formation; Tj, Juncal Formation; Tl, Lospe Formation; Tm, Monterey Formation; Tma, Matilija Sandstone; Tps, Point Sal Formation; Tr, Rincon Shale; Ts, Sisquoc Formation; Tsa, Sacate Formation; Tsi, Simmler Formation; Tt, Topanga Formation.

³Lithology: dol., dolomite; mdst., mudstone; ss., sandstone; sh., shale; slts., siltstone.

⁴Uncertainty calculated as 95 percent confidence limits.

⁵References:

- A = present study
- B = M.B. Underwood (written commun., 1985)
- C = Frizzell and Claypool (1983); number in parentheses under "Sample No." is map number listed in Frizzell and Claypool (1983, table 4); see Frizzell and Claypool (1983) for more detailed locality information.
- D = Frederiksen (1985) and N.O. Frederiksen (written commun., 1985); see Frederiksen (1985) for more detailed locality information.
- E = Kablanow and Surdam (1984)
- F = Surdam and Stanley (1984)
- G = Isaacs (1980) and C.M. Isaacs, unpub. data
- H = Isaacs and Tomson (1990)
- I = Stanley and others (1993, 1995)
- J = T.H. McCulloh (written commun., 1995)

⁶Map number 2 comprises 18 samples collected along the coast from the San Simeon Creek area to south of Point Estero (map A, pl.1); 16 of these samples yield percent R_o values in the range 0.6 to 1.2, and two samples yield percent R_o greater than 1.2.

⁷VRE of surface rocks, extrapolated from drill-hole data.

⁸Vitrinite reflectance based on one measured value.

⁹Map number 30 comprises 16 samples collected through a 283.7-m (approximately 931-ft) thick vertical section of lower Miocene Lospe Formation and overlying lower Miocene Point Sal Formation in the North Beach section of Stanley and others (1995); percent R_o values range from 0.68 to 1.56, with a mean of 1.29.

¹⁰Series of samples recovered from Eocene rocks between 235 m (771 ft) and 2,900 m (9,514 ft) depth yield percent R_o values ranging from 0.48 (at 771 ft) to 2.1 (at 9,514 ft).

¹¹Sample is plotted incorrectly in Frederiksen (1985) (N.O. Frederiksen, written commun., 1985). Sample site is on Piru Creek in sec. ?27 (projected), T. 6 N., R. 18 W., in Los Angeles County, about 305 m (1,000 ft) north of the point where Piru Creek crosses the Ventura-Los Angeles county line.

¹²Position in section: WC-1: 305 m (1,000 ft) below Cretaceous/Eocene (K/E) contact; WC-2--WC-4: 30-46 m (100-150 ft) above K/E contact; WC-5, WC-6: 914-975 m (3,000-3,200 ft) above K/E contact; WC-7, WC-8: 701-732 m (2,300-2,400 ft) above K/E contact; WC-9, WC-10: 1,676 m (5,500 ft) above K/E contact; WC-12: 2,743 m (9,000 ft) above K/E contact; WC-13: 2,957 m (9,700 ft) above K/E contact; WC-14: 244 m (800 ft) below K/E contact; WC-15: 457 m (1,500 ft) below K/E contact (P.C. van de Kamp, written commun., 1987).

¹³Camino Cielo Sandstone Member.

¹⁴Position in section: DV 1: 152 m (500 ft) above lower Eocene-middle Eocene (IE-mE) contact; DV 2: 366 m (1,200 ft) above IE-mE contact; DV 3: 335 m (1,100 ft) above IE-mE contact; DV 4: 274 m (900 ft) above IE-mE contact (P.C. van de Kamp, written commun., 1987).

¹⁵Map number 73 comprises 51 samples collected in a measured section through the Tajiguas Landfill, located on the east side of Cañada de la Pila, about 40 km (about 25 mi) west of Santa Barbara; T_{max} values range from 409 to 432, with a mean of 425 (Stanley and others, 1992).

¹⁶Subsurface samples from Miocene (Rincon Shale) into Eocene (Juncal Formation) at 4,606-ft (1,404-m) depth are immature (Helmold, 1980); see also Helmold and van de Kamp (1984) and Frederiksen (1985).

¹⁷Uncertainty calculated as sum of standard error of the mean and a factor (0.10 x mean percent R_o) added to reflect the error that may have been introduced by measuring more than one variety of vitrinite in any given sample (Bostick and others, 1978).

¹⁸Rocks contain foraminiferal faunas indicative of Natland's (1957) basal "Repettian" benthonic foraminiferal stage and are "almost certainly Pliocene in age" (Bostick and others, 1978).

¹⁹Vitrinite reflectance based on two measured values.

and R_o , TAI, T_{max} , PI, and H/C ratios from 20 other published and unpublished sources in the public domain. Available maturity data in some parts of the study area are very sparse (map A, pl. 1; table 5), necessitating broad assumptions and extrapolations in mapping (map A, pl. 1) and leaving open the likelihood that, certainly in detail, maturity is more complex than indicated.

Region 1—Basement: This region of the southern Coast Ranges north of the Santa Maria basin is dominated by the Franciscan Complex that forms most of the coastal region from the northern edge of the map area south to Estero Bay and at the northern end of San Luis Obispo Bay and extends inland to southeast of San Luis Obispo. The rocks are assumed to be everywhere overmature with respect to oil generation ($VRE > 1.3$ percent). Data from two samples at map number (map no.) 1 (map A, pl. 1; table 5) indicate that VRE of the enclosed Upper Jurassic and Lower Cretaceous Toro Formation is > 1.3 percent.

Region 2—Tertiary sliver in area of T. 27 S., R. 10 E.: One of several small slivers of Miocene rocks within the area dominated by the Franciscan Complex rocks of Region 1 and Cretaceous rocks of Region 4. Additional areas of Miocene rock occur in Regions 1 and 4 (Jennings, 1958) but are too small to show on maps A and B, pl. 1. These Miocene rocks were not sampled but are assumed to have $VRE < 0.6$ percent, except possibly where associated with Miocene volcanic rocks (Jennings, 1958).

Region 3—Cretaceous: Vitrinite reflectance measurements on 18 samples collected along the coast from San Simeon Beach State Park (T. 27 S., R. 8 E.) south to northern Estero Bay (T. 28 S., R. 10 E.) (map no. 2) indicate that the Upper Cretaceous rocks (Jennings, 1958; Vedder and others, 1983) in this area are thermally mature ($VRE = 0.6$ to 1.3 percent).

Region 4—Cretaceous: In the northern part of this region, R_o , TAI, T_{max} , and PI data from samples collected from Cretaceous(?) rocks in outcrops more than 20 km apart (map no. 3, 7) indicate overmaturity, with a VRE of greater than or equal to approximately 1.75 percent. Rocks at map no. 3 were collected in an area close to the basement-Cretaceous contact, and their age assignment is uncertain. Rocks at map no. 7 were identified as Cretaceous by Frizzell and Claypool (1983) but are located within an area mapped as Franciscan Complex by Jennings (1958). Cretaceous rocks in the northern part of Region 4 are mapped as overmature with respect to oil generation (> 1.3 percent VRE) (map A, pl. 1) based on the data from map no. 3 and 7, but, because of the uncertainty in the age of the analyzed rocks, more data are needed to confirm the level of maturity of the Cretaceous section.

To the south, a sample collected from Upper Cretaceous rocks (Jennings, 1958) (map no. 5) near the Miocene Monterey Formation (map no. 4, 6) of Region 7 is only marginally mature ($VRE \approx 0.6$ percent).

Region 5—Upper Jurassic and Cretaceous: Maturity data indicate that Cretaceous strata in this area range from mar-

ginally mature ($VRE \approx 0.6$ percent) to overmature ($VRE > 1.3$ percent) with respect to oil generation, although in some samples there is less internal consistency among maturity indicators than in samples from Region 4 (as, for example, in the sample at map no. 25, table 5). Maturity is greatest ($VRE > 1.3$ percent) in a sample of Lower Cretaceous Jollo Formation (map no. 18) and in Upper Cretaceous rocks (Jennings, 1977; Vedder and others, 1983) (map no. 19, 20) in the central part of the area. What are probably the least mature samples were collected in Upper Cretaceous and lower Tertiary rocks (at map no. 26) near the contact with lower Miocene(?) rocks (Jennings, 1959) of Region 7.

Region 6—Basement: These rocks are considered overmature with respect to oil generation on the basis of Rock-Eval pyrolysis T_{max} values determined on Franciscan Complex samples from the northeastern and southwestern edges of the outcrop area (map no. 21, 22).

Region 7—Tertiary rocks, Santa Maria basin and Huasna-Pismo basin area: Tertiary strata dominate exposed rocks in the Santa Maria and Huasna-Pismo basins. Available data from TAI measurements on Paleogene rocks on the basin margins (map no. 9, 53); TAI, Rock-Eval pyrolysis, and H/C data from the Miocene Monterey Formation in the extreme northeast of the region (map no. 4, 6, 8, 16); and VRE extrapolated from R_o , TAI, PI, and H/C maturity data from scattered drill holes (map no. ?10, 14, 15, 24, 27-29, 32, 40) indicate that VRE of exposed Tertiary rocks in the Santa Maria and Huasna-Pismo basins is < 0.6 percent. The one known exception to this general rule occurs near Point Sal (map no. 30), where samples collected from the lower Miocene Lospe Formation and overlying lower Miocene Point Sal Formation yielded unusually high R_o values, ranging from 0.68 to 1.56 percent with a mean of 1.29 percent. These high values possibly result from heating associated with a local high-temperature hydrothermal system and (or) emplacement of a gabbro sill (Stanley and others, 1993, 1995). Similarly, Miocene rocks may also be more mature in local areas, as in the vicinity of the West Huasna fault, where they are associated with Miocene volcanic rocks (Jennings, 1958, 1959).

The drill-hole data (map no. 14, 15, 24, 27-29, 32, 40) further suggest that Tertiary rocks are immature to significant depths in the subsurface. Samples of lower Pliocene-upper Miocene Sisquoc Formation, Miocene Monterey Formation, and lower Miocene Point Sal Formation yield VRE values ranging from < 0.6 percent to approximately 0.6 percent (in the lower part of well *d*, map no. 15) to depths as great as about 2,620 m (about 8,600 ft) below surface, based on R_o , TAI, PI, and (or) H/C data (table 5). Below about 2,620 m (about 8,600 ft) (in drill holes *h* and *j*; map no. 28, 32), maturity indicators in the Monterey Formation yield internally conflicting results. In particular, TAI and to some extent H/C ratios indicate higher maturity than indicated by vitrinite reflectance (Isaacs and Tomson, 1990) and suggest that VRE may be > 0.6 percent. The interpretation of the TAI and H/C data is uncertain, however. In drill hole *i* (map no.

29) TAI measurements on samples from the Sisquoc Formation similarly suggest higher maturity than indicated by R_o , but these samples were recovered from depths of only 158 m to 371 m (520 ft to 1,216 ft) below surface and are underlain by Monterey and Point Sal rocks in which TAI, R_o , and H/C ratios all indicate VRE less than 0.6 percent (table 5).

In summary, available maturity data indicate that, with the exception of areas such as Point Sal, Tertiary strata in the Santa Maria and Huasna-Pismo basins yield VRE<0.6 percent, and thus are immature, everywhere at the surface and to significant depths in the subsurface. This simple picture, however, almost certainly obscures the actual maturity of these rocks with respect to oil generation, both because of the scarcity of maturity data in Region 7 and because of the questionable reliability of the maturity indicators in these rocks, particularly in the Monterey Formation.

Few data are available from the Paleogene part of the Tertiary section. On the southern margin of the Santa Maria basin, just north of the Santa Ynez fault, Paleogene strata (for example, Eocene Cozy Dell Shale at map no. 53), along with isolated Upper Jurassic and Lower Cretaceous Espada Formation (Dibblee, 1950) outcrops (sampled at map no. 54, 55), are mapped as immature but may be mature; the only maturity data available for these rocks are Frederiksen's (1985) TAI measurements that elsewhere in the study area appear to yield anomalously low maturity values (see discussion under "Thermal Alteration Index" and "Region 11"). However, in the Point Conception OCS-Cal 78-164 no. 1 (COST) well, located about 16 km (10 mi) offshore southwest of Point Conception (lat 34°28'56.6" N., long 120°47'0" W.), the Espada Formation yields an R_o of only 0.68 percent at 3,185 m (10,450 ft) drilled depth (Bostick, 1979; T.H. McCulloh, written commun., 1995). This suggests that Espada Formation rocks sampled onshore at map no. 54 and 55 and Eocene rocks at map no. 53 may in fact be immature, although maturity may be higher than the about <0.2 to about 0.5 percent VRE indicated by TAI measurements. Frederiksen's (1985) TAI measurements are also the only maturity data available from the only other Paleogene strata sampled in Region 7 (Oligocene and lower Miocene Simmler Formation at map no. 9).

In the Neogene section, all of the surface samples and all but a few of the subsurface samples that yield VRE<0.6 percent are from the Monterey Formation. A number of studies present evidence of the anomalous behavior of conventional maturity indicators, particularly R_o , in Monterey and equivalent source rocks in coastal California basins. In particular, they cite cases in which R_o values (a) are as low as 0.3-0.4 percent, significantly below the conventional boundary of the "oil window," in rocks that almost certainly have generated oil; (b) indicate lower maturity than one or more other maturity indicators; and (or) (c) show poor correlation with depth or inferred maximum temperatures through a significant vertical thickness of rock (for example, McCulloh, 1979; Petersen and Hickey, 1983, 1987; Walker and others,

1983; Isaacs and Magoon, 1984; Orr, 1984; Isaacs and Petersen, 1987; Isaacs, 1988; Pytte, 1989; Baskin and Peters, 1992; Stanley and others, 1995; T.H. McCulloh, written commun., 1995). The low R_o values in these rocks are variously attributed to one or both of the following:

(1) Early generation of oil in the Monterey at thermal exposures significantly lower than those normally attributed to the onset of oil generation, possibly due to the presence of high-sulfur kerogen in these rocks and the relative ease of breaking carbon-sulfur bonds, as compared with carbon-carbon bonds (see also Dunham and others, 1991).

(2) Suppression of R_o , possibly due to the presence of oil, significant concentrations of hydrogen-rich amorphous algal material, and (or) high concentrations of hydrogen in the vitrinite macerals.

Resolving the relative role of these two mechanisms is complicated by the fact that Rock-Eval pyrolysis, TAI, and (or) H/C data may also behave anomalously as maturity indicators in the Monterey Formation and some other source rocks (Snowdon, 1995). Additionally, thermal models, such as the Time-Temperature Index (TTI), may produce unreliable estimates of maturity because of the marked variability of present-day geothermal gradients in coastal and offshore California, the uncertainty of past geothermal gradients in the tectonically complex California coastal area, and (particularly in the Monterey) the difficulty of accurately estimating paleothicknesses and paleoconductivities (Petersen and Hickey, 1983, 1987; Isaacs and Magoon, 1984; Isaacs and Petersen, 1987; Isaacs, 1988; Dunham and others, 1991; Williams and others, 1994).

In any case, the important point in the present study is recognition of the possibility that, at least in some areas, Monterey strata that appear to be immature because they yield VRE<0.6 percent may be capable of generating large volumes of crude oil, much of it sulfur rich and heavy.

Within Region 7, slivers of Jurassic and Cretaceous rocks and Franciscan Complex and ophiolite basement rocks crop out in several places, including (1) in the Point Arguello and Point Sal area, (2) immediately north of the Santa Ynez fault, and (3) in the vicinity of the West Huasna fault, but these outcrops are generally too small to show on map A (pl. 1). As noted below, some of these rocks, such as the Espada Formation sampled at map no. 54 and 55, may be immature, but others are almost certainly mature (VRE=0.6-1.3 percent) or overmature (VRE>1.3 percent) with respect to oil generation.

Region 8—Upper Jurassic and Cretaceous, San Rafael Mountains: The only data from this region are from 12 samples collected from the Upper Jurassic and Lower Cretaceous Espada Formation in T. 8 N., R. 29 W. (map no. 31). TAI analyses by Frederiksen (1985) and R_o , TAI, T_{max} , and PI data (this study) indicate that these rocks are mature (VRE=0.6-1.3 percent). Based on these data, Region 8 has been mapped as mature (map A, pl. 1). This may be an oversimplified picture, however, judging from the variable matu-

urity of Cretaceous rocks in Region 5 to the north and the lack of any maturity data from the Upper Cretaceous rocks in Region 8.

Region 9—Upper Jurassic and Cretaceous, southeastern San Rafael Mountains: R_o , TAI, T_{max} , and PI data from four samples collected in the Upper Jurassic and Lower Cretaceous Espada Formation in T. 6 N., R. 27 W. (map no. 52) indicate that these rocks are mature (table 5), but, as in Region 8, further sampling is needed to define the thermal maturity of this region. Map no. 52 includes samples that demonstrate the discrepancy between TAI and other maturity data (table 3).

Region 10—Basement: This region is dominated by Franciscan Complex with minor ophiolite. No maturity data are available, but these rocks are assumed to be overmature with respect to oil generation (VRE>1.3 percent).

Region 11—Tertiary: Eocene and younger rocks are exposed between the Big Pine fault to the north, Pine Mountain fault to the northeast, and Santa Ynez fault to the south. Rock-Eval pyrolysis T_{max} and PI (Frizzell and Claypool, 1983) and TAI (Frederiksen, 1985) have been determined for more than 60 samples collected from Eocene rocks (Juncal Formation, Matilija Sandstone, Cozy Dell Shale, and Coldwater Sandstone) in this region. In many localities, Rock-Eval and TAI values were determined on samples collected from the same formation and, at least in some cases, probably from very close to the same outcrop. Comparison of the data shows that T_{max} values indicate higher maturity than TAI values, when TAI is interpreted using Frederiksen's (1985) TAI- R_o correlation (table 2). The series of analyses from map no. 48, 51, 60, and elsewhere illustrate this relationship (table 5). This is consistent with the observation that in cases where TAI, T_{max} , and other maturity data are known to have been determined on the same samples (table 3), maturity indicated by Frederiksen's (1985) TAI- R_o correlation is low. For this reason, and because of the generally good agreement between maturity indicated by Frizzell and Claypool's (1983) data and other maturity data elsewhere in the study area, more weight has been placed on the Rock-Eval data than on the TAI in interpreting maturity.

T_{max} values from Region 11 indicate that, except for two samples from the Juncal Formation near the Santa Ynez fault (map no. 64) that yield VRE>1.3 percent, the Eocene section is marginally mature to mature with respect to oil generation. The post-Eocene section, including some outcrops too small to show on map A (pl. 1), is almost certainly immature.

Region 12—Tertiary: Eocene rocks are exposed on the northeastern side of the study area, between the Big Pine Fault to the north and Pine Mountain fault to the south. Along the northeastern side of the region, where Eocene rocks are thrust over Pliocene nonmarine rocks along the San Guillermo fault to the north and are in depositional contact with the granite of Alamo Mountain to the south (Dibblee, 1987), the Eocene Juncal Formation varies from immature (map no. 34, 36, 44)

to marginally mature (map no. 33) to mature (map no. 35, 37, 43), based on T_{max} values (table 5). To the south, in the Pine Mountain area north of the Pine Mountain fault, Eocene rocks assignable at least in part to the younger Matilija Sandstone, Cozy Dell Shale, and Coldwater Sandstone range from immature to mature, based on T_{max} (map no. 45-47), R_o extrapolated from well samples (map no. 49), and TAI measurements (map no. 38).

Region 13—Tertiary and Quaternary, northern onshore Santa Barbara-Ventura basin: North of the Santa Barbara coast where the Santa Ynez Mountains form the northern margin of the onshore Santa Barbara-Ventura basin, a steeply southward dipping homocline exposes a wide expanse of dominantly Eocene and younger rocks south of the Santa Ynez fault. The Santa Ynez Mountains-Santa Barbara coast area has been studied extensively by a number of investigators, using the full range of thermal maturity indicators in table 5. The data, which generally yield a consistent picture of thermal maturity, indicate that Miocene and younger rocks, including the Monterey Formation, are everywhere immature at the surface. The main maturity variation is in the Cretaceous and Paleogene section that has been sampled in the subsurface at Point Conception (map no. 87) and is exposed in the southward-dipping homocline south of the Santa Ynez fault, where it has been upthrown about 1,500 m to 3,000 m (5,000 ft to 10,000 ft) (Bailey and Jahns, 1954; Vedder and others, 1969). The California State Highway 33 (Wheeler Gorge) (map no. 61-63) and Gibraltar Road (map no. 66-68) sections illustrate the progression from overmaturity with respect to oil generation (VRE>1.3 percent) in the oldest strata near the Santa Ynez fault to less mature younger rocks to the south. Limited data in the Refugio Pass area (map no. 70, 71) suggest similar maturity patterns there. Rocks shown as VRE greater than 1.3 percent in map A (pl. 1) encompass map no. 61 and 66 and other limited outcrops of basement, Cretaceous, and Eocene rocks south of the Santa Ynez fault. The boundary between mature and immature rocks (the 0.6-percent VRE contour) is drawn within the Eocene section. However, evidence that Eocene and Oligocene rocks are in part immature is based on Frederiksen's (1985) TAI and Helmold's (1980) R_o values (for example, at map no. 63, 68, 71, 74) that may be anomalously low (see discussion under "Thermal Alteration Index (TAI)").

Although Helmold's (1980) R_o and Frederiksen's (1985) TAI data may yield anomalously low maturity in the Eocene section, T_{max} , TAI, and R_o determined by these and other laboratories are internally consistent in indicating that within individual Eocene formations, maturity levels in the subsurface at Point Conception are lower than in the section exposed in the California State Highway 33 section to the east. The westward decrease in maturity corresponds to a westward decrease in present-day thickness of the Eocene section from north of Ventura to near Point Conception (Bailey and Jahns, 1954), and to an east-to-west decrease in estimated maximum burial depth and increase in comparable sandstone porosities and

permeabilities of individual Eocene formations (Helmold and van de Kamp, 1984). The limited data in table 5 suggest that in progressively younger rocks within the Eocene section [from the Juncal Formation (oldest) through the Sacate Formation (Kelley, 1943)/Coldwater Formation], the difference in maturity between the State Highway 33 and Point Conception sections becomes less noticeable, consistent with the decrease in the difference between these two sections in the estimated maximum burial depth of progressively younger rocks (Helmold and van de Kamp, 1984).

As a consequence of the east-to-west decrease in maturity, the position of the 0.6-percent VRE contour moves downsection from the State Highway 33-Gibraltar Road sections, where it lies within the Cozy Dell or younger formations, to the Gerber No. 1 well at Point Conception where the boundary between immature and mature rocks probably occurs within the Juncal Formation and certainly in rocks no younger than Matilija Sandstone [based on data from Helmold (1980) and P.C. van de Kamp, written commun., 1987].

East of the Agua Blanca Thrust (map no. 41, 56, 57), Eocene rocks assignable at least in part to the Juncal Formation range from mature to overmature with respect to oil generation.

In the southeastern part of Region 13 near Ventura, the deep central part of the onshore Santa Barbara-Ventura basin contains one of the thickest Pliocene and Pleistocene marine sequences in the world; about 4,000 m to 4,600 m (13,000 ft to 15,000 ft) of generally marine Pliocene sediments are conformably overlain by about 1,200 m to 2,000 m (4,000 ft to 6,500 ft) or more of Pleistocene marine strata. Tectonism has deformed the section and exposed Pliocene and Pleistocene rocks north and east of Ventura (Bailey and Jahns, 1954; Vedder and others, 1969; Bostick and others, 1978; Crowell, 1987; De Rito and others, 1989). Northwest and northeast of Ventura, Miocene Rincon Shale and Monterey Formation rocks yield VRE less than 0.6 percent (map no. 42, 58, 79-81, 88). Immediately south of Ventura, Pliocene and Pleistocene rocks yield R_o values <0.6 percent to depths of 5,706 m (18,721 ft) or greater in the subsurface (map no. 90, 91) (Bostick and others, 1978).

Region 14—Tertiary and Quaternary of the southern onshore Santa Barbara-Ventura basin and Santa Monica Mountains: Very few data are available in this geologically complex (Crowell, 1987) area. Over much of the region, Miocene and younger rocks are assumed to be immature at the surface, although the only maturity data determined directly from immature Tertiary rocks are from two drill holes south of the Oak Ridge fault a few kilometers east of map no. 90. Extrapolation of vitrinite reflectance data determined on Pliocene and Pleistocene Pico Formation samples from these wells indicates VRE of surface rocks is <0.6 percent (Hathon, 1992). In the Simi Hills, Paleogene rocks may also be immature (see Region 15).

In contrast, in the western part of the Santa Monica Mountains, which are essentially a broad, generally westward-

plunging anticline, lower Miocene and older sedimentary rocks were overlain by up to about 4,570 m (15,000 ft) or more of middle and upper Miocene marine strata and as much as about 1,500 m (5,000 ft) or more of upper middle Miocene submarine flows. Diabasic sills and dikes, some of which were probably feeders for the submarine flows, intruded the Miocene section between 17 Ma and 12 Ma (Bailey and Jahns, 1954; Crowell, 1987). In this area, Miocene rocks are at least locally mature to possibly overmature with respect to oil generation (map no. 96). The 0.6-percent VRE contour line (map A, pl. 1) has been drawn to encompass the deepest part of the section, but the contour is very poorly constrained. It is likely that within the area shown as immature, Miocene rocks near Miocene intrusions and upper middle Miocene volcanic units are locally mature to overmature with respect to oil generation.

Region 15—Cretaceous, Simi Hills: Three samples of Upper Cretaceous Chatsworth Formation (Colburn and others, 1981) collected in T. 2 N., R. 17 W. (map no. 89) yield R_o , TAI, and T_{max} values that indicate the rocks are immature, suggesting that nearby Paleocene-Miocene strata of Region 14 are also immature.

Region 16—Basement, Cretaceous, and lower Tertiary blocks: Areas of marginally mature (map no. 93) to mature (map no. 94) Upper Cretaceous rocks and overmature (VRE greater than 1.3 percent) basement (Upper Jurassic Santa Monica Slate) (map no. 92) and Cretaceous and lower Tertiary (map no. 95) rocks occur in a structurally complex area affected by Tertiary intrusion and volcanism (see Region 14). Several other small areas of Cretaceous and lower Tertiary rocks within Region 14 (Jennings and Strand, 1969) [not shown on maps A and B (pl. 1)] may be marginally mature to overmature, but no maturity data are available. VRE contours are poorly constrained.

SUMMARY

Mesozoic to Quaternary rocks are exposed at the surface in the structurally and tectonically complex region of the onshore Santa Maria and Santa Barbara-Ventura basins. In the onshore Santa Maria basin and southern Coast Ranges, Mesozoic basement rocks, including the Franciscan Complex, are assumed to be overmature with respect to oil generation (VRE > 1.3 percent), although few maturity data are available. Upper Jurassic and Cretaceous sedimentary rocks range from overmature to marginally mature (VRE ≈ 0.6 percent). The exposed Tertiary section in the onshore Santa Maria basin and smaller Huasna-Pismo basin to the north is almost entirely lower Miocene and younger. VRE is generally <0.6 percent at the surface and less than or equal to approximately 0.6 percent to depths up to about 2,620 m (about 8,600 ft) or more in the subsurface. The only known Tertiary surface rocks with VRE greater than 0.6 percent are near Point Sal, where lower Miocene strata intruded by a gabbro sill yield R_o val-

ues as high as 1.56 percent. However, because of the possibility of early generation and the suggested unreliability of maturity indicators, particularly in the Miocene Monterey Formation, VRE values may underestimate the actual maturity of the surface and subsurface Neogene section.

To the south and east, surface rocks in the onshore Santa Barbara-Ventura basin area are almost entirely Tertiary and younger. Outcrops of basement and Cretaceous sedimentary rocks are restricted to limited areas south of the Santa Ynez fault and in the Simi Hills and Santa Monica Mountains. In contrast to the onshore Santa Maria basin, the Tertiary sequence includes an extensive, thick Paleogene section with a wide range in maturity. In the area between the Santa Ynez and Big Pine faults, VRE of Eocene rocks ranges from <0.6 percent to >1.3 percent. South of the Santa Ynez fault, VRE decreases from >1.3 percent in Cretaceous-Eocene rocks near the fault to <0.6 percent in younger rocks to the south. Within the Eocene section, maturity also decreases from east to west, from north of Ventura west toward Point Conception, reflecting at least in part an east-to-west decrease in estimated maximum burial depths of the Eocene section.

Neogene rocks, including the Miocene Monterey Formation, that crop out along the Santa Barbara coast and in the Ventura area everywhere yield VRE <0.6 percent. Southeast of Ventura, Pliocene and Pleistocene marine sediments yield VRE <0.6 percent to depths of 5,706 m (18,721 ft) or greater in the subsurface, reflecting at least in part the short effective heating time and low geothermal gradient (Bostick and others, 1978; De Rito and others, 1989) in this area of extremely rapid Pliocene and Pleistocene marine sedimentation. The only exposed rocks in the southern part of the study area known to have VRE >0.6 percent are in the Santa Monica Mountains, where Miocene strata were deeply buried and intruded and are associated with Miocene volcanic rocks, and where there are isolated blocks of higher maturity basement and Cretaceous rocks.

REFERENCES CITED

- Alpha, T.R., Detterman, J.S., and Morley, J.M., 1988, Atlas of oblique maps—A collection of landform portrayals of selected areas of the world: U.S. Geological Survey Miscellaneous Investigations Series I-1799.
- Bailey, T.L., and Jahns, R.H., 1954, Geology of the Transverse Range Province, southern California, in Jahns, R.H., ed., Geology of southern California, Chapter II, Geology of the natural provinces: California Division of Mines Bulletin 170, p. 83-106.
- Baskin, D.K., and Peters, K.E., 1992, Early generation characteristics of a sulfur-rich Monterey kerogen: American Association of Petroleum Geologists Bulletin, v. 76, p. 1-13.
- Bostick, N.H., 1979, Vitrinite reflectance, in Cook, H.E., ed., Geologic studies of the Point Conception Deep Stratigraphic Test Well OCS-CAL 78-164 No. 1, outer continental shelf, southern California, United States: U.S. Geological Survey Open-File Report 79-1218, p. 125-128.
- Bostick, N.H., Cashman, S.M., McCulloh, T.H., and Waddell, C.T., 1978, Gradients of vitrinite reflectance and present temperature in the Los Angeles and Ventura basins, California, in Oltz, D.F., ed., A symposium in geochemistry—Low temperature metamorphism of kerogen and clay minerals: Los Angeles, Pacific Section, Society of Economic Paleontologists and Mineralogists, p. 65-96.
- Bustin, R.M., Barnes, M.A., and Barnes, W.C., 1985, Diagenesis 10—Quantification and modelling of organic diagenesis: Geoscience Canada, v. 12, no. 1, p. 4-21.
- California Division of Oil and Gas, 1991, California oil and gas fields, Volume II, Southern, central coastal, and offshore California [3d ed.]: Sacramento, California Department of Conservation Division of Oil and Gas Report TR12, 689 p.
- Claypool, G.E., and Magoon, L.B., 1988, Oil and gas source rocks in the National Petroleum Reserve in Alaska: U.S. Geological Survey Professional Paper 1399, p. 451-481.
- Colburn, I.P., Saul, L.R., and Almgren, A.A., 1981, The Chatsworth Formation: A new formation name for the Upper Cretaceous strata of the Simi Hills, California, in Link, M.H., Squires, R.L., and Colburn, I.P., eds., Simi Hills Cretaceous turbidites, southern California, volume and guidebook: Los Angeles, Pacific Section, Society of Economic Paleontologists and Mineralogists, p. 9-16.
- Crawford, F.D., 1971, Petroleum potential of the Santa Maria province, in Cram, I.H., ed., Future petroleum provinces of the United States—Their geology and potential: American Association of Petroleum Geologists Memoir 15, v. 1, p. 316-328.
- Crouch, J.K., and Suppe, J., 1993, Neogene tectonic evolution of the Los Angeles basin and inner borderland: A model for core complex-like crustal extension: Geological Society of America Bulletin, v. 105, p. 1415-1434.
- Crowell, J.C., 1976, Implications of crustal stretching and shortening of coastal Ventura basin, California, in Howell, D.G., ed., Aspects of the geologic history of the California continental borderland: American Association of Petroleum Geologists Miscellaneous Publication 24, p. 365-382.
- 1987, Late Cenozoic basins of onshore southern California—Complexity is the hallmark of their tectonic history, in Ingersoll, R.V., and Ernst, W.G., eds., Cenozoic basin development of coastal California: Englewood Cliffs, N.J., Prentice-Hall, p. 207-241.
- Curran, J.F., 1982, Petroleum in the Transverse Ranges—A summary, in Fife, D.L., and Minch, J.A., eds., Geology and mineral wealth of the California Transverse Ranges: Santa Ana, Calif., South Coast Geological Society, p. 252-273.
- Curran, J.F., Hall, K.B., and Herron, R.F., 1971, Geology, oil fields and future petroleum potential of Santa Barbara Channel area, California, in Cram, I.H., ed., Future petroleum provinces of the United States—Their geology and potential: American Association of Petroleum Geologists Memoir 15, v. 1, p. 192-211.
- De Rito, D.F., Lachenbruch, A.H., Moses, T.H., Jr., and Munroe, R.J., 1989, Heat flow and thermotectonic problems of the central Ventura Basin, California: Journal of Geophysical Research, v. 94, p. 681-699.
- Dibblee, T.W., Jr., 1950, Geology of southwestern Santa Barbara County, California: Point Arguello, Lompoc, Point Conception, Los Olivos and Gaviota quadrangles: California Division of Mines Bulletin 150, 95 p.
- 1966, Geology of the central Santa Ynez Mountains, Santa Barbara County, California: California Division of Mines and

- Geology Bulletin 186, 99 p.
- 1987, Geology of the Sierra Madre and Pine Mountain area, California, in Davis, T.L., and Namson, J.S., eds., Structural evolution of the western Transverse Ranges, volume and guidebook: Los Angeles, Pacific Section, Society of Economic Paleontologists and Mineralogists, v. 48A, p. 43-53.
- Dickinson, W.W., 1989, Analysis of vitrinite maturation and Tertiary burial history, northern Green River basin, Wyoming, Chapter F, in Law, B.E., and Spencer, C.W., eds., Geology of tight gas reservoirs in the Pinedale anticline area, Wyoming, and at the Multiwell Experiment site, Colorado: U.S. Geological Survey Bulletin 1886, p. F1-F17.
- Dunham, J.B., Bromley, B.W., and Rosato, V.J., 1991, Geologic controls on hydrocarbon occurrence within the Santa Maria basin of western California, in Gluskoter, H.J., Rice, D.D., and Taylor, R.B., eds., Economic geology, U.S.: Boulder, Colo., Geological Society of America, The Geology of North America, v. P-2, p. 431-446.
- Frederiksen, N.O., 1985, Map showing thermal-alteration indices in roadless areas and the Santa Lucia Wilderness in the Los Padres National Forest, southwestern California: U.S. Geological Survey Miscellaneous Field Studies Map MF-1655-F, scale 1:250,000.
- Frizzell, V.A., Jr., and Claypool, G.E., 1983, Petroleum potential map of Mesozoic and Cenozoic rocks in roadless areas and the Santa Lucia Wilderness in the Los Padres National Forest, southwestern California: U.S. Geological Survey Miscellaneous Field Studies Map MF-1655-D, scale 1:250,000.
- Gautier, D.L., Dolton, G.L., Takahashi, K.I., and Varnes, K.L., eds., 1995, 1995 National assessment of United States oil and gas resources—Results, methodology, and supporting data: U.S. Geological Survey Digital Data Series DDS-30 [CD-ROM].
- Hathon, L.A., 1992, Burial diagenesis of the Sespe Formation, Ventura basin, California: Columbia, Mo., University of Missouri—Columbia, Ph.D. thesis, 261 p.
- Helmold, K.P., 1980, Diagenesis of Tertiary arkoses, Santa Ynez Mountains, California: Stanford, Calif., Stanford University, Ph.D. thesis, 225 p.
- Helmold, K.P., and van de Kamp, P.C., 1984, Diagenetic mineralogy and controls on albitization and laumontite formation in Paleogene arkoses, Santa Ynez Mountains, California, in McDonald, D.A., and Surdam, R.C., eds., Clastic diagenesis: American Association of Petroleum Geologists Memoir 37, p. 239-276.
- Hornafius, J.S., Luyendyk, B.P., Terres, R.R., and Kamerling, M.J., 1986, Timing and extent of Neogene tectonic rotation in the western Transverse Ranges, California: Geological Society of America Bulletin, v. 97, p. 1476-1487.
- Howard, J.L., 1995, Conglomerates of the upper middle Eocene to lower Miocene Sespe Formation along the Santa Ynez fault—Implications for the geologic history of the eastern Santa Maria basin area, California, in Keller, M.A., ed., Evolution of sedimentary basins/onshore oil and gas investigations—Santa Maria province: U.S. Geological Survey Bulletin 1995-H, 37 p.
- Howell, D.G., Champion, D.E., and Vedder, J.G., 1987, Terrane accretion, crustal kinematics, and basin evolution, southern California, in Ingersoll, R.V., and Ernst, W.G., eds., Cenozoic basin development of coastal California: Englewood Cliffs, N.J., Prentice-Hall, p. 242-258.
- Ingle, J.C., Jr., 1981, Cenozoic depositional history of the northern continental borderland of southern California and the origin of associated Miocene diatomites, in Isaacs, C.M., ed., Guide to the Monterey Formation in the California coastal area, Ventura to San Luis Obispo: American Association of Petroleum Geologists Special Publication 52, p. 1-8.
- Isaacs, C.M., 1980, Diagenesis in the Monterey Formation examined laterally along the coast near Santa Barbara, California: Stanford, Calif., Stanford University, Ph.D. thesis, 329 p.
- 1988, Marine petroleum source rocks and reservoir rocks of the Miocene Monterey Formation, California, U.S.A., in Wagner, H.C., Wagner, L.C., Wang, F.F.H., and Wong, F.L., eds., Petroleum resources of China and related subjects: Houston, Tex., Circum-Pacific Council for Energy and Mineral Resources Earth Science Series 10, p. 825-848.
- Isaacs, C.M., and Magoon, L.B., 1984, Thermal indicators of organic matter in the Sisquoc and Monterey Formations, Santa Maria basin, California [abs.]: Abstracts, Society of Economic Paleontologists and Mineralogists Annual Midyear Meeting, San Jose, Calif., August 10-13, p. 40.
- Isaacs, C.M., and Petersen, N.F., 1987, Petroleum in the Miocene Monterey Formation, California, in Hein, J.R., ed., Siliceous sedimentary rock-hosted ores and petroleum: New York, Van Nostrand Reinhold, p. 83-116.
- Isaacs, C.M., and Tomson, J.H., 1990, Reconnaissance study of petroleum source-rock characteristics of core samples from the Sisquoc and Monterey Formations in a north-south subsurface transect across the onshore Santa Maria basin and in surface sections along the Santa Barbara-Ventura coast, southern California: U.S. Geological Survey Open-File Report 89-108, 43 p.
- Jennings, C.W., compiler, 1958, Geologic map of California—San Luis Obispo sheet: Sacramento, California Division of Mines and Geology, scale 1:250,000.
- 1959, Geologic map of California—Santa Maria sheet: Sacramento, California Division of Mines and Geology, scale 1:250,000.
- 1977, California geologic data map series, map 2, geologic map of California: Sacramento, California Division of Mines and Geology, scale 1:750,000.
- Jennings, C.W., and Strand, R.G., compilers, 1969, Geologic map of California—Los Angeles sheet: Sacramento, California Division of Mines and Geology, scale 1:250,000.
- Johnson, S.Y., and Stanley, R.G., 1994, Sedimentology of the conglomeratic lower member of the Lospe Formation (lower Miocene), Santa Maria basin, California, in Keller, M.A., ed., Evolution of sedimentary basins/onshore oil and gas investigations—Santa Maria province: U.S. Geological Survey Bulletin 1995-D, 21 p.
- Johnsson, M.J., Howell, D.G., and Bird, K.J., 1993, Thermal maturity patterns in Alaska: Implications for tectonic evolution and hydrocarbon potential: American Association of Petroleum Geologists Bulletin, v. 77, p. 1874-1903.
- Kablanow, R.I., II, and Surdam, R.C., 1984, Diagenesis and hydrocarbon generation in the Monterey Formation, Huasna basin, California, in Surdam, R.C., ed., Stratigraphic, tectonic, thermal, and diagenetic histories of the Monterey Formation, Pismo and Huasna basin, California: Society of Economic Paleontologists and Mineralogists Annual Midyear Meeting, San Jose, Calif., 1984, Guidebook 2, p. 53-68.
- Keller, M.A., 1984a, Diagenesis and lithostratigraphy of the Monterey Formation near Ojai, California: Los Angeles, Ca-

Selected Series of U.S. Geological Survey Publications

Books and Other Publications

Professional Papers report scientific data and interpretations of lasting scientific interest that cover all facets of USGS investigations and research.

Bulletins contain significant data and interpretations that are of lasting scientific interest but are generally more limited in scope or geographic coverage than Professional Papers.

Water-Supply Papers are comprehensive reports that present significant interpretive results of hydrologic investigations of wide interest to professional geologists, hydrologists, and engineers. The series covers investigations in all phases of hydrology, including hydrogeology, availability of water, quality of water, and use of water.

Circulars are reports of programmatic or scientific information of an ephemeral nature; many present important scientific information of wide popular interest. Circulars are distributed at no cost to the public.

Fact Sheets communicate a wide variety of timely information on USGS programs, projects, and research. They commonly address issues of public interest. Fact Sheets generally are two or four pages long and are distributed at no cost to the public.

Reports in the **Digital Data Series (DDS)** distribute large amounts of data through digital media, including compact disc-read-only memory (CD-ROM). They are high-quality, interpretive publications designed as self-contained packages for viewing and interpreting data and typically contain data sets, software to view the data, and explanatory text.

Water-Resources Investigations Reports are papers of an interpretive nature made available to the public outside the formal USGS publications series. Copies are produced on request (unlike formal USGS publications) and are also available for public inspection at depositories indicated in USGS catalogs.

Open-File Reports can consist of basic data, preliminary reports, and a wide range of scientific documents on USGS investigations. Open-File Reports are designed for fast release and are available for public consultation at depositories.

Maps

Geologic Quadrangle Maps (GQ's) are multicolor geologic maps on topographic bases in 7.5- or 15-minute quadrangle formats (scales mainly 1:24,000 or 1:62,500) showing bedrock, surficial, or engineering geology. Maps generally include brief texts; some maps include structure and columnar sections only.

Geophysical Investigations Maps (GP's) are on topographic or planimetric bases at various scales. They show results of geophysical investigations using gravity, magnetic, seismic, or radioactivity surveys, which provide data on subsurface structures that are of economic or geologic significance.

Miscellaneous Investigations Series Maps or Geologic Investigations Series (I's) are on planimetric or topographic bases at various scales; they present a wide variety of format and subject matter. The series also includes 7.5-minute quadrangle photogeologic maps on planimetric bases and planetary maps.

Information Periodicals

Metal Industry Indicators (MII's) is a free monthly newsletter that analyzes and forecasts the economic health of five metal industries with composite leading and coincident indexes: primary metals, steel, copper, primary and secondary aluminum, and aluminum mill products.

Mineral Industry Surveys (MIS's) are free periodic statistical and economic reports designed to provide timely statistical data on production, distribution, stocks, and consumption of significant mineral commodities. The surveys are issued monthly, quarterly, annually, or at other regular intervals, depending on the need for current data. The MIS's are published by commodity as well as by State. A series of international MIS's is also available.

Published on an annual basis, **Mineral Commodity Summaries** is the earliest Government publication to furnish estimates covering nonfuel mineral industry data. Data sheets contain information on the domestic industry structure, Government programs, tariffs, and 5-year salient statistics for more than 90 individual minerals and materials.

The Minerals Yearbook discusses the performance of the worldwide minerals and materials industry during a calendar year, and it provides background information to assist in interpreting that performance. The Minerals Yearbook consists of three volumes. Volume I, Metals and Minerals, contains chapters about virtually all metallic and industrial mineral commodities important to the U.S. economy. Volume II, Area Reports: Domestic, contains a chapter on the minerals industry of each of the 50 States and Puerto Rico and the Administered Islands. Volume III, Area Reports: International, is published as four separate reports. These reports collectively contain the latest available mineral data on more than 190 foreign countries and discuss the importance of minerals to the economies of these nations and the United States.

Permanent Catalogs

"Publications of the U.S. Geological Survey, 1879–1961" and **"Publications of the U.S. Geological Survey, 1962–1970"** are available in paperback book form and as a set of microfiche.

"Publications of the U.S. Geological Survey, 1971–1981" is available in paperback book form (two volumes, publications listing and index) and as a set of microfiche.

Annual supplements for 1982, 1983, 1984, 1985, 1986, and subsequent years are available in paperback book form.

ISBN 0-607-91825-X



9 780607 918250